The Dissertation Committee for Meng Zhao Certifies that this is the approved version of the following dissertation:

Genetic and Biochemical Studies on the Differential Modulation of RNA Decay and Processing by Inhibitory Proteins in *Escherichia coli*

Committee:

George Georgiou, Supervisor

Ian J. Molineux

Charles F. Earhart, Jr.

Vishwanath Iyer

Richard J. Meyer

Genetic and Biochemical Studies on the Differential Modulation of RNA Decay and Processing by Inhibitory Proteins in *Escherichia coli*

by

Meng Zhao, B.M., M.S.

Dissertation

Presented to the Faculty of the Graduate School of

The University of Texas at Austin

in Partial Fulfillment

of the Requirements

for the Degree of

Doctor of Philosophy

The University of Texas at Austin

December, 2006

Dedication

To my family, to whom I owe everything

Acknowledgements

First, I want to thank my advisor, George Georgiou, for being such a great mentor the past five (or so) years. Your trust in my ability, encouragement, support and guidance will never be forgotten. I am grateful to my committee members, Ian Molineux, Charles Earhart, Vishwanath Iyer, and Richard Meyer, for their interest in this work and helpful suggestions. I would like to thank Yasuaki Kawarasaki and Li Zhou for their assistance on the RraA and RraB regulation work; Junjun Gao, Kangseok Lee and Stanley Cohen, for their collaborations on the characterization of RraB function; Chainaya Jain for his suggestion on the design of genetic screen. I would also like to thank Aiko Umeda, Ashwini Devkota, and Jeff Chan, for their help on making the degradosome component expression constructs. I am grateful to Alan Lambowitz and Andy Ellington, who allowed me to use their labs for the RNA related experiments. I acknowledge Robert Simons, Charles Yanofsky, Andrew Emily, Sidney Kushner and Lin-Chao Sue for sharing strains and antibodies. I thank Danielle Tullman-Ercek and Clinton Leysath for proofreading this dissertation. Then there are so many other lab members –Karl Griswold, Andrew Hayhurst, Xiaoming Zhan, Lluis Masip, Laura Segatori, and Navin Varadarajan who all helped me so much with both research and keeping my sanity. And thanks also to everyone else who has made the lab such a fun place to work. Beyond the lab, special praise goes to Jo Frederick and her family. Thank you for introducing the love of God to me, which has changed my life. I would like to express my deepest appreciation to my parents and my sister for their unconditional love and support. And finally, my husband, Yibin, gets the most thanks for his love, understanding and support, over the last four and a half years.

Genetic and Biochemical Studies on the Differential Modulation of RNA Decay and Processing by Inhibitory Proteins in *Escherichia coli*

Publication No._____

Meng Zhao, Ph.D.

The University of Texas at Austin, 2006

Supervisor: George Georgiou

The regulation of mRNA decay is a critical post-transcriptional step in the control of gene expression. In *E. coli*, RNase E carries out the first and rate-limiting step in the decay of most mRNAs, as well as in the processing of ribosomal, transfer RNAs and small regulatory RNAs. The RNase E protein has two domains: the catalytic N-terminal half and the C-terminal half containing the scaffold region for the assembly of an RNA degrading machine termed the degradosome. Earlier studies in our lab identified the trans-acting proteins, RraA and RraB, which inhibit RNase E activity through direct-interaction with the enzyme.

The present work explores several mechanistic, physiological and biotechnology-related aspects of the modulation of *E. coli* RNA decay and processing by inhibitory proteins. We found that, in contrast to RraA, RraB interacts with a different site on RNase E, results in distinct changes in degradosome composition, and interferes with cleavage of a different set of transcripts. Therefore, our results revealed a novel

mechanism whereby a selective remodeling of the degradosome by endonuclease binding proteins serves to differentially regulate RNA decay and processing in *E. coli*.

We developed protocols to express and purify the C-terminal truncated forms of RNase E. A system to reconstitute part of the degradosome and determine the consequences of RraA and RraB binding to the kinetics of RNA degradation *in vitro* was established.

We showed that *rraA* is transcribed predominantly from its own promoter (PrraA) located in the *menA* - *rraA* intergenic region. Transcription from PrraA is σ^s-dependent and is induced upon entry into stationary phase. Moreover, the synthesis of RraA is regulated at the post-transcriptional level by RNase E, suggesting the existence of a feedback regulatory circuit between RraA and RNase E.

RraB is transcribed from a promoter (P*rraB*) which is divergent from the *argI* promoter. Contrary to the previous data, we could not find any evidence that *rraB* promoter activity, mRNA abundance and protein level are affected by changes in tryptophan or arginine metabolism. In contrast to RraA, the expression of RraB does not change during different growth phases.

Table of Contents

Chapter 1: Introduction and Background

POST-TRANSCRIPTIONAL CONTROL OF GENE EXPRESSION: mRNA DECAY IN *ESCHERICHIA COLI*

Studies over the past 50 years have revealed that virtually every event involved in gene expression appears to be subject to regulation. The rates of gene transcription and of mRNA decay determine the steady-state level of transcripts. Transcript levels, together with translation rates, then dictate the amount of protein produced. The various steps of gene expression are highly coordinated and inter-dependent with each other. Whereas the effect of transcription and protein turnover on protein abundance in the cell has been appreciated for some time, mRNA decay is only now emerging as a critical post-transcriptional control point and as a major contributor to the regulation of gene expression. The significance of mRNA decay as a mechanism for controlling gene expression in either eukaryotic or prokaryotic cells is well established (Kushner 2004). For example, in *E. coli*, the different abundance of the protein products from the polycistronic *pap* operon is readily explained by the difference in their mRNA stability (the *papA* mRNA half-life is estimated to be 20 min, whereas the half-life of the *papBA* transcript is 2.5 min) (Nilsson and Uhlin 1991). In human cells, the mechanisms controlling mRNA stability are relevant in determining the level of chemokine gene expression during chronic inflammatory conditions (Mata et al. 2005).

While in eukaryotic cells, the typical mRNA lifetimes range from 25 minutes (yeast) to 16 hours (in human HeLa cells) (Singer and Penman 1973; Warner and Gorenstein 1978), in bacteria mRNAs are subject to very rapid turnover. The continuous

breakdown and re-synthesis of prokaryotic mRNA allows rapid changes in protein synthesis to occur and is important for the rapid adaptation of micro-organisms to a changing environment. Nonetheless the decay rates of specific bacterial mRNAs can differ significantly. In *E. coli*, the half-life of individual mRNAs range from just a few seconds to more than an hour (Belasco 1993).

The work described in this dissertation is focused on *E. coli.* However, it is worth mentioning that recent results show that the similarities between mRNA decay in the prokaryotes and eukaryotes are greater than were generally believed. Despite the clearly distinct molecular mechanisms of mRNA turnover in these two biological realms, evidence has been established that mRNA degradation in all organisms is regulated by trans-acting factors, as well as cis-acting RNA sequences. Moreover, both prokaryotes and eukaryotes adjust the activity of trans-effectors and the accessibility of the cis-acting regulatory sequences in order to provide fine-tuning of the mRNA degradation process. Furthermore, recurrent themes exist in both phyla, e.g. common RNA structural elements and functionally analogous multicomponent RNA/protein complexes such as the "degradeosome" and "exosome," all involved in RNA processing and decay (BAKER and CONDON 2004).

Ribonucleases control RNA decay and processing

The most direct trans-acting factors controlling mRNA stability in both eukaryotes and prokaryotes are ribonucleases (RNases). After more than 30 years of studies, it is now known that *E. coli* contains more than a dozen ribonucleases, and the list is still growing. Based on the manner in which they cleave the substrate, RNases can be broadly classified into two groups: endoribonucleases, which cleave internal

phosphodiester bonds within RNA, and exoribonucleases, which cleave RNA chains from the 3' or the 5' terminus. In contrast to eukaryotes, no 5' to 3' exoribonuclease has been found in eubacteria and archaea (Zuo and Deutscher 2001).

The first, and rate limiting, step of mRNA decay (as well as in the maturation of tRNAs and of the 5S ribosomal RNA) in *E. coli* and many other bacteria is primarily due to endonucleolytic attack, generally carried out by the essential enzyme, RNase E (Misra and Apirion 1979; Deutscher 2006). As discussed later, studies of total mRNA turnover and breakdown of individual messages have confirmed the important role of RNase E in RNA decay and processing. Nevertheless, a number of other endoribonucleases such as RNase G, RNase P, and RNase III also participate in mRNA decay to a limited degree. RNase G is a homolog of RNase E, which might serve as a backup in both mRNA decay and 5S rRNA maturation when RNase E is inactivated (Lee et al. 2002; Ow et al. 2003). RNase III, whose action is specifically on double-stranded RNAs, is primarily involved in the maturation of rRNA and the processing of certain polycistronic operons. However, RNase III probably does not play a major role in initiating mRNA decay since this enzyme is not essential for cell viability (Kushner 2004). Finally, RNase P is an enzyme acting primarily on tRNA precursors and certain polycistronic operons (Li and Deutscher 2004).

Following an initial endonucleolytic cleavage, additional cleavages break the mRNA into fragments. In *E. coli*, three processive 3'-5' exoribonucleases, i.e. PNPase (polyribonucleotide nucleotidyltransferase), RNase II and RNase R, are primarily responsible for degradation of the mRNA fragments. PNPase is a phosphorolytic nuclease which releases nucleoside 5'-diphosphates (Soreq and Littauer 1977). RNase II and RNase R are hydrolytic and generate nucleoside monophosphates (Gupta et al. 1977; Cheng et al. 1998). Interestingly, mutant cells lacking one of the three nucleases

grow normally, indicating that the three enzymes have significant functional overlap. PNPase seems to have broad specificity to carry out all essential functions in mRNA decay (after the initial endonucleolytic attack) since cells lacking both RNase II and RNase R do not exhibit any significant defects. As detailed later, degradation by PNPase is further stimulated by its interaction with the RhlB RNA helicase, particularly when it is associated with the RNase E-based degradosome (Coburn et al. 1999).

All three processive exoribonucleases are single-strand specific nucleases and their action is inhibited by secondary structure. None of these enzymes can complete the degradation of mRNA fragments because they are relatively inactive against short oligonucleotides. These residual products are digested to mononucleotides by oligoribonuclease, an exoribonuclease belonging to the DEDD exonuclease superfamily which is named after the characteristic core comprised of four invariant acidic amino acids and display specificity for very short nucleotide chains (4-7 nt). In fact, this step has been shown to be essential for cell viability (Zhang et al. 1998; Ghosh and Deutscher 1999) (Figure 1.1).

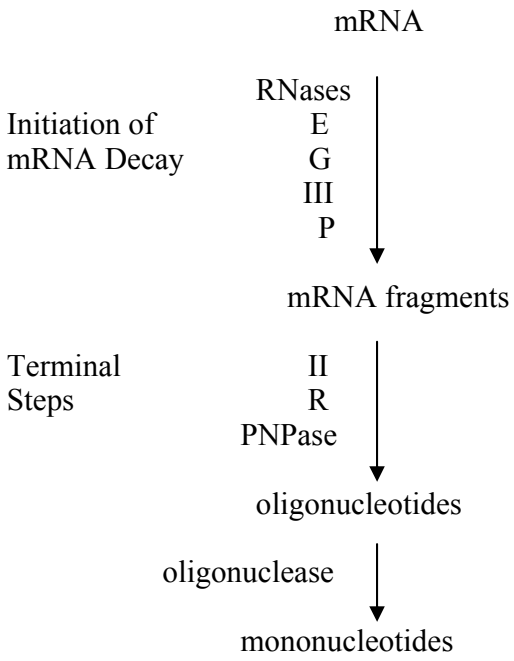

Figure 1.1 mRNA decay in *E. coli.* The endoribonucleases, RNase E, G, III and P, carry out the initial cleavages during mRNA decay. Depending on the process, a particular enzyme may play the primary role. Terminal steps in mRNA degradation involve the processive exoribonucleases, PNase II, R or PNPase, followed by oligoribonuclease to remove 5' terminal oligonucleotides.

5'- end events in mRNA decay

The influence of the 5' terminus on the susceptibility of mRNA to degradation is well documented for both bacteria and higher organisms. In eukaryotes, the 5'methyl guanosine cap prevents 5'-3' exonucleolytic decay. Thus its removal from the mRNA by the decapping complex often constitutes the rate-limiting step in mRNA turnover (Coller and Parker 2004). In *E. coli*, differences in mRNA longevity are frequently determined by features of the 5' untranslated region. The presence of a stem-loop structure at an

RNA 5' end often increases RNA stability, a finding that is somewhat surprising in view of the absence of prokaryotic 5' exoribunuclease and the central role of endonucleolytic cleavage in bacterial RNA degradation. For example, the 5'-most stem-loop and a 30-nt single-stranded region surrounding the ribosome binding site (RBS) of the *ompA* mRNA are found to account for the unusual stability of the *ompA* transcript (t1/2=17 minutes) (Emory et al. 1992). On the other hand, the addition of as few as five unpaired nucleotides to the 5' end of the stem-loop can significantly reduce the stability of the *ompA* mRNA. These results suggest that the initial step in degradation requires access to the mRNA by an RNase that needs a single-stranded region at the 5' end for binding (Lundberg et al. 1990). As will be detailed later, this decay-initiating RNA cleavage event is catalyzed by RNase E, and the 5'-terminal triphosphate in an intact transcript acts to stabilize the mRNA from this endoribonucleatic attack (Mackie 1998, 2000). In fact, RNase E strongly favors monophosphorylated RNA substrates, which is believed to ensure that once decay of an mRNA is initiated, continued degradation of the 3' cleavage product is preferred over an intact triphosphorylated RNA.

3'-end events in mRNA decay

Just like the 5' terminus of an mRNA is important to its stability, the 3' end also plays a critical role in controlling degradation through the polyadenylation process. In contrast to eukaryotes in which stable poly (A)-tails at the 3'end helps maintain mRNA stability, polyadenylation stimulates RNA degradation in prokaryotes and in eukaryotic

organelles (Kushner 2002). At least a fraction of *E. coli* mRNAs, including the *rpsO*, *lpp*, and *ompA* mRNAs, are polyadenylated as a prerequisite for degradation (Hajnsdorf et al. 1994; Hajnsdorf et al. 1995). None of the exonucleases (PNPase, RNase II or RNase R), are able to act on a completely double-stranded RNA molecules due to their inability to bind the substrate (Deutscher 2006). Thus the polyadenylation of structured RNA seems to destabilize the transcript by creating a single-stranded RNA binding site that provokes exonucleolytic digestion of the substrate by various 3'-5' exonucleases. We now know that polyadenylation in bacteria results from a balance between the activities of a poly(A) polymerase I (PAP I) and of exoribonucleases that remove poly(A) tails. PAP I adds adenylate residues to the 3' end of RNA using ATP as a donor (August et al. 1962; Cao et al. 1996). Deletion of the *pcnB* gene (encoding PAP I) reduces polyadenylylation by over 90% and dramatically stabilizes the *lpp*, *ompA*, and *trxA* mRNAs (O'Hara et al. 1995). It was thought that only a small fraction of *E. coli* mRNA was polyadenylated at any time. However, recent comparisons of the transcriptomes of wild-type and the *pcnB* deletion strains demonstrated that majority mRNAs undergo some degree of polyadenylylation by PAP I. The studies on the molecular mechanism of polyadenylation-dependent mRNA degradation suggest that in *E. coli* Rho-independent transcriptional terminators at the 3' end of many mRNAs serve as the specific polyadenylation signals for PAP I. The binding of the Sm-like protein, Hfq, to the terminator modifies this substrate specificity and enhances activity for polyadenylation catalyzed by PAP I. Specifically, inactivation of the *hfq* gene leads to a reduction in the ability of PAP I to add poly(A) tails at the 3' end of full-length mRNAs containing Rho-independent transcription terminators. Under these conditions, PNPase

performs the primary poly(A)/polynucleotide-adding activity in the cell, producing short heteropolymeric additions on RNA decay intermediates (Mohanty et al. 2004). Paradoxically, the binding of Hfq to poly(A) tail is also shown to protect the 3' terminus from exonucleolytic attack by RNase II and PNPase (Folichon et al. 2005). Clearly, further investigation is required to clarify the role of Hfq in regulating polyadenylation-dependent mRNA degradation.

Small regulatory RNAs

In recent years there has been increased evidence for the interaction of small regulatory RNAs (sRNA) with their target mRNAs and their role in decay. Bacteria use a very heterogeneous group of small non-coding RNAs which have been identified as crucial regulatory elements in stress responses and in virulence. More than 70 small, non-coding RNAs, usually 80-100 nt in length, have been confirmed in *E. coli*, based on genome-wide searches (1–2% of the number of known protein-coding genes) (Gottesman 2005). A major class of *E. coli* sRNAs, which comprise about one third of all known sRNAs, act by base-paring with the target mRNAs, i.e. by antisense mechanisms, to carry out their regulatory functions (Zhang et al. 2003). The bacterial regulatory RNAs are bound to the RNA chaperone Hfq, and are presented to their pairing targets, generally the 5' end of the mRNA, to affect their stability or translation (Storz et al. 2004). Hfq is a well-conserved homohexameric ring protein which is closely related to Sm and Sm-like proteins involved in RNA splicing in eukaryotes (Sauter et al. 2003). Through strong interactions with the single-stranded AU-rich regions on both small non-coding RNAs

and the target mRNAs, Hfq stimulates pairing between small RNAs and their targets. A well-studied *E. coli* small regulatory RNA is RyhB, which is expressed in response to iron limitation as a result of the released repression by Fur protein. RyhB causes the rapid degradation of several target mRNAs encoding nonessential Fe-binding proteins, such as the *sodB* mRNA which encodes an iron superoxide dismutase, thus reducing the intracellular requirement for Fe (Masse and Gottesman 2002). Interestingly, degradation of both mRNA targets and small regulatory RNAs, i.e. *sodB* and RyhB, has been shown to depend on RNase E. Since Hfq and RNase E bind similar sites on the RNA, it is suggested that pairing may precipitate the loss of Hfq and access of RNase E (Lin-Chao et al. 1999; Masse et al. 2003). Nevertheless, as will be discussed later, a model of the ribonucleoprotein complexes formed by RNase E, Hfq and sRNA has been implicated in degradation as well (Morita et al. 2005).

It should be pointed out that mediating mRNA decay is only one of the multifaceted functions of the small RNAs. The outcome of the sRNA-target mRNA pairing can be inhibition of translation (e.g. OxyS negatively regulates the synthesis of two transcriptional regulators, RpoS and FhlA); stimulation of translation (e.g. DsrA and RprA increase levels of translation of RpoS) and stabilization of mRNA (e.g. GadY increased levels of the GadA and GadB glutamate decarboxylases (Gottesman 2005)).

RNASE E AND THE DEGRADOSOME

RNase E

RNase E has received intensive study for its role in RNA decay ever since it was first identified in the late 70s. In 1978, Ghora and Apirion characterized RNase E in a temperature-sensitive mutant (*rne-3071*) based on the observation that 5S rRNA precursor accumulated at the nonpermissive temperature (Ghora and Apirion 1978). Independent work by Ono and Kuwano identified the *ams-1* (altered mRNA stability) gene because its inactivation significantly slowed down the decay of total pulse-labeled RNA at elevated temperature (Ono and Kuwano 1979). It took several research groups almost 10 years to confirm that the *ams-1* and *rne-3071* mutations are alleles of the same gene, now named *rne* (Mudd et al. 1990; Babitzke and Kushner 1991; Melefors and von Gabain 1991; Taraseviciene et al. 1991). Located at 24.6 min on the linkage map of *E. coli*, the *rne* open reading frame (ORF) is 3.4 kb long. The promoter of the *rne* gene is located 361 nucleotides upstream of the initiation codon. Right after the stop codon there is a typical Rho-independent terminator consisted of an inverted repeat followed by 6 consecutive Us.

More than 25 years of extensive studies have revealed that the functions of RNase E in RNA metabolism include the processing of ribosomal and transfer RNAs (Li and Deutscher 2002; Ow and Kushner 2002); the degradation of sRNAs such as DsrA (Masse et al. 2003), RyhB (Masse and Gottesman 2002), and SgrS (Morita et al. 2004); and, most importantly, the turnover of numerous cellular mRNAs (Mudd et al. 1990; Mackie 1991; Regnier and Hajnsdorf 1991; Bernstein et al. 2002). Complete deletion of the *rne* gene is lethal. Initially, defects in 9S rRNA processing and mRNA decay were thought to be responsible for the defect in viability associated with the inactivation of RNase E (Ghora and Apirion 1978). However, recent data suggest that the essential role of RNase E is the initiation of tRNA maturation (Ow et al. 2000; Ow and Kushner 2002).

The *E. coli* RNase E protein contains 1,061 amino acids, with a calculated molecular mass of 118 kDa, and is one of the larger proteins in this organism. Based on amino acid composition and the presence of functional sites, the full-length RNase E protein can be divided into two functional portions: an N-terminal half (NTH, amino acid residues 1–500), and a C-terminal half (CTH, aa residues 501-1061) (Figure1.2). Also known as the catalytic domain, the NTH carries out the catalytic function of RNase E (McDowall and Cohen 1996). The crystal structure of the catalytic domain of RNase E (aa residues 1–529) was recently solved as trapped allosteric intermediates with RNA substrates. This 529 aa RNase E fragment is composed of two globular portions, referred to as the 'small' (aa residues 400-529) and 'large' domains (aa residues 1–400). The 'large' domain is further divided into subdomains according to the established folds. The N-terminal 279 aa residues are structurally related to the RNase H endoribonuclease family. Embedded in the RNase H fold are an S1 domain (aa residues 36–118) which is a widely occurring RNA-binding structural motif, and a 5' sensor fold (aa residues 119–215) which participates in the recognition of the 5' terminus of the bound RNA. The remaining component of the large domain (aa residues 280-440) encompassing the active site is structurally congruent to the endo-deoxyribonuclease, DNase I, making a surprising link in the evolution of RNA and DNA nucleases. The catalytic domain of RNase E forms a homotetramer which is organized as a dimer-of-dimers. This quaternary organization requires that the intra-domain linkers cross and coordinate a zinc ion through a pair of cysteine residues (Figure 1.2). Importantly, mutation of the coordinating four cysteine residues results in disruption of the RNase E tetramer into stable dimers, which are capable of binding RNA but have no catalytic activity. On the other hand, tetrameric RNase E, formed by chemical crosslinking in the absence of zinc, is catalytically active. These results suggest that a tetrameric quaternary structure is

required for RNase E to carry out its core enzymatic functions (Adams et al. 2001; Callaghan et al. 2003; Callaghan et al. 2005).

The S1 domain has also been found in at least three other *E. coli* ribonucleases, including RNase G, RNase II and PNPase (Bycroft et al. 1997). The first clue suggesting that the S1 domain is important for the activity of RNase E comes from the fact that two separate point mutations within the domain, *rne-3071* (L68F) and *ams-1* (G66S), are both lethal at nonpermissive temperatures (McDowall et al. 1993). Using site-directed mutagenesis and structural modeling, Joel Belasco and co-workers suggest the role of the RNase E S1 domain is more complex than simply providing an RNA-binding surface. They identified two functionally distinct regions on the surface of the S1 domain: one group, including Phe-57, Phe-67 and Tyr-112, is important for the ribonucleolytic activity of the enzyme, while the other group, comprising Lys-37 and Tyr-60, is dispensable for catalysis *in vitro* but is required for feedback regulation of RNase E expression (Diwa et al. 2002). Moreover, structural studies of the S1 domain of RNase E as determined by both X-ray crystallography and NMR spectroscopy indicate that the S1 domain serves a role in dimerization, to assist the formation of the tetrameric quaternary structure of RNase E. Thus, functional investigations of the S1 domain in RNase E point to a complex role in facilitating substrate recognition, autoregulation and subunit assembly (Schubert et al. 2004).

The NTH is essential for cell viability (Kido et al. 1996) and has numerous homologues, most notably the paralogue RNase G encoded by the *rng* gene (Wachi et al. 1999). In contrast, the C-terminal half (CTH) of RNase E, containing residues 501-1061, is poorly conserved and is dispensable for cell survival (Kido et al. 1996; Kaberdin et al. 1998; Ow et al. 2000). Based on functionality, the CTH can be further divided into two functional domains. One is the central domain (residues 501-750) containing a

secondary RNA binding site which is arginine-rich (ARRBS, residues 604-688) (McDowall and Cohen 1996). However, in contrast with the S1 domain located in the NTH of RNase E, the ARRBS appears to have a more marginal role in RNA recognition since it is not required for ribonucleolytic activity, feedback regulation or cell growth (Abee and Wouters 1999; Diwa and Belasco 2002).

The rest of RNase E C-terminal half (residues 734-1061) is called the "scaffold region" because it is involved in interactions with other proteins. A. J. Carpousis *et al.* first reported that, when purified from *E. coli* cells, RNase E is present in a large multiprotein complex, i.e., the RNA degradosome, that also contains the exoribonuclease polynucleotide phosphorylase (PNPase), the DEAD-box RNA helicase RhlB, and the glycolytic enzyme enolase (Carpousis et al. 1994; Py et al. 1994; Py et al. 1996). Several other degradosome-associated proteins including the protein chaperones GroEL and DnaK (Miczak et al. 1996), polyphosphate kinase (PPK) and PAP I (Raynal and Carpousis 1999) may also be present in sub-stoichiometric amounts (Blum et al. 1997). Through a combination of deletion, yeast two-hybrid analysis and co-immunopurification experiments, the binding sites of the three major degradosome components were mapped to adjacent but different sites on the C-terminal domain of RNase E. Residues 734-738 are required for RhlB binding, while enolase binds to residues 738-845 on RNase E. The binding site for PNPase is within the last 217 residues at the C-terminus, which consists of residues 844-1045 (Vanzo et al. 1998). Recently, the protein–protein interactions among degradosome components were further examined using chemical cross-linking, size-exclusion chromatography, partial proteolysis and Nanoflow mass spectrometry analysis. The residues within the 728–784 regions are found to be important for the interaction with RhlB. The enolase-binding site was narrowed down to residues 833–850 of RNase E. Moreover, the crystal structure of enolase in complex with a synthetic

peptide corresponding to this 18 amino acid stretch of RNase E (833–850) was recently obtained and showed that a single molecule of an RNase E-derived peptide binds asymmetrically in a conserved cleft at the interface of the enolase dimer. The segment containing residues 1022-1061 of RNase E was shown to bind PNPase, which is in agreement with the earlier finding that PNPase binds at the end of C-terminus (Callaghan et al. 2004). Although the reported molar ratios of these four major components from purified degradosomes vary, it is recognized that RNase E associates with a molar excess molar of PNPase and an equal molar amount of RhlB (Carpousis et al. 1994; Khemici et al. 2004; Lin and Lin-Chao 2005).

The degradosome-organizing domain of RNase E has little structure under native conditions and is unlikely to be extensively folded within the degradosome. Among the few segments of structural propensity in RNase E CTH, a larger segment of 80 residues is predicted to form a coiled coil and could possibly interact with RNA. The other three isolated segments of 10–40 residues are possibly the site of self-recognition and protein-protein interaction. It has been suggested that the "scaffold region" of RNase E may act as a flexible tether of the degradosome components since binding of the three major degradosome components does not induce significant folding of the CTH (Callaghan et al. 2004). Given its intrinsically unstructured nature, it is not surprising that the CTH domain is highly divergent amongst the members of the RNase E family. The presence of the CTH may confer selective advantages to *E. coli* and closely related bacteria in term of fine-tuning the transcript dynamics within the cell through the assembly of the degradosome.

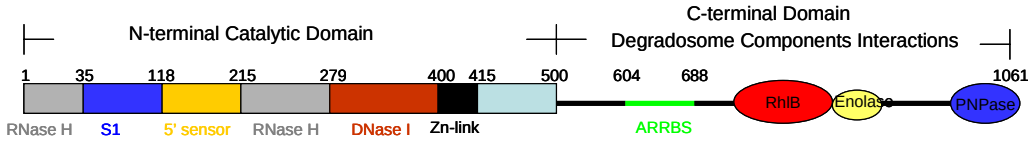

Figure 1.2 Schematic representation of the structure of RNase E. Linear representation of the subdomain boundaries within the N-terminal catalytic domain. The degradosome-scaffolding C-terminal domain has binding regions for RNA/helicase, enolase and PNPase (Modified from Callaghan, 2005).

Function of the degradosome

Many cellular functions are carried out *in vivo* by multicomponent macromolecular complexes (i.e., cellular machines) rather than by individual freely diffusable proteins. Well recognized and extensively studied examples of such complexes include ribosomes, replisomes, and proteasomes. The *E. coli* RNA degradosome is the prototype of a family of multiprotein machines involved in the processing and degradation of RNA. Complexes analogous to the degradosome, sometimes sharing homologous components are found in eukaryotic cells as well. For example, the exosome and mtEXO are degradosome-like complexes involved in RNA processing and degradation identified in yeast and its mitochondria (Margossian et al. 1996; Mitchell et al. 1997). The mtEXO complex contains a PNPase homologue and a putative DExH-box helicase. Similarly, two ATP-dependent RNA helicases are associated with the exosome (Anderson and Parker 1998; de la Cruz et al. 1998). Finally, a PNPase homologue is part of a multiprotein complex implicated in the regulation of chloroplast message stability (Hayes et al. 1996). The identification of multiprotein complexes in both prokaryotic and

eukaryotic cells suggests that assemblies of ribonucleases with other enzymes such as RNA helicases is a common feature in RNA processing and decay.

The association of an endoribonuclease, an exoribonuclease and an RNA helicase would seem to make the degradosome ideally suited to breakdown RNA molecules. The different steps in the degradation of mRNAs are speculated to be orchestrated by the degradosome in a coordinated manner: when the degradation of mRNA is initiated by RNase E-mediated endonucleolytic cleavage, the newly generated 3' ends can be directly attacked by PNPase which is capable of breaking down RNAs from the 3' end to the 5' end; thus eliminating the potentially slow step in which free PNPase locates the 3' end of the substrate. The presence of an ATP-dependent RNA helicase, RhlB, in the degradosome presumably helps unwind unfavorable RNA secondary structures that could block the action of PNPase and RNase E, both of which are single-strand specific ribonucleases.

Notwithstanding the isolation of multicomponent RNase E-based complexes from *E. coli*, it has been difficult to demonstrate its physiological significance,for several reasons. (1) Truncated RNase E protein lacking the CTH, and therefore not capable of assembling the degradosome, is sufficient for cell survival and for RNA degradation *in vivo*. (2) Purified RNase E devoid of other degradosome components is functional *in vitro*. (3) The scaffold region that interacts with other degradosome proteins is not conserved in the RNase E homologues in certain other bacteria, e.g. *Synechocystis sp*.

Recent evidence that reveals physiological roles of the degradosome have begun to emerge. Electron microscopy studies using immunogold labeling and freeze-fracture methods demonstrate that degradosomes exist *in vivo* in *E. coli* as multicomponent structures that associate with the cytoplasmic membrane via the N-terminal region of RNase E (Liou et al. 2002). Nearly all the RNase E C-terminal truncation mutants

exhibit some degree of impaired growth. Furthermore, deletion of the CTH of RNase E containing both ARRBS and the scaffold region significantly slows down the degradation of bulk RNA, although the processing of rRNA is not affected (Ow et al. 2000). A recent, more extensive analysis of degradosome function using DNA microarrays revealed that all four degradosome components, including RNase E, PNPase, RhlB, and enolase, are necessary for normal mRNA degradation in *E. coli*. Decay of some *E. coli* mRNAs *in vivo* also depends on the action of assembled degradosomes (Bernstein et al. 2004).

In addition, there is increasing experimental evidence that individual degradosome components functionally interact during decay of at least some RNAs. PNPase is a major 3' to 5' exoribonuclease of *E. coli* and functions both in the degradation of mRNA and stable RNA species and as a poly(A) polymerase. PNPase cooperates with RNase E in the degradation of RNA I, an antisense regulator of replication of ColE1-type plasmids (Xu and Cohen 1995).

RhlB is one of the five DEAD-box proteins in *E. coli*; the other four are CsdA (formerly called DeaD), DbpA, RhlE and SrmB (Iost and Dreyfus 2006). They are members of a family of RNA helicases that contain a characteristic DEAD-box core (350 amino acids). The DEAD-box proteins are now known to be part of the widely distributed DExD/H-box family of helicases that participate in many RNA unwinding and remodeling reactions (Tanner and Linder 2001). The DExD/H-box proteins together with other RNA and DNA unwinding enzymes constitute a helicase superfamily containing a structurally conserved ATPase domain with RecA-like architecture (Gorbalenya and Koonin 1993; Caruthers and McKay 2002). The sequence alignment of the DEAD-box proteins shows that the conserved catalytic core is flanked by C-terminal extensions that differ both in size (from 70 to 290 amino acids) and sequence. These non-conserved extensions are thought to mediate the interactions of DEAD-box proteins with

their specific partners or with RNA substrates (Silverman et al. 2003). As one of the smallest members of the DExD/H-box family, RhlB contains little more than the common DEAD-box core. In contrast with the other four DEAD-box proteins, RhlB lacks detectable ATPase and RNA helicase activities unless it is stimulated by binding to the CTH of RNase E. Interestingly, studies with different RNase E fragments reveal that the stimulation of the helicase activity is dependent on an arginine-rich region of RNase E (residues 789–820), which might contribute to RNA binding and thus facilitate the interaction of RNA substrate with the helicase core (Vanzo et al. 1998; Silverman et al. 2003; Iost and Dreyfus 2006).

Inactivation of the *rhlB* gene severely impedes the degradation of mRNAs containing stable secondary structures, such as REP (repeated extragenic palindrome) elements (Py et al. 1996; Coburn et al. 1999; Khemici and Carpousis 2004). Studies using *in vitro* reconstituted degradosome show that a complex containing all three components, RNase E, PNPase and RhlB, is required to degrade the highly structured *malE* REP sequence (Coburn et al. 1999). RhlB also facilitates the degradation of ribosome-free, highly RNase E-sensitive mRNAs *in vivo*. The mRNAs transcribed by bacteriophage T7 RNA polymerase contain long stretches of ribosome-free mRNAs because transcription outpaces translation as a result of higher mRNA elongation rate by the bacteriophage T7 RNA polymerase compared with the *E. coli* counterpart. These ribosome-free mRNAs are exceptionally sensitive to inactivation and degradation by RNase E (Iost and Dreyfus 1995). Deletion of the *rhlB* gene stabilizes the ribosome-free *lacZ* and other mRNAs transcribed by bacteriophage T7 RNA polymerase. Primer extension analysis confirmed that RhlB facilitates the endoribonucleolytic cleavage of *lacZ* mRNA by RNase E (Khemici et al. 2005). These results suggest that RhlB mediates the unwinding of these structures that otherwise would impede the processivity of RNase E and PNPase.

The 48 kDa enolase is a universally conserved enzyme of glycolytic metabolism that is found in archaea, eubacteria and eukaryotes. The enzyme catalyzes the interconversion of phosphoenolpyruvate and 2-phospho-d-glycerate, which proceeds through the reversible elimination of water. In *E. coli*, roughly 10% of the total enolase is sequestered in the degradosome (Liou et al. 2001). Unlike RNase E, RhlB or PNPase, whose presence in the degradosome is well explained by their individual roles in RNA metabolism, the function of the enolase is not clear. In fact, a functionally active "minimal" degradosome containing only RNase E, RhlB and PNPase can be reconstituted from individually purified components (Coburn et al. 1999). However, analysis of transcript levels using DNA microarrays has shown that disruption of enolase's interaction with RNase E in *E. coli* affects the turnover of some mRNAs, particularly, the transcripts encoding enzymes of energy-generating metabolic routes (Lee et al. 2002; Bernstein et al. 2004). It has also been reported that the association of enolase with RNase E is required for the response to excess phosphosugar (Morita et al. 2004; Kawamoto et al. 2005). Under this condition, the small regulatory RNA, SgrS, is induced and recruited to the degradosome via Hfq, resulting in the targeted degradation of the transcript encoding the transmembrane glucose transporter, *ptsG* (Morita et al. 2005). These results suggest that the function of enolase may serve to link cellular metabolic status with post-transcriptional gene regulation. Nevertheless, the direct interaction of enolase and RNase E is not required for the induction of SgrS or for *ptsG* transcript turnover. Additional investigations will be needed to reveal the exact function of enolase in the degradosome.

The emerging picture of the RNA degradosome suggests RNase E-based complexes that are much more versatile than originally thought. For example, recent work indicates that degradosomes vary in composition in response to altered

environment. A specialized degradosome containing CsdA, whose expression is induced by cold shock, is found to form at low temperatures. Reconstitution of a complex containing RNase E, PNPase and CsdA shows that CsdA can furnish an ATP-dependent activity that facilitates the efficient degradation of a model mRNA at low temperatures (Prud'homme-Genereux et al. 2004). In addition, two other DEAD-box helicases, SrmB and RhlE, are also able to interact with RNase E *in vitro*. Interestingly, mutation analyses show that SrmB, RhlE and CsdA bind to RNase E at a site that is different from the RhlB binding site. RhlE can fully replace RhlB and display RNA-dependent ATPase activity in functional assays using the reconstituted minimal degradosomes prepared from purified components (Khemici et al. 2004). Thus, RhlB, RhlE and CsdA are interchangeable in assays of RNA degradation performed *in vitro*. Just like CsdA, the recruitment of SrmB and RhlE to the degradosome might also depend on physiological conditions which have yet to be identified. Taken together, these findings suggest that the RNA degradosome is flexible and capable of adapting to changing cellular environments.

To make the picture more complete, other recent work indicates that RNase E may be part of multiple RNP complexes, and that the RNA degradosome is just one of them. For example, RNase E forms variable ribonucleoprotein complexes with Hfq/sRNAs (e.g. SgrS and RyhB) through its C-terminal scaffold region. These complexes are distinct from the RNA degradosome since the Hfq/sRNAs appears to be able to associate with RNase E only when its C-terminal scaffold region is not occupied by other degradosome components (Morita et al. 2005). It is therefore suggested that these RNase E-based ribonucleoprotein complexes may act as specialized RNA decay machines that initiate the degradation of mRNAs targeted by individual sRNA.

It is also of considerable interest that recent data suggest degradosome proteins are also found unattached to RNase E. While RNase E and the RhlB helicase are present in *E. coli* cells in approximately equimolar amounts throughout cell growth, only 5–10% of cellular enolase and 10–20% of PNPase are estimated to be present in the degradosome complex in *E. coli.* Moreover, the molar ratios of enolase and PNPase to RNase E fluctuate with the growth phase, suggesting a dynamic regulation of degradosome composition *in vivo* (Py et al. 1996; Liou et al. 2002). Therefore mutations in degradosome constituents may affect the actions of unassociated constituents as well as the actions of proteins in assembled degradosomes. Consistent with the possibility that degradosome components may function independent of the degradosome, RhlB helicase has been shown to interact directly with PNPase independently of RNase E (Lin and Lin-Chao 2005). Notably, the PNPase-RhlB complex, is analogous to eukaryotic cell exosome complexes, which carry out 3' to 5' exonucleolytic RNA degradation and contain homologous PNPase and RNA helicase (Mitchell et al. 1997; Anderson and Parker 1998). Collectively, these findings indicate that different types of ribonuclease complexes exist, enabling bacterial cells to effectively process and degrade a wide range of RNA substrates.

RNASE E ACTION

RNase E cleavage specificity

Given its central role in RNA processing and degradation in *E. coli*, the biochemical properties of RNase E have been extensively investigated. Particularly, knowledge of the substrate specificity allows the understanding of how different elements of RNA structure

individually contribute to the efficiency and specificity of RNase E cleavage. Through an analysis of mutants in a bacteriophage T4 mRNA processing site, a consensus pentanucleotide ((A/G)AUU(A/U)) that determines RNA substrate susceptibility to RNase E cleavage was suggested (Ehretsmann et al. 1992). However, studies on the degradation of *rpsT* mRNA indicate that rather than recognizing a particular consensus sequence, RNase E is a single-strand-specific enzyme with few primary structural constraints (Mackie 1992). Through introducing random mutations at the 5' end of RNA I and studying their effect on the position of the cleavage *in vivo* and *in vitro*, McDowall *et. al.* demonstrated that an unstructured, AU-rich region is required for efficient cleavage by RNase E (McDowall et al. 1994). A recent study utilizing an oligonucleotide-based assay suggests the presence of a weak consensus motif (G,A)(C,A)N(G)(G,U,A)↓(A,U)(C,U)N(C,A)(C,A) and that the G at position -2 is highly conserved for efficient cleavage (Kaberdin 2003). It is now suggested that the preference of RNase E for the AU-rich substrates arises mainly as a consequence of the recognition of the RNA conformation, rather than the exact sequence. Specifically, the crystal structure of the RNase E catalytic domain in complex with bound RNA shows that the RNA follows the same stacking arrangement over the surface of the RNA-binding channel, and only one of the bases directly contacts with RNase E through a hydrogen bond. No other sequence recognition exists aside from that contact (Callaghan et al. 2005).

While the exact nature of an RNase E cleavage site is still unclear, it has been shown that *in vitro*, RNase E prefers a 5' monophosphate terminus to a 5' triphosphate. Since the cleavage product of RNase E is a 5' monophosphate, the preference for

monophosphorylated RNA substrates ensures that once decay of an mRNA by RNase E is initiated, continued degradation of the 3' cleavage product is preferred over an intact triphosphorylated RNA (Mackie 1998; Jiang and Belasco 2004). This indicates that RNase E must somehow recognize an internal cleavage site and a 5'-terminal unpaired nucleoside monophosphate residue as well. The crystal structure of the RNase E catalytic domain shed some light on the mechanism whereby the recognition of the 5'-terminus of the RNA triggers catalysis. In the proposed induced-fit model, the engagement of the 5'monophosphate of the RNA in the 5' sensing pocket causes an allosteric change in RNase E, thus inducing the S1 domain to clamp down on the RNA downstream and triggering cleavage (Callaghan et al. 2005). The sensitivity of RNase E to the phosphorylation status at the 5' end of RNA was previously attributed simply to the relative affinity of the enzyme for monophosphorylated versus triphosphorylated mRNA. However, a recent study using fluorogenic RNA substrates that allow more accurate quantification of RNase E activity argues that 5' monophosphate facilitates the endoribonucleolytic reaction by increasing the catalytic efficiency and promoting dimer/tetramer formation of RNase E (Jiang and Belasco 2004). This is in agreement with the X-ray structure and biochemical studies which suggest that *E. coli* RNase E protein functions as a homotetramer formed by the Zn linkage of dimers. Nevertheless, this current model that a tetrameric quaternary structure is essential for the core enzymatic functions of RNase E is challenged by the identification of a conserved minimal RNase E peptide (aa residues 1-395) which preserves the core catalytic functions. Despite its lack of the Zn-coordination site which is required for tetramer formation, the RNase E 1-395 fragment is sufficient to carry out the various known

functions of RNase E, as well as to complement an *rne* deletion *in vivo* (Caruthers et al. 2006).

In an effort to understand how RNase E identifies its cleavage sites, Feng *et al.* used synthetic oligoribonucleotides containing repeats of identical target sequences with 2'-O-methyl modifications at defined positions. They showed that the uncleavable target sequence (i.e. 2'-O-methyl-modified nucleotides) impedes cleavages at unmodified sites located 5' to, but not 3' to, the uncleavable target sequence. This observation indicates that RNase E catalytic domain binds selectively to 5'-monophosphate RNA termini but has an inherent mode of cleavage in the 3' to 5' direction in a quasi-prosesive manner. Interestingly, RNase G, which has extensive structural homology with N-Rne, and can functionally complement an *rne* null mutation, has a non-directional mode of action (Feng et al. 2002).

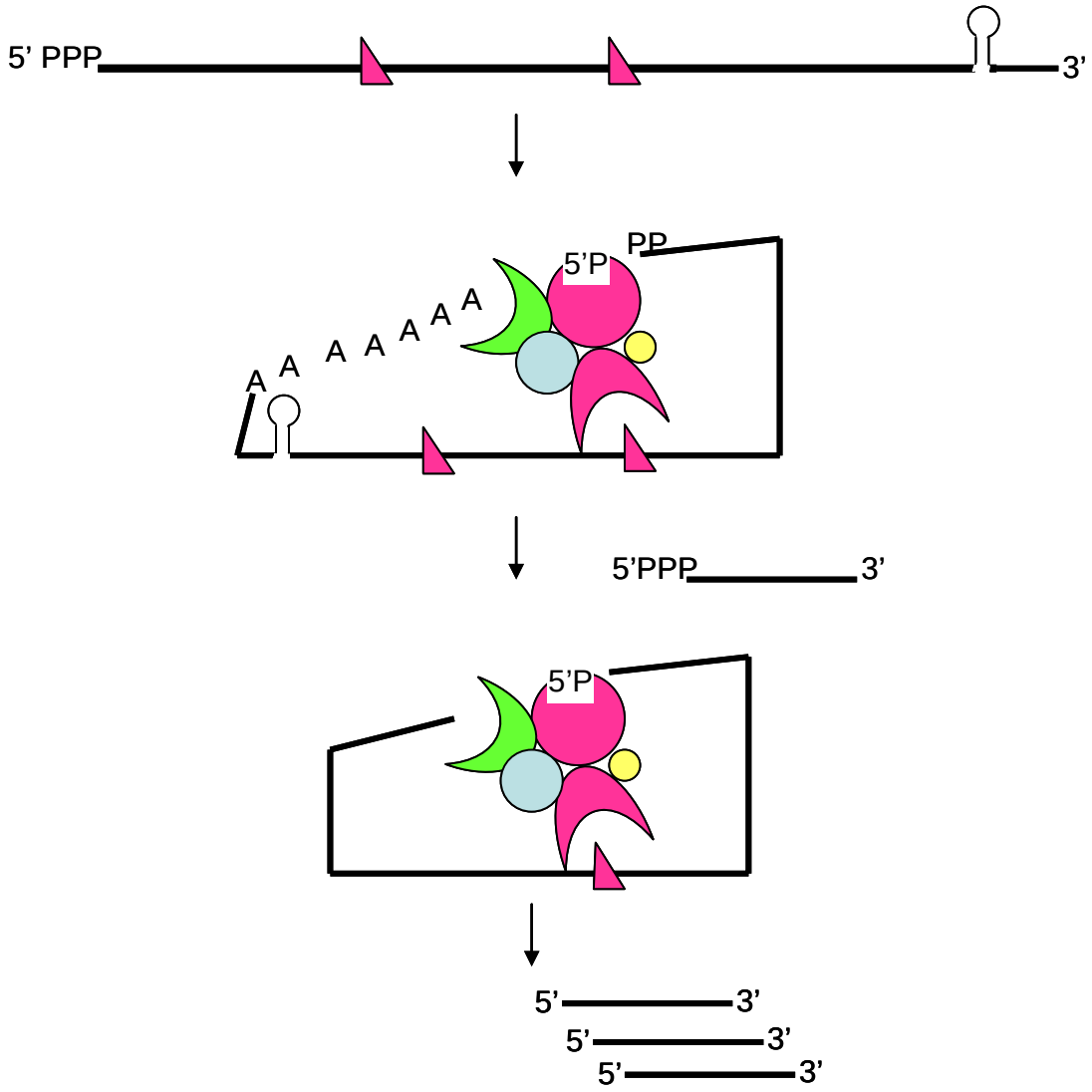

Figure 1.3 mRNA decay catalyzed by the RNase E based degradosome. The degradosome contains RNase E, PNPase, RhlB and enolase. RNase E is present in the degradosome as a dimer or higher oligomer. RNase E recognizes an internal cleavage site and a 5'-terminal unpaired nucleoside residue. A monocistronic mRNA terminated with a Rho-independent transcription terminator (stem-loop structure) is shown as an example. Prior to the initiation of decay, the 3' end of the transcript is polyadenylated by PAP I. The PNPase protein binds to the poly(A) tail while RNase E binds (inefficiently) to the 5' triphosphate terminus. A 5' monophosphate terminus generated by the first endonucleolytic cleavage by RNase E stimulates the activity of RNase E. At the same time, PNPase is degrading exonucleolytically from the 3' terminus releasing nucleoside monophosphates. The oligonucleotides generated by RNase E cleavage would subsequently be degraded by the terminal steps as shown in figure 1.1. Mauve: RNase E and RNase E cleavage sites, Green: PNPase, Blue: RhlB, Yellow: Enolase.

RNase E autoregulation

The expression level of RNase E is tightly controlled by a negative feedback loop. RNase E represses its own synthesis through the reduction of the cellular level of the *rne* transcript which is cleaved by the enzyme (Mudd and Higgins 1993). The cleavage site is within the 5'-terminal segment which contains the 361-nucleotide of 5' untranslated region (5'-UTR) and the first 28 codons of the *rne* protein-coding region. This 5'-terminal 0.45-kb segment is sufficient to confer the feedback regulatory property onto a heterologous transcript to which it is fused. As a consequence of autoregulation, the half-life of the *rne* mRNA varies from less than 40 seconds in strains hosting a multicopy plasmid to more than 8 minutes in an *rne* temperature-sensitive mutant strain, thus maintaining the RNase E protein level within a narrow range (Jain and Belasco 1995).

RRAA, THE TRANS-ACTING FACTOR MODULATING RNASE E ACTIVITY

As discussed above, RNase E plays a central role in RNA decay and processing in *E. coli.* The activity of RNase E is affected by the growth conditions. For example, the processing of RNAs by RNase E is affected by anaerobiosis during cell growth (Georgellis et al., 1993) and also to occur prominently in transcripts that encode proteins involved in energy-generating pathways (Lee et al. 2002 and Bernstein et al. 2002).

The prototypical trans-acting modulator of RNase E activity, RraA (regulator of ribonuclease activity A), was isolated in a genetic screen aimed at the identification of genes whose overexpression enhances disulfide isomerase (DsbC) activity in *E. coli.*

Briefly, an *E. coli* genomic DNA library, cloned into the expression vector pTrc99A downstream from the IPTG-inducible Trc promoter was screened for ability to confer increased folding yield of the v-tPA (a truncated variant of human tissue plasminogen activator [h-tPA]) by monitoring the formation of a clearance zone on fibrin plates. h-tPA, a protease that converts plasminogen to plasmin and contains a total of 17 disulfide bonds, is expressed in a catalytically active form in *E. coli* only in cells that produce elevated levels of DsbC (Qiu et al. 1998). Thus, DsbC activity can be measured using h-tPA as a model substrate. This screen yielded a clone corresponding to a fragment containing an open reading frame (ORF) previously annotated as *menG* in the NCBI database (Qiu 2001), later renamed as RraA based on its function.

The level of *dsbC* mRNA is highly sensitive to cellular RNase E activity, e.g. the half-life of a *dsbC* transcript is less than a minute in the *rne* wild-type strain, however its stability is increased by three-fold in *rne* mutants. Further experiments revealed that the observed increase in DsbC protein level with RraA overexpression resulted from the stabilization of the *dsbC* transcript. Adventitious expression of RraA inhibits the RNase E mediated degradation of *dsbC* transcript, resulting in more than 5-fold increase in its half-life (0.8 min to >4 min) (Zhan et al. 2004).

Subsequent extensive biochemical and genetic studies demonstrated that RraA interacts with RNase E and inhibits it catalytic activity *in vivo* and *in vitro* (Lee et al. 2003). Overexpression of RraA inhibits the autoregulatory cleavage of RNase E at its 5'-UTR and results in a 3-4 fold increase in β-galactosidase activity from a chromosomal *rne-lacZ* fusion (Jain and Belasco 1995) in which the 5'-terminal segment responsible for feedback regulation of *rne* was fused upstream of *lacZ*. Purified RraA inhibits the

cleavage of various well-defined RNA substrates by full-length RNase E *in vitro*. The direct interaction between RraA and RNase E *in vivo* was confirmed by co-precipitation of RNase E by biotin-tagged RraA after nuclease treatment. Moreover, gel shift assays demonstrated that RraA does not interact detectably with RNA substrates or inhibit the binding of substrate RNA to RNase E. These findings argue that RraA affects the ability of RNase E to disrupt phosphodiester bonds between nucleotides by a mechanism that is independent of substrate binding. The absence of experimental evidence for binding of RraA to RNA substrates is supported by the crystal structure of RraA, which is found to form a ring-like trimer with a central cavity of approximately 12 Å in diameter lacking any structural motif characteristic of nucleic acid binding (Figure 1.4) (Monzingo et al. 2003). RraA interacts with full-length RNase E with an equilibrium dissociation constant (K_D) of 26 μM, which is of the same order as the one for proteins that perform regulatory functions such as, for example, the interaction of transcription factors with the core RNA polymerase enzyme.

RraA exhibited higher affinity and displayed more effective inhibition of RNA processing by the full-length RNase E relative to a fragment containing only the catalytic domain. For example, the processing of a well studied RNA substrate, pM1, by full-length RNase E was inhibited by 50% at a 10:1 molar ratio of RraA monomer to purified RNase E. The inhibitory effect of RraA on the cleavage of pM1 by the N-terminal catalytic domain of RNase E was much weaker and the maximum inhibition of pM1 processing was 45% at the highest concentration of RraA used (200-fold molar excess of monomer over N-terminal catalytic domain protein). Furthermore, no binding between RraA and the N-terminal catalytic domain has been detected *in vivo* or *in vitro*. These

observations suggest that the C-terminal scaffold region of RNase E enhances the ability of the catalytic domain of the ribonuclease to interact with RraA.

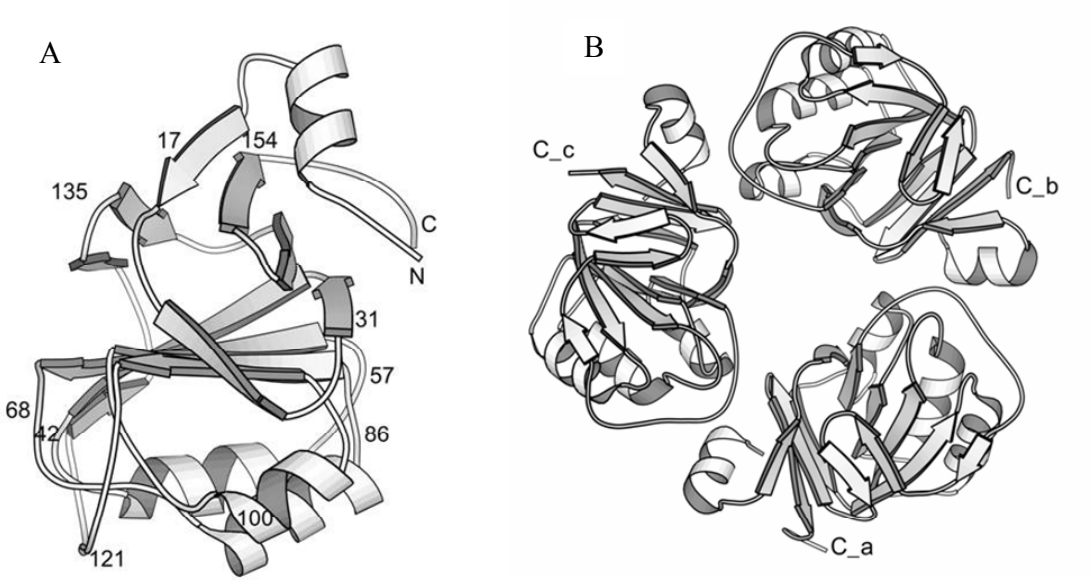

Figure 1.4 Models of RraA. (A) The backbone model of an RraA monomer. This stereo picture illustrates the fold of the protein and displays its secondary structural elements. Residues along the backbone are labeled to aid in following the polypeptide path. (B) The trimeric arrangement of RraA. RraA functions as a trimer, and a trimer is the asymmetric unit of the crystal. Three monomers pack around a pseudo 3-fold axis (Monzingo, 2003).

Microarray profiling shows that overexpression of RraA circumvents the effects of an autoregulatory mechanism that normally maintains the RNase E cellular level within a narrow range, resulting in the genome-wide accumulation of RNase E-targeted transcripts (more than 2000). The absence of *rraA* destabilized the abundance of numerous (~80)

transcripts at least 2-fold, consistent with the inhibitory effect of RraA on the endoribonucleolytic activity of RNase E (Lee et al. 2003).

RraA-like genes are widely distributed in nature with homologues found in many organisms that contain endonuclease genes homologous to RNase E, including Archae, proteobacteria, and Arabidopsis. RraA also efficiently inhibited the cleavage of pM1 RNA by RNase ES, a functional ortholog of *E. coli* RNase E in *S. coelicolor*. The conservation of function between RraA and RNase E homologues from two distantly related bacterial species (i.e., *S. coelicolor* and *E. coli*) suggests that RraA may have a phylogenetically conserved function in modulating ribonuclease activity.

RESEARCH OUTLINE

RraA represents a prototype for cellular proteins that modulate RNA decay and processing by binding to ribonucleases and inhibiting their activity. The characterization of additional cellular proteins that inhibit RNase E activity will improve our understanding of the action mechanisms of these protein modulators. Together with RraA, RraB was isolated in the same functional screen for genes that enhance disulfide bond isomerization in the *E. coli* periplasm as a consequence of its ability to stabilize the *dsbC* transcript. Subsequent research (Chapter 2) reveals RraB is a second adaptor protein which interacts with a different site on RNase E and interferes with cleavage of a different set of transcripts. Importantly, biochemical and genetic studies (Chapter 2 and Chapter 3) led to the discovery of a novel mechanism whereby the selective remodeling

of the degradosome by endonuclease-binding proteins serves to dramatically alter the steady state level of hundreds of transcripts in *E. coli.* An *in vitro* reconstitution system for the mechanistic analysis of selective inhibition of RNA processing by RraA and RraB is discussed in Chapter 3.

As with other post-translational mechanisms of regulation, the physiological significance of inhibition of RNase E activity by RraA/RraB is probably to facilitate rapid alterations in RNA degradation and/or processing in response to specific environmental stimuli. Examining this hypothesis requires a better understanding of the regulation of *rraA*/*rraB* expression. Previously, the regulation of *rraA* was thought to be linked to the synthesis of the redox mediator menaquinone. In chapter 4, I present evidence that transcription of *rraA* from its own promoter is elevated upon entry of stationary phase in an *rpoS*-dependent manner and that the stability of the *rraA* transcript is also dependent on RNase E activity. This suggests that the biological role for the σ^s-dependent P*rraA* activity in early stationary phase may be to provide a means for the protection of σ^s-dependent transcripts from the decay catalyzed by RNase E. Finally, I have examined in some detail the regulation of the second RNase E modulator, *rraB* (Chapter 5).

Chapter 2: RraB: A second RNase E-inhibitory protein that differentially modulates the mRNA abundance

INTRODUCTION

RNase E, an essential endoribonuclease of *E. coli*, is a major player in RNA metabolism including the turnover of numerous cellular mRNAs, the processing of ribosomal and tRNAs, and the degradation of small regulatory RNAs (Ghora and Apirion 1978; Li et al. 1999; Lin-Chao et al. 1999; Steege 2000; Bernstein et al. 2002; Kushner 2002; Li and Deutscher 2002; Masse et al. 2003). Not surprisingly, the regulation of cellular level and activity of RNase E in *E. coli* is complex. First, the efficiency of RNase E cleavage depends on the structural features of RNA substrates and the factors affecting the accessibility of the cleavage sites. Binding to a 5' monophosphate terminus significantly stimulates enzymatic activity and promotes dimer and tetramer formation (Mackie 1998; Jiang and Belasco 2004). In addition, RNA binding proteins, such as Hfq, can reduce the efficiency of RNA processing, competing with RNase E for the same A/U rich regions (Moll I et al. 2003). Second, the amount of RNase E in the cell is another parameter which probably effects efficiency of RNA processing. RNase E autoregulates its synthesis by modulating decay of its own mRNA, the stability of which varies inversely with the cellular RNase E activity (Mudd and Higgins 1993; Jain and Belasco 1995). Third, RNA decay is regulated by interaction with RraA (*r*egulator of *r*ibonuclease *a*ctivity A). RraA is an evolutionarilly conserved small protein which binds directly to RNase E and inhibits its endonucleolytic cleavages (Lee et al. 2003). Adventitious expression of RraA circumvents the effects of the autoregulatory

mechanism and modulates the accumulation of over 2,000 RNase E-targeted transcripts (Lee et al. 2003).

The work described here was undertaken to determine whether cellular proteins other than RraA might participate in the regulation of RNase activity *in vivo.* An *E. coli* genomic DNA library was screened for clones that would increase disulfide isomerization activity, which hinges on a protein encoded by an RNase E-cleavable transcript with a short half-life (Zhan et al. 2004). This screen takes advantage of the high sensitivity of disulfide isomerase (*dsbC*) mRNA to the action of RNase E, although the screen for activities does not specifically require a regulator of RNase E. Here we report the isolation and characterization of a second protein modulator of RNase activity, previously annotated as YjgD and renamed as RraB (*r*egulator of *r*ibonuclease *a*ctivity B) based on its function. RraB and RraA share a number of common characteristics. Both inhibit RNase E activity *in vitro* and *in vivo* by binding to the enzyme. Despite these similarities, there are also striking differences between RraB and RraA. They interact with RNase E at separate sites within RNase E and exert dramatic and distinct effects on the composition of the degradosome. The combined action of the two proteins differentially alters mRNA decay in a transcript-specific manner. Our results reveal a novel mechanism for the global control of steady state mRNA abundance in *E. coli* that appears to be mediated by dynamic remodeling of the degradosome composition in response to elevated expression of RraA or RraB.

The work described in this chapter was done through collaboration between researchers in the Georgiou laboratory and the Cohen laboratory (Stanford University). Specifically, Dr. Junjun Gao (U. Texas) performed surface plasmon resonance analysis，the SPA purification of degradosomes and proteomic analyses; Dr. Kangseok Lee

(Stanford) performed the *in vitro* cleavage assay and microarray analysis of the transcription profile.

MATERIALS AND METHODS

Strains and plasmids

The strains and plasmids used in this work are listed in Table 2.1. The construction of the chromosomal *rne* deleted *E. coli* strain KSL2000, KSL2009, and the *rraA* null strain JQ004 have been previously described (Lee et al. 2002; Lee et al. 2003). The *rraB* null strain JG002 was constructed using the chromosomal gene inactivation method describe by Datsenko and Wanner (Datsenko and Wanner 2000). The *rraA rraB* double null strain JG004 was constructed by transducing the allele into strain JQ004 with P1 phage.

Plasmids pDW363-RraA and pDW363-RraB encoding a biotag-RraA and biotag-RraB fusion were constructed by cloning the *rraA* or *rraB* gene into the *Xho*I-*Bam*HI site of vector pDW363 (Tsao et al. 1996). The chloramphenicol-resistant pTrc-RraA-Cm plasmid was constructed by inserting the Cm^r cassette into the Amp^r cassette of the pTrc-RraA plasmid.

β-galactosidase assay

E. coli cells transformed with pTrc-RraA or pTrc-RraB or empty vector were cultured in LB media at 37°C. When culture A_{600} reached around 0.2, IPTG was added

to the final concentration of 0.5 mM. Cells were harvested after 1.5 hours and 100 μl of the cell culture was chilled on ice for 10 minutes. Afterwards 400 μl of Z Buffer (60 mM Na_2HPO_4, 40 mM NaH_2PO_4, 10 mM KCl, 1 mM $MgSO_4$, 50 mM β-mercaptoethanol), 100 μl of $CHCl_3$ and 50 μl of 0.1% SDS were added to the sample. The mixture was vortexed vigorously for 20 seconds to completely lyse the cells. The reaction was started by addition of 200 μl of ONPG (o-Nitrophenyl-β-D-galactoside, 4 mg/ml) to the mixture. After sufficient yellow color had developed, the reaction was stopped by the addition of 250 μl of 1 M Na_2CO_3 solution and the total reaction time for each reaction was recorded. The reaction mixture was centrifuged at 13,000 rpm for 5 minutes to remove any cell debris. The optical density of the reaction at wavelength 405 nm was measured. The unit of β-galactosidase was defined as 1 Miller Unit = 1000 x A_{405} / Time (in minutes) x Volume (in milliliters) x A_{600}.

RNA work

RNase protection assays were performed in cells grown, induced and harvested as above. An aliquot was harvested 1.5 hour after induction to determine the steady state level of *rne* transcripts and the rest of the cells were treated with rifampicin at a final concentration of 200 μg/ml. Subsequently, cell samples harvested at different time points were rapidly chilled in a liquid nitrogen bath and total RNA was prepared using an RNeasy® kit (Qiagen, CA). The amount of RNA was quantified spectrophotometrically at 260 nm and RNase protection assays were carried out using the RPA III kit (Ambion, TX) with a probe containing sequence complementary to to the -359 to +33 bp region of *rne* transcript. The band intensity from each sample was quantified using the ImageQuant® software.

Table 2.1 Strains and plasmids

Strain / Plasmid	Description	Reference or Source
JCB570	MC1000, *phoR zih12*::*Tn10*	(Bardwell et al.,1991)
JQ004	JCB570, *rraA*	(Lee et al., 2003)
JG002	JCB570, *rraB*	This work
JG004	JCB570, *rraA rraB*	This work
BL21 (DE3)	F^- *ΔompT* $hsdS_B(r_B^-m_B^-)$ *gal dcm* (DE3)	Novagen
MC1061	*araD39* Δ(*ara,leu*)*7697* Δ*lacX74 galU*$^-$ *galK*$^-$ *hsr*$^-$*hsm*$^+$ *strA*	(Casadaban and Cohen, 1980)
CJ1825	MC1061, *(λez1)*	(Jain et al., 2002)
CJ1825/BZ99	MC1061, *rne(1-602) (λez1)*	C. Jain
N3433	*lacZ43, relA, spoT, thi-1*	(Goldblum and Apririon, 1981)
KSL2000	*lacZ43, relA, spoT, thi-1, rne*::*cat*, *recA*::*Tn10* [pBAD-RNE]	(Lee et al., 2002)
KSL2009	*lacZ43, relA, spoT, thi-1, rne*::*cat*, *recA*::*Tn10* [pBAD-NRNE]	(Lee et al., 2002)
AC21	MC1061, *zce-726::Tn10*	(Carpousis et al., 1994)
AC23	MC1061, *zce-726::Tn10*, *rne(ams)*	(Vanzo et al., 1998)
AC24	AC23, *rneΔ10(aaΔ844-1045)*	(Leroy et al., 2002)
AC26	AC23, *rneΔ18(aaΔ728-845)*	(Leroy et al., 2002)
AC27	AC23, *rne131*	(Leroy et al., 2002)
AC28	AC23, *rneΔ14(aaΔ636-845)*	(Leroy et al., 2002)
AC29	*AC23, rneΔ17(aaΔ636-693)*	(Leroy et al., 2002)
AC31	*AC23, rneΔ21(aaΔ603-627)*	(Leroy et al., 2002)
AC32	*AC23, rneΔ22(aaΔ603-693)*	(Leroy et al., 2002)
pBAD-stII-htPA	p15A *ori*, Cm^r, h-tPA with stII leader under PBAD	(Qiu et al., 1998)
pTrc-RraA	ColE1 ori, Amp^r, *rraA* under *trc* promoter	(Lee et al., 2003)
pTrc-RraB	ColE1 ori, Amp^r, *rraB* under *trc* promoter	This work
pTrc-RraA-Cm	ColE1 ori, Cm^r, *rraA* under *trc* promoter	This work
pDW363	pBR *ori*, Amp^r, *birA*	(Tsao et al., 1996)
pDW363-RraA	pBR *ori*, Amp^r, *birA*, *rraA-biotag* under *trc* promoter	(Lee et al., 2003)
pDW363-RraB	pBR *ori*, Amp^r, *birA*, *biotag-rraB* under *trc* promoter	This work
pDW363-DsbA	pBR *ori*, Amp^r, *birA*, *dsbA* under *trc* promoter	(Lee et al., 2003)
pBAD-RNE	pSC101 *ori*, Km^r, *rne* under PBAD	(Lee et al., 2002)
pBAD-NRNE	pSC101 *ori*, Km^r, *N-rne* under PBAD	(Lee et al., 2003)
pLAC-RNE2	pSC101 *ori*, Amp^r, *rne* under PLAC	This work
pET28A-RraA	f1 ori, Kan^r, *rraA* under T7 *lac* promoter	(Lee et al., 2003)
pET28A-RraB	f1 ori, Kan^r, *rraB* under T7 *lac* promoter	This work

Microarray procedures

Relative mRNA levels were determined by parallel two-color hybridization to DNA microarrays (Schena et al. 1995) on glass slides containing 4405 known and predicted ORFs. Comparative measurements of transcript abundance were performed by directly determining the abundance of each gene's transcript relative to the wild-type sample, described by Khodursky *et al.* (2000). Analysis of data was performed using the software available at http://genome-www5.stanford.edu/microarray/SMD and http://rana.lbl.gov.

Surface plasmon resonance analysis

Surface plasmon resonance analysis was performed at 25°C using a BIACORE® 3000 instrument (Biacore AB, Sweden). 2,500 RU each of purified RNase E and bovine serum albumin were immobilized on different flow cells of a CM5 sensor chip using amine-coupling chemistry as described by the manufacturer (BIACORE® 3000 instrument handbook, Biacore AB). Purified RraB in the concentration range between 0 and 100 μM was injected at a constant flow rate of 30 μl/min.

Pull-down assay

E. coli AC21 and derivatives were transformed with pDW363-RraA or pDW363-RraB and cultured in LB media containing 8 μg/ml of biotin (Sigma, MO) at 37 °C. Expression of biotinylated RraA or biotinylated RraB was initiated by addition of 1 mM

of IPTG when the cell culture A_{600} reached ~0.4. Three hours after induction, the cells were harvested by centrifugation at 5,000 rpm for 10 minutes and re-suspended in 1/5 volume of ice-cold NP-40 lysis buffer (150 mM sodium chloride, 1.0% NP-40, 50 mM Tris, pH 8.0). Cells were lysed by passing through a French press (2,000 psi). The lysate was centrifuged for 15 minutes at 4 ^{o}C to remove intact cells and cell debris and the protein concentration in the supernatant was determined. Aliquots containing 5 mg of protein were mixed with 100 µl of streptavidin bead slurry (Amersham Biosciences, Sweden) and the volume was adjusted to 800 µl. Following rotation at 4 ^{o}C for one hour, samples were centrifuged at 6,000 rpm for 5 minutes and the pellets were washed extensively 5 times with ice-cold NP-40 buffer. Finally, the streptavidin beads were recovered and proteins were released by boiling for 10 minutes in 2XSDS protein loading buffer (100 mM Tris-Cl [pH 6.8], 4% SDS, 200 mM β-mercaptoethanol). The presence of RNase E was analyzed by Western blotting using polyclonal anti-RNase E antiserum.

SPA purification of degradosomes

The protocol was adapted from Butland et al. (Butland et al., 2005) with modifications. One liter of *E. coli* cultures was grown in Terrific Broth (TB) at 32 °C to an A600 ~0.6. Expression of RraA or RraB was induced with 1 mM IPTG for 3 hours. Harvested cells were re-suspended in lysis buffer (10 mM Tris•Cl pH 7.9, 100 mM NaCl, 0.2 mM EDTA, 0.5 mM DTT, 10% glycerol) with Complete® protease inhibitor cocktail (Roche, IN) and lysed by French press. Cell debris was removed by centrifugation at 20,000Xg for 30 minutes. The whole cell extracts were first treated with Benzonase® nuclease (Novagen, CA) for 30 minutes and Triton X-100 was added to the final concentration of 0.1%. 100 µl of Anti-FLAG M2 agarose beads (Sigma, MO) were added

and incubated for 3 hours with rotation. After extensive washing, the beads were re-suspended in 200 µl TEV buffer (50 mM Tris•Cl pH 7.9, 100 mM NaCl, 0.2 mM EDTA, 1mM DTT, 0.1% Triton X-100) and digested with 5 µl of TEV protease overnight at 4 °C. Following digestion, 400 µl TEV buffer and 1.2 µl of 1 M CaCl2 were added to the eluate and then incubated with 50 µl calmodulin-sepharose beads (Amersham Biosciences, Sweden) for 3 hours. After incubation, 400 µl of calmodulin binding buffer (10 mM Tris•Cl, 100 mM NaCl, 2 mM CaCl2, 10 mM 2-mercaptoethanol, 0.1% Triton X-100, pH 7.9), followed by 100 µl of calmodulin wash buffer (10 mM Tris•Cl, 100 mM NaCl, 0.1 mM CaCl2, 10 mM 2-mercaptoethanol, 0.1% Triton X-100, pH 7.9) were used to wash the beads. The purified complex proteins were recovered using 300 µl of calmodulin elution buffer and analyzed by SDS-PAGE using NuPAGE® Novex 4-12% Bis-Tris gel (Invitrogen, CA). The gel was visualized by colloidal blue staining (Invitrogen, CA).

Mass spectrometry

The stained protein bands were cut out and in-gel digested with proteomic grade trypsin (Sigma, MO) at 37 °C overnight. The tryptic peptide mixtures were subjected to Q-TOF Premier® mass spectrometer (Waters, MA) and the ProteinLynx (version 2.2) software was used to analyze each dataset for protein identification.

RESULTS

Transcript-specific inhibition of the endonuclease activity of RNase E by RraB

Consistent with the notion that RraB overexpression may decrease the activity of RNase E, analysis of the β-galactosidase level expressed from a chromosomal *rne-lacZ* fusion in *E. coli* strain CJ1825 (Jain and Belasco 1995), showed a 2-3 fold increase in β-galactosidase activity following induction of RraB synthesis (Figure 2.1A). The increase in β-galactosidase activity is similar to that observed for RraA. Further analysis indicated that the observed increase in β-galactosidase activity resulted from decreased RNase E cleavage of the fusion transcript, which previously had been shown to occur in the 5' UTR segment of the *rne*-encoded segment (Mudd and Higgins 1993; Jain and Belasco 1995). The effect of RraB on the processing of the *rne* 5' UTR was statistically indistinguishable from that conferred by RraA expressed from an identical plasmid. Examination of the processing kinetics of the *rne* 5' UTR using RNase protection assays revealed that the cleavage was inhibited in cells expressing RraB with the $t_{1/2}$ increasing from 90 seconds to over 225 seconds. The steady-state abundance of *rne* mRNA was also increased under RraB overexpression condition (Figure 2.1B). Strain CJ1825/BZ99 contains a truncated version of the *rne* gene encoding a protein that consists only of the catalytic, N-terminal domain of the enzyme (amino acids 1-602) and additionally, contains the *rne-lacZ* fusion described above. Expression of RraB in this strain resulted in a modest increase in β-galactosidase activity (Figure 2.1 A).

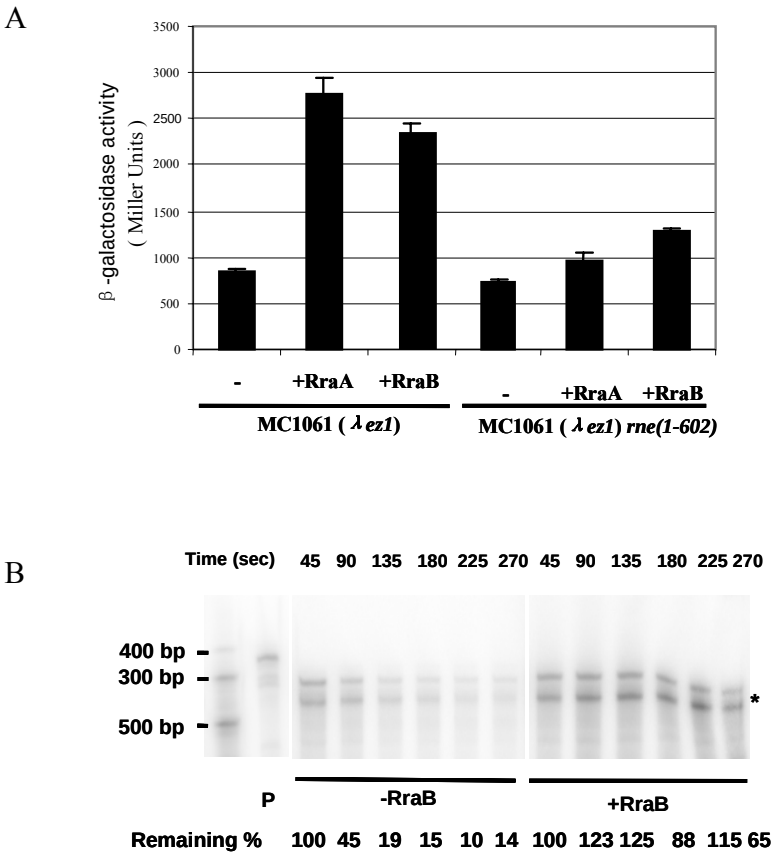

Figure. 2.1. RraB inhibits the activity of RNase E *in vivo.* (A) β-Galactosidase activity expressed from a chromosomal *rne-lacZ* fusion and measured as described in the Methods and Materials. Cells transformed with pTrc99A, pTrc-RraA or pTrc-RraB were grown in LB media and induced at A600=0.2. After 1.5 h induction, the cells were harvested and assayed for β-galactosidase activity. The result shown is the average from three independent experiments. (B) *rne* 5' UTR decay. Cells were induced with 0.5 mM IPTG and 90 minutes after induction, rifampicin was added to stop transcription. One ml aliquots were collected every 45 seconds, RNA was extracted and 5 μg of total RNA were used in RNase protection assays. The percentage of remaining *rne* 5' UTR at each time point was calculated by dividing with the signal intensity of the first lane (45 s sample). The experiment was carried out in triplicate and the variation in the t1/2 values between repetitions was <5%. P, free probe containing sequence complementary to the −360 to +33 region of *rne* transcript. Asterisks (*) indicate the position of *rne* 5' UTR transcript.

While the above results argue that RraB, like RraA, is an inhibitor of RNase E activity, examination of the steady state level of RNAs on a global scale indicated that RraA and RraB differentially affect the ability of RNase E to attack various substrate RNAs. The transcript profile of *E. coli* cells expressing either RraA or RraB was examined by microarray analysis. These experiments were performed in *E. coli* strain KSL2000 and KSL2009 in which the synthesis of RNase E and the N-terminal catalytic domain, respectively, is under the control of the arabinose promoter. In addition, the *rne* transcript produced in these two strains lacks the 5' UTR site that is subject to attack by RNase E. As a result, in strains KSL2000 and KSL2009 the level of RNase E is adjusted by the concentration of arabinose and is not subject to autocatalytic control (Lee et al. 2002).

Relative RNA levels in the presence or absence of RraA or RraB were determined by two-color hybridization to DNA microarrays containing 4,405 known and predicted *E. coli* ORFs (Blattner et al. 1997). In these experiments the effect of RraA or RraB was compared with the consequence of RNase E depletion by arabinose withdrawal (Figure 2.2A). Transcripts exhibiting the most dramatic increase (> three-fold) were individually clustered and are shown in Figure 2.2B-F.

Adventitious expression of either RraA or RraB increased the steady state level of 18% of all *E. coli* transcripts (corresponding to 792 out of 4,405 known and predicted ORFs) at least two-fold. In particular, RraA uniquely affected the abundance of 371 transcripts (8.4%), while RraB altered the steady-state level of a distinct set of 85 transcripts (1.9%). An additional 127 RNAs (2.9%) accumulated to a greater degree during adventitious expression of either RraA or RraB; however, their abundance was not affected by RNase E depletion alone. The transcription profiles of RraA or RraB expression are distinct from that of RNase E depletion alone. Thus, the microarray

analyses reveal that instead of simply acting as general inhibitors of RNase E, RraA and RraB specifically modulate RNA decay and therefore affect the intracellular levels of distinct sets of transcripts.

RraA and RraB had a marginal effect on transcript abundance in cells expressing the catalytic domain of RNase E (strain KSL2009) rather than the full-length protein (strain KSL2000) (Figure 2.2), implying that the C-terminal half of RNase E is required for these effects. Consistent with the notion that an elevated level of RraA and RraB is important for the inhibition of RNase E activity, 28 transcripts showed significantly decreased cellular levels relative to the isogenic parent in the *rraA rraB* double mutant.

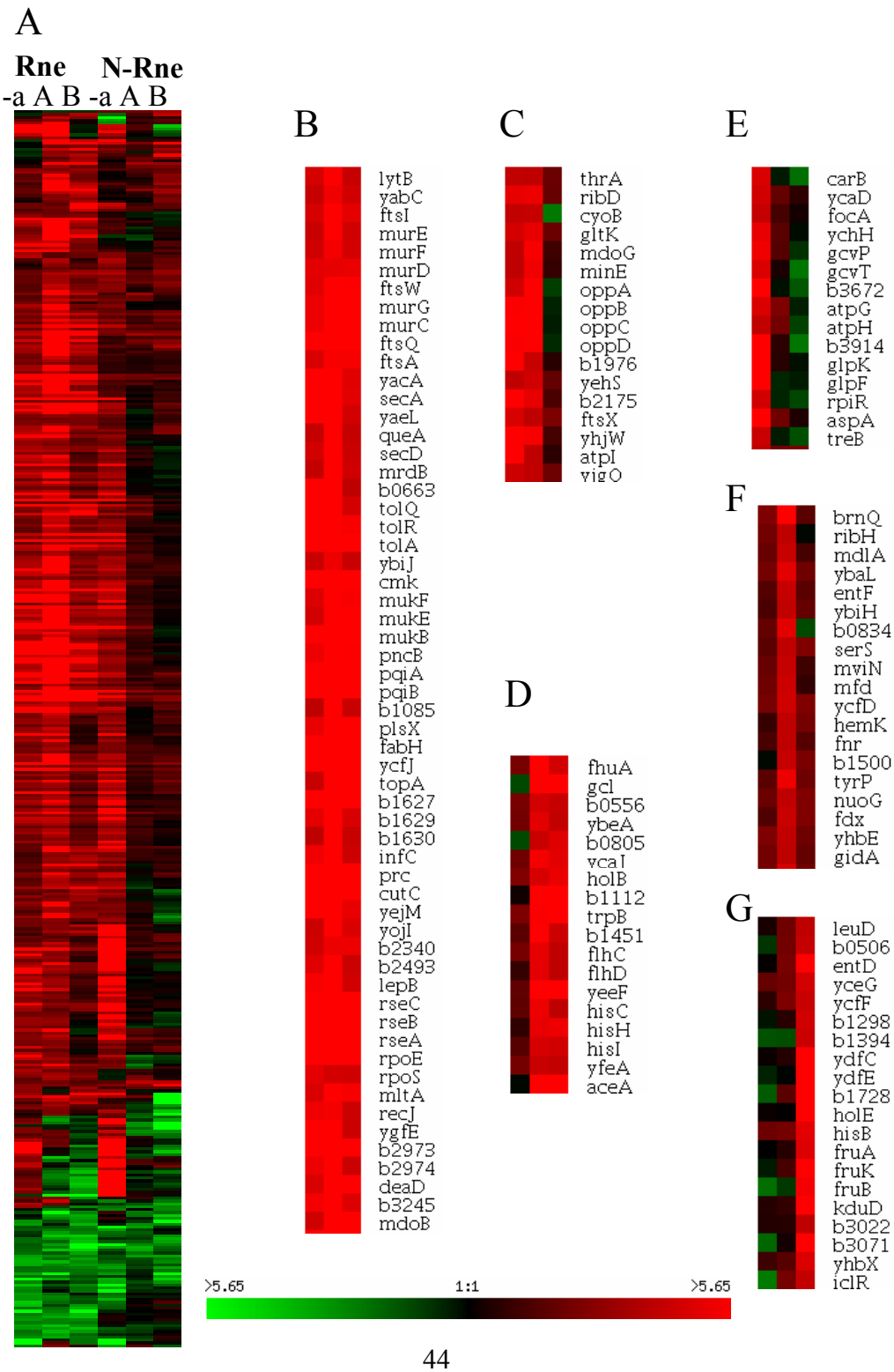
A
Rne
N-Rne
-a A B -a A B
B
lytB
yabC
ftsI
murE
murF
murD
ftsW
murG
murC
ftsQ
ftsA
yacA
secA
yaeL
queA
secD
mrdB
b0663
tolQ
tolR
tolA
ybiJ
cmk
mukF
mukE
mukB
pncB
pqiA
pqiB
b1085
plsX
fabH
ycfJ
topA
b1627
b1629
b1630
infC
prc
cutC
yejM
yojI
b2340
b2493
lepB
rseC
rseB
rseA
rpoE
rpoS
mltA
recJ
ygfE
b2973
b2974
deaD
b3245
mdoB
C
thrA
ribD
cyoB
gltK
mdoG
minE
oppA
oppB
oppC
oppD
b1976
yehS
b2175
ftsX
yhjW
atpI
vigO
D
fhuA
gcl
b0556
ybeA
b0805
ycaI
holB
b1112
trpB
b1451
flhC
flhD
yeeF
hisC
hisH
hisI
yfeA
aceA
E
carB
ycaD
focA
ychH
gcvP
gcvT
b3672
atpG
atpH
b3914
glpK
glpF
rpiR
aspA
treB
F
brnQ
ribH
mdlA
ybaL
entF
ybiH
b0834
serS
mviN
mfd
ycfD
hemK
fnr
b1500
tyrP
nuoG
fdx
yhbE
gidA
G
leuD
b0506
entD
yceG
ycfF
b1298
b1394
ydfC
ydfE
b1728
holE
hisB
fruA
fruK
fruB
kduD
b3022
b3071
yhbX
iclR
>5.65
1:1
>5.65

Figure 2.2 Effect of RraB and RraA expression on the *E. coli* transcript profile. (A) Gene clusters whose relative mRNA levels were 2-fold or more changed in at least 2 out of 4 slides. Cy-5-labeled cDNAs were synthesized with RNA samples taken from strains: −a, KSL2000 plus pTrc99A (Rne) or KSL2009 plus pTrc99A (N-Rne) followed by withdrawal of arabinose for 1.5 hours; A, KSL2000 plus pTrc-RraA or KSL2009 plus pTrc-RraA; B, KSL2000 plus pTrc-RraB or KSL2009 plus pTrc-RraB. RNA samples from KSL2000 plus pTrc99A (Rne) or KSL2009 plus pTrc99A (N-Rne) grown in the presence of 0.1% arabinose were labeled with Cy-3 and comparisons between paired cultures were done directly. (B) Cluster of genes whose transcript abundance was at least three-fold increased when RNase E is depleted or RraA is overexpressed or RraB is overexpressed in strain KSL2000. (C) Cluster of genes whose transcript abundance was at least three-fold increased when RNase E is depleted or RraA is overexpressed in strain KSL2000. (D) Cluster of genes whose transcript abundance was at least three-fold increased when RraA is overexpressed or RraB is overexpressed in strain KSL2000. (E) Cluster of genes whose transcript abundance was at least three-fold increased when RNase E is depleted in strain KSL2000. (F) Cluster of genes whose transcript abundance was at least three-fold increased when RraA is overexpressed in strain KSL2000. (G) Cluster of genes whose transcript abundance was at least three-fold increased when RraB is overexpressed in strain KSL2000.

RraA and RraB interact differently with the CTH domain of RNase E

The differential effect of RraA and RraB on the catalytic activity of RNase E suggests that the mode of interaction of the two inhibitors with the enzyme may be distinct. First, we examined the binding of purified RraB with RNase E by surface plasmon resonance analysis on a BIACORE® 3000 instrument. Binding of RraB to the purified RNase E immobilized on the CM5 chip was detected as an increase in response units (RU). An equilibrium dissociation constant (K_D) of 28.2 μM was calculated by steady state analysis (Gao et al, 2006). This value is statistically indistinguishable from the K_D of 26 μM determined earlier for the interaction of RraA with full length RNase E (Lee et al. 2003). Binding of the purified RNase E catalytic domain (amino acids 1-498) to RraB could not be detected by surface plasmon resonance.

The contribution of the various domains of RNase E to the binding of RraA or RraB was evaluated *in vivo* by co-precipitation analysis using a set of RNase E truncation mutants. Carpousis and co-workers constructed a series of isogenic strains in which the chromosomal *rne* gene was replaced by mutant alleles containing various C-terminal deletions (Leroy et al. 2002). For our analysis, RraB was fused to a 21 amino acid extension (Biotag), which encodes a peptide substrate of the *E. coli* biotin holoenzyme synthetase (Schatz 1993). While fusion of the Biotag peptide at the C-terminus destabilized the protein and gave no detectable expression, fusion at the N-terminus did not impact the steady state accumulation of RraB relative to unfused protein (data not shown). Furthermore, no significant change in solubility or localization of RraB after biotinylation was observed. Expression of the Biotag-RraB fusion protein gave the same phenotypes as unmodified RraB, including increased DsbC accumulation and higher β-galactosidase activity expressed from the chromosomal *rne-lacZ* fusion.

Biotinylated RraB synthesized in the AC series of RNase E C-terminal truncation mutants (Leroy et al. 2002) was precipitated with streptavidin beads and the presence of RNase E in the precipitate was detected by Western blot analysis using an antibody that recognizes the N-terminal domain. As expected, full-length RNase E was readily observed in the precipitate from cells expressing Biotag-RraB (Figure 2.3B, first lane). Pre-treatment of cell lysate with RNase A or Benzonase® nuclease (Novagen, WI) did not affect the co-precipitation of RNase E, indicating that nucleic acids are not involved in the ability of these two proteins to interact. No RNase E band was detected in cells expressing the Rne131 protein lacking the whole CTH (amino acids 585-1061) or in strain CJ1825/BZ99 expressing RNase E amino acids 1-602 (data not shown). Similarly,

the RneΔ14 protein lacking amino acids 636-845 was not co-precipitated with the biotinylated RraB whereas RNase E mutant proteins lacking amino acids 603-693 and 728-845 gave a clear signal. This analysis suggests that the region between amino acids 694-727 is important for the binding of RraB to RNase E.

A similar experiment was performed using an RraA-Biotag fusion and the results are presented in Figure 2.3C. Interaction between RraA and RNase E was detected for all truncation mutants except for the Rne131 protein (RneΔ585-1061). It has been shown that RraA at a large molar excess inhibits the catalytic activity of the RNase E NTH *in vitro* but the interaction between the two proteins is weak and shows a K_D in excess of 200 uM (Lee et al. 2003). Thus, while it appears that RraA requires the C-terminal half of RNase E for high affinity binding, we could not map the interaction of the two proteins to a single contiguous epitope. This is in contrast to RraB and all the major degradosome components which bind to defined continuous epitopes in the CTH.

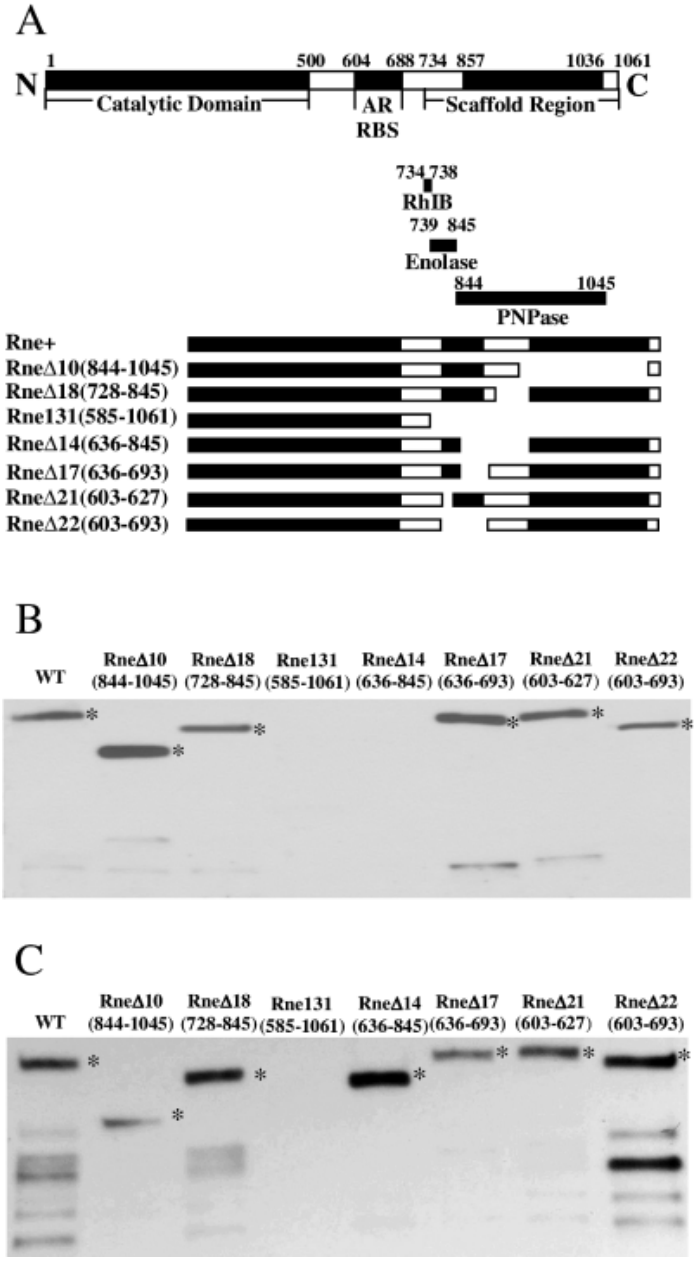

Figure 2.3 Mapping the binding site of RraB and RraA on RNase E by co-precipitation analysis. (A) Schematic illustration of the structure of wild-type and truncated RNase E, adapted from Vanzo et al. 1998 and Leory et al. 2002. (B) Western blot analysis of proteins co-precipitated with in vivo synthesized Biotag-RraB. The same amount of cell lysate protein was used in each co-precipitation. Asterisks (*) indicate the expected electrophoretic migration of the RNase E truncated mutant proteins in the absence of proteolytic degradation. WT, wild-type. (C) The same as above except that RraA-Biotag was used for the co-precipitation analysis.

Consistent with their distinctive interaction pattern with RNase E, RraA and RraB demonstrated different inhibitory effects on partially purified full-length RNase E or on the catalytic domain. p23 RNA is a truncated pM1 RNA that is processed by RNase E to a product termed 23 RNA (Kim et al. 1996). Addition of RraA *in vitro* resulted in a greater degree of inhibition than RraB throughout the concentration range tested. For example, at a 40-fold excess of inhibitor protein/RNase E, RraB resulted in 23% inhibition of p23 RNA processing over the control, whereas RraA inhibited processing by 45%. RraB did not inhibit the processing of p23 by the purified N-terminal domain of RNase E. In contrast, RraA inhibited the processing of p23 by the N-terminal domain, albeit to a lesser extent than what was observed for the full-length protein (Figure 2.4).

Binding of RraA and RraB affects the degradosome composition

The fact that RraA and RraB interact with the scaffold region of RNase E at different locations led us to speculate that these two inhibitors might differentially affect the binding of other proteins to the CTH. To address this question, we took advantage of a recently developed affinity purification system for the analysis of protein complexes in *E. coli* (Butland et al. 2005). In strain DY330 *rne-SPA,* the chromosomal *rne* gene had been fused to a DNA cassette that encodes a carboxyl-terminal sequential peptide affinity (SPA) tag. The SPA tag is composed of a 3×FLAG tag and a calmodulin-binding peptide (CBP) separated by a tobacco etch virus (TEV) protease cleavage site. The tagged RNase E was used as the bait to purify its interacting proteins by sequential

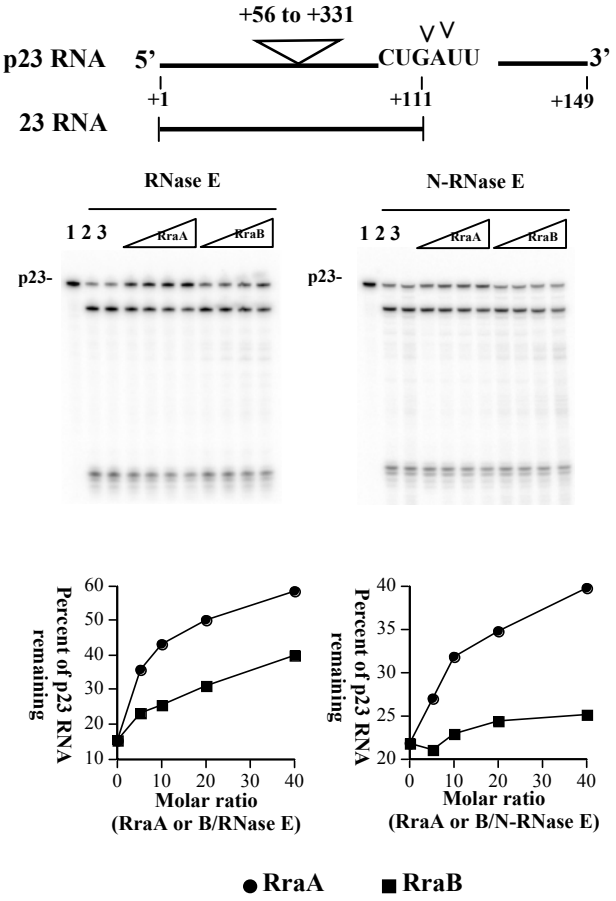

Figure 2.4 RraB inhibits the *in vitro* cleavage of p23 RNA. Two picomoles of internally labeled p23 RNA were incubated with BSA only (**1**), RNase E or N-RNase E only (**2**, **3**), or 100 ng of RNase E or 200 ng of N-RNase E with varying concentrations of RraA or RraB in 20 µl of 1×cleavage buffer at 37°C for 30 minutes for RNase E, or for 90 minutes for N-RNase E or BSA only controls. The percentage of uncleaved p23 RNA in the gel was quantitated using a Molecular Dynamics Phosphoimager and plotted as a function of the molar ratio of RraA/RNase E or RraB/RNase E in the assay.

affinity purification. The integrity and expression level of RNase E in the tagged strain are not affected, as judged by Western blot analysis (data not shown).

The components of purified degradosomes were resolved by SDS-PAGE and visualized by colloidal blue staining (Figure 2.5). To compare the relative abundance of individual degradosome components, protein samples loaded on each lane were normalized to the same amount of RNase E. The region of gel containing each of the detected bands was individually excised, proteolytically digested, and subjected to mass spectrometry analysis. As seen in Figure 2.5, overexpression of RraA or RraB had a dramatic effect on the degradosome composition, most strikingly on the abundance of RNase E-bound PNPase. In degradosomes purified from control cells without RraA or RraB overexpression, the molar ratios of the major protein components to RNase E were as follows: PNPase, 5.4; RhlB, 2; enolase, 1.3. For clarity, all the above ratios were calculated based on relative polypeptide amounts without taking into account the oligomeric states of the respective proteins. The relative abundance we determined for these degradosome components in our experiments is comparable to those reported earlier by others (Py et al. 1996; Coburn et al. 1999). By contrast, in degradosomes isolated from cells expressing RraA, the ratios of PNPase, RhlB, and enolase to RNase E were substantially lower, namely 0.7, 0.3, and 0.1, respectively. Similarly, in cells expressing RraB the ratios of RNase E-bound PNPase, RhlB, and enolase dropped to 1.1, 0.9, and 0.6, respectively. Interestingly, RNase E from cells expressing RraA was found associated with markedly less RhlB compared to cells expressing RraB (RhlB to RNase E ratio of 0.3 vs. 0.9). It is also noteworthy that expression of RraB, but not RraA, resulted in a moderate increase in RNase E-associated amounts of two non-stoichiometric components of degradosomes: DnaK and CsdA (DeaD).

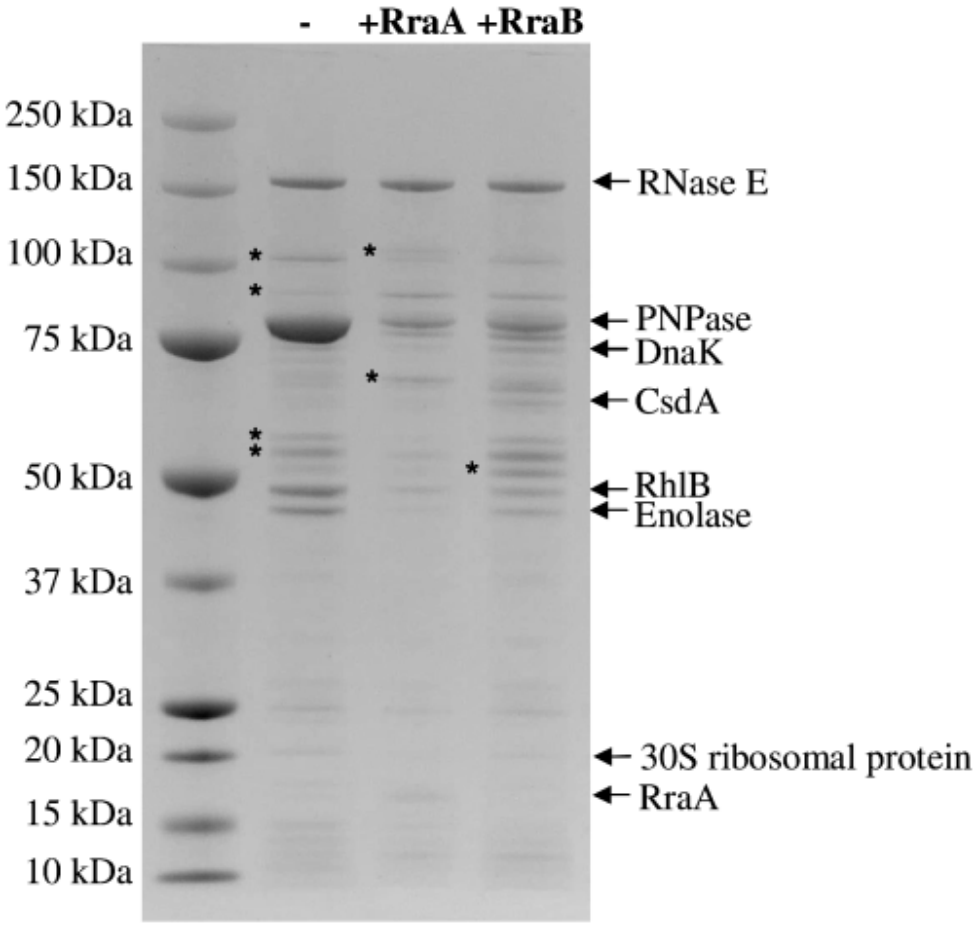

Figure 2.5 RraA and RraB differently affect the composition of degradosomes. Purified degradosomes with and without overproduction of RraA or RraB were separated by SDS-PAGE and visualized by colloidal blue staining. The identities of protein bands were confirmed by mass spectrometry. Bands denoted with an asterisk correspond to RNase E degradation products.

DISCUSSION

Both RraA and RraB were isolated genetically as a result of their ability to facilitate disulfide bond isomerization in the periplasmic space of *E. coli.* In a manner similar to RraA, RraB stabilized the *dsbC* transcript and resulted in accumulation of the disulfide isomerase, DsbC. RraB, like RraA, inhibited endoribonucleolytic cleavage of the 5' UTR of *rne* transcripts strongly enough to circumvent the autoregulation of *rne* that normally maintains the level of the enzyme within a narrow range (Figure 2.1). Genome-wide analysis of mRNA abundance by DNA microarrays revealed that the abundance of 18% of all *E. coli* transcripts (corresponding to 792 out of 4,405 known and predicted ORFs, excluding small RNAs, Figure 2) were affected by 2-fold or more when either RraA or RraB is expressed. Strikingly, however, not all RNAs were affected equally by both inhibitors. Global analysis of steady state level of mRNA revealed that while a large set of transcripts was affected similarly by either inhibitor protein, other equally large sets of transcripts were stabilized exclusively by RraA or by RraB. In particular, 336 transcripts corresponding to 7.6% of the transcriptome were stabilized equally by either protein inhibitor, 371 transcripts (8.4%) were affected uniquely by the expression of RraA and 85 transcripts (1.9%) were stabilized only by RraB. These results clearly demonstrate that the two inhibitor proteins exert a differential effect on the ability of RNA processing machinery to cleave various mRNAs, in turn giving rise to distinct transcript profiles.

Neither the crystal structure of RraA (Monzingo et al. 2003) nor the solution structure of the *Vibrio cholerae* RraB homologue, VC0424, contain putative nucleotide binding sites (Ramelot et al. 2003). Not surprisingly, RraA and RraB do not appear to interact directly with substrate RNAs (Lee et al. 2003). Instead, inhibition of RNA

cleavage results from the direct interaction of the two proteins with RNase E. RraA and RraB exhibit nearly identical affinities for RNase E, with K_D values determined by surface plasmon resonance spectroscopy in the micromolar range. Similar weak binding affinities have been measured for other proteins that modulate the specificity of macromolecular machines. Examples include the binding of the adaptor protein SspB with ClpX (Wah et al. 2002) and the interaction between the active forms of ClpB and DnaK (K_D= 17 mM) (Schlee et al. 2004).

Co-precipitation analysis using a set of RNase E mutants containing deletions in the CTH (Leroy et al. 2002) revealed that RraA and RraB interact with the enzyme in distinct ways. Even though RraA and RraB have a low pI they do not bind to the positively charged arginine-rich motif of RNase E (amino acids 604 to 688). Amino acids 694-727 were required for the binding of RraB to RNase E, similar to the major degradosome components which bind to specific, continuous regions within the CTH (Py et al. 1994; Miczak et al. 1996; Py et al. 1996; Vanzo et al. 1998; Coburn et al. 1999). This region partially overlaps a stretch of amino acids extending from position 685 to 712 which is predicted to form half of a putative coiled-coil that may be important for binding of the enzyme to structured RNAs (Callaghan et al. 2004). As expected, the endonucleolytic activity of the N-terminal catalytic domain which lacks the CTH region was unaffected by RraB, even when present at a large stoichiometric excess. In contrast, RraA inhibited the endonuclease activity of the N-terminal catalytic domain *in vitro*, albeit more weakly compared to the inhibition of the full length RNase E. Although this inhibitory effect strongly suggests a physical interaction between the two proteins, we could not detect the formation of a protein complex using surface plasmon resonance analysis, presumably because of the low binding affinity.

On the basis of these results we propose that the distinct mode of interaction of the two inhibitor proteins with RNase E is responsible for the selective stabilization of different sets of transcripts. The selective stabilization of some transcripts but not others is likely to be related to the way in which RraA and RraB mediate the remodeling of the degradosome. The two inhibitors had a similar effect on the amount of some degradosome components but reduced the level of other components in a distinct manner that was specific to each of the two proteins. *E. coli* degradosomes contain an excess of PNPase per RNase E polypeptide chain (Py et al. 1996; Coburn et al. 1999). However, in degradosomes isolated from cells expressing RraA or RraB, PNPase and RNase E were present in nearly equal amounts. On the other hand, RraA reduced the amount of RhlB and enolase associated with RNase E by 7-fold and 13-fold respectively, whereas RraB led to only a 2-fold reduction for both degradosome components. As a result of these effects, the stoichiometry of PNPase to RhlB and enolase bound to RNase E is different for control *E. coli*, for cells expressing RraA and for cells expressing RraB. Recently, Lin-Chao and coworker (2005) reported that PNPase and the RhlB helicase form an RNA-degrading complex independently of the attachment of both proteins to RNase E. By changing the composition of the degradosome, RraA and RraB may also be exerting an indirect effect on the amount of free, i.e. not RNase E-bound, PNPase and RhlB, in turn affecting other RNA degrading complexes.

In addition to changes in the amount of PNPase, RhlB, and enolase bound to RNase E, RraB gave rise to degradosomes that contained the non-canonical components DnaK and CsdA. Such an effect was not observed in degradosomes isolated from cells expressing RraA. The chaperone protein DnaK, which normally is present in degradosomes in small amounts (Miczak et al. 1996), has been found to increase significantly under certain stress conditions such as low temperature, RNase E

overexpression, or in cells lacking PNPase (Regonesi et al. 2005). CsdA was previously found associated with the RNA degradation machinery only under cold-shock conditions (Prud'homme-Genereux et al. 2004).

Comparison of the microarray data reported here with the genomic scale RNA stability data of Bernstein et al. (Bernstein et al. 2002) did not reveal any substantial difference between the $t_{1/2}$ of transcripts that are affected by RraA and those affected by RraB. We also failed to identify a pattern in the length or in the function of the 371 RraA-specific or the 85 RraB-specific transcripts. Therefore more complex factors, possibly related to secondary structure considerations, might determine whether a particular RNA is stabilized through the action of RraA or RraB. While homologues of RraA are widely distributed among archea, proteobacteria and plants, RraB homologues are found only in γ-proteobacteria—suggesting that these proteins may have a more specialized role in modulating RNA degradation. The existence of two proteins that exert a differential effect on RNA decay via their interactions with RNase E and degradosome remodeling argues that modulation of RNA stability may be a mechanism for global control of transcript abundance in response to dynamic changes in the extracellular or intracellular environment.

Chapter 3: Reconstitution of Degradosomes and Kinetic Analysis of RNA Degradation *in vitro*

INTRODUCTION

RNase E functions as the core component of a multiprotein complex termed the RNA degradosome. The degradosome is a 500-700 KDa complex formed by the assembly of the exoribonuclease polynucleotide phosphorylase (PNPase), the DEAD-box RNA helicase RhlB, and the glycolytic pathway enzyme, enolase, onto the CTH of the RNase E protein. Several other proteins including the protein chaperones GroEL and DnaK may also be present in sub-stoichiometric amounts. The overall significance of the degradosome has been established by recent studies, however, the details regarding how the individual components cooperate in carrying out RNA degradation and how changes in the degradosome composition affect the decay of different transcripts remains to be discovered.

As described in Chapter 2, the Georgiou laboratory recently discovered a novel mechanism whereby the distinct, inhibitor-specific remodeling of the degradosome, by RraA or RraB, is associated with the selective alteration of the steady state level of different transcripts in *E. coli*. Nevertheless, little is known regarding the molecular details of this mechanism and its importance in gene regulation. For example, is the stabilization of transcripts due to the direct inhibitory effect of RraA/RraB on the endonucleolytic activity of RNase E or is it due to the degradosome remodeling? Why are certain transcripts stabilized by RraA, others by RraB and yet a third class is not stabilized by either inhibitor? How does the binding of RraA or RraB and the resulting

changes in degradosome composition affect the detailed kinetics of hydrolysis of different RNAs?

To answer these questions, we sought to develop a system for the reconstitution of degradosomes and determine the consequences of RraA and RraB binding to the kinetics of RNA degradation *in vitro*. This will allow us to carry out a systematic analysis of the contribution of: 1) the sequence and structure of the RNA substrate, including the importance of the phosphorylation status at the 5' end, 2) the effect of the different domains within the CTH of RNase E, and 3) the effects of minor degradosome components.

The purpose of the studies described in this chapter was to produce purified proteins for subsequent reconstitution experiments. Unfortunately, the 1061 aa RNase E that forms the core of the degradosome is very susceptible to proteolytic degradation during purification. To date, there has not been any evidence that the full length RNase E can be purified in any significant amounts. A recent biophysical study suggests the CTH of RNase E is mainly unstructured and highly susceptible to degradation, which accounts for the low yield of the intact protein (Callaghan et al. 2004). To overcome this problem, we made a series of C-terminal truncated forms of RNase E, which contain the binding sites for the degradosome components RhlB and enolase and part of the epitope recognized by PNPase, as well as the binding sites for RraA and RraB. In this study, we show that the C-terminal truncated forms of RNase E are amenable to preparative expression and purification. In addition to truncated RNase E, we also purified individual degradosome components (PNPase, RhlB and enolase). Using this truncated RNase E and purified degradosome components, we can now pursue the reconstitution of RNA degrading complexes containing at least some of the components of the intact degradosome.

Previous studies of RNA hydrolysis by RNase E have been based on limited kinetic data under conditions that have not been rigorously defined. With this in mind, we have adopted the fluorescence resonance energy transfer (FRET) methodology, originally described by Belasco's group (Jiang and Belasco 2004), that allows the determination of the kinetic parameters in RNA cleavage in a continuous, real-time fashion. We have optimized the reaction condition for truncated forms of RNase E and determined the Michaelis-Menten parameters for these enzymes. A pilot study on the consequences of RraA/RraB binding to the kinetics of RNA degradation *in vitro* is also presented here.

Dr. Junjun Gao assisted in making the C-terminal truncated RNase E constructs.

MATERIALS AND METHODS

Strains and plasmids

The strains and plasmids used in this work are listed in Table 3.1. The C-terminal truncated RNase E expression plasmids, pET28a- *Rne*752-His, pET28a-*Rne*845-His, and pET28a-*Rne*1045-His were constructed as follows. Different fragments of the *rne* gene were PCR amplified from the *E. coli* genome using the primers: *Rne*-NTH-up, *Rne*-752-Dn, *Rne*-845-Dn and *Rne*-1045-Dn. The PCR products were digested with BsaI / XhoI and cloned into the commercial expression plasmid pET28a (Novagen, WI), which had been linearized with NcoI/XhoI. The constructs encode for C-terminal hexa-histidine tagged truncated versions of RNase E. To facilitate the purification of individual degradosome components, the individual genes, either *pnp*, *rhlB*, or *eno*, with a DNA

cassette that encodes a carboxy-terminal SPA tag (Butland et al. 2005), were PCR amplified from the *E. coli* genome. The PCR products were digested with NdeI and HindIII and moved into the pET21a expression vector (Novagen, WI), which had been linearized with NdeI/HindIII.

Table 3.1 Strains and plasmids

Strain / Plasmid	Description	Reference or Source
JCB570	MC1000, *phoR zih12*::*Tn10*	(Bardwell et al.,1991)
N3433	*lacZ43, relA, spoT, thi-1*	(Goldblum and Apririon, 1981)
BL21 (DE3)	F^- *ΔompT* $hsdS_B(r_B^-m_B^-)$ *gal dcm* (DE3)	Novagen
MC1061	*araD39* Δ(*ara,leu*)*7697* Δ*lacX74 galU*$^-$ *galK*$^-$ *hsr*$^-$*hsm*$^+$ *strA*	(Casadaban and Cohen, 1980)
KSL2002	N3433*, rne*::*cat*, *recA*::*Tn10* [pN*RNE*5]	(Lee et al., 2002)
pET28a- *Rne*752-His	f1 ori, Kan^r, *rne*752 under T7 *lac* promoter	This work
pET28a-*Rne*845-His	f1 ori, Kan^r, *rne*845 under T7 *lac* promoter	This work
pET28a-*Rne*1045-His	f1 ori, Kan^r, *rne*1045 under T7 *lac* promoter	This work
pN*RNE*5	pSC101 *ori*, Ap^r, *N-rne* under PlacUV5	(Lee et al., 2002)
pET28a-RraA	f1 ori, Kan^r, *rraA* under T7 *lac* promoter	(Lee et al., 2003)
pET-RraB-His-28a	f1 ori, Kan^r, *rraB* under T7 *lac* promoter	(Qiu, 2001)
DY330	W3110, Δ*lacU169 gal490 λc1857 Δ(cro-bioA)*	(Zeghouf et al.,2004)
pET21a-Pnp-SPA	f1 ori, Amp^r, Pnp-SPA under T7 *lac* promoter	This work
pET21a-RhlB-SPA	f1 ori, Amp^r, RhlB-SPA under T7 *lac* promoter	This work
pET21a-Eno-SPA	f1 ori, Amp^r, Eno-SPA under T7 *lac* promoter	This work

Expression and purification of truncated versions of RNase E

The carboxy-terminally his_6 tagged, truncated form of RNase E lacking the C-terminal 562 residues, i.e. N-RNase E (RNase E 1-499aa), was purified from KSL2002 expressing the N-terminal catalytic domain of RNase E from the plasmid pN*RNE*5. Cells were grown to mid-log phase, induced with 1 mM IPTG for 3 hrs and harvested by centrifugation. The N-terminal catalytic domain of RNase E was purified under native conditions by nickel-nitrilotriacetic acid (Ni-NTA) metal-affinity chromatography with modifications, as suggested by the vendor (Qiagen, Valencia, CA). Briefly, the cell pellet was washed and re-suspended in ice-cold native lysis buffer (50 mM NaH_2PO_4, 500 mM NaCl, 10 mM Imidizole, 0.1%TritonX-100, pH 8.0) with Complete® protease inhibitor cocktail (Roche, IN) at the manufacturer's suggested working concentration. Cells were lysed by passing through a French press (2,000 psi). The lysate was centrifuged for 15 minutes at 4 ^oC to remove intact cells and cell debris and the supernatant was clarified by syringe filtration [with a Whatman 0.45-µm poly(vinylidene difluoride) filter disk]. 4ml cell lysate supernatant was combined with 1 ml of Ni-nitrilotriacetic acid resin, and gently agitated for 1hr at 4°C. The resin was separated by gravity filtration and washed with five volumes of lysis buffer, and the tagged protein was eluted with a step gradient of imidizole (60mM, 80, 100, 120, 150mM) in lysis buffer. The elution of protein peaked at 120 mM imidazole. The protein in the peak was concentrated using an Amicon Ultra concentrator (Millipore, MA) and dialyzed against the RNase E storage buffer (pH 7.5, 50 mM Tris-HCl, 1 mM EDTA, 500 M NaCl, 20 % (v/v) glycerol, 0.5% TritonX-100, and 1 mM dithiothreitol). All steps were performed at 4^oC.

The *E. coli* BL21(DE3) cells hosting C-terminal truncated RNase E expression plasmids (other than the 1-499 aa protein whose purification is described above) were

grown in Terrific Broth (TB) media at 25˚C until the O.D. reached 0.5. IPTG was added to a final concentration of 1 mM, and cells were harvested after three hours of induction. Protein purifications were conducted under denaturing conditions and all steps were performed at room temperature. Briefly, cell pellets were re-suspended in freshly made denaturing lysis buffer A (100 mM NaH_2PO_4, 10 mM Tris·Cl, 8M urea, pH 8.0) (due to the dissociation of urea, the buffer pH was adjusted immediately prior to use) with Complete® protease inhibitor cocktail (Roche, IN) at the manufacturer's suggested working concentration. After lysis by French press at 2,000 psi, insoluble material was removed by centrifugation at 15,000 rpm for 45 min at 4°C. The supernatant was clarified by syringe filtration [with a Whatman 0.45-μm poly(vinylidene difluoride) filter disk], combined with 1 ml of Ni-nitrilotriacetic acid resin, and gently agitated for 45 min at 25°C. The resin was separated by gravity filtration and washed twice with 4 ml buffer C (100 mM NaH_2PO_4, 10 mM Tris·Cl, 8M urea, pH 6.3). Elution was carried out by washing 4 times, each time with 0.5 ml of buffer D (100 mM NaH_2PO_4, 10 mM Tris·Cl, 8M urea, pH 5.9), followed by another 4 washes, each with 0.5 ml of buffer E (100 mM NaH_2PO_4, 10 mM Tris·Cl, 8M urea, pH 4.5). The eluted proteins were concentrated using an Amicon Ultra concentrator (Millipore, MA) and the purity of each collected fraction was examined by SDS-PAGE. Only the fractions containing purified target proteins were pooled and refolded by dialyzing against the RNase E storage buffer (pH 7.5, 50 mM Tris-HCl, 1 mM EDTA, 500 M NaCl, 20 % (v/v) glycerol, 0.5% TritonX-100, and 1 mM dithiothreitol) overnight at 4^{o}C. The final protein concentration was determined by the Bradford assay (Bio-Rad Laboratories, Hercules, CA).

Production and purification of RraA, RraB, PNPase, RhlB and Enolase

RraA was expressed from BL21(DE3) transformed with pET28a-RraA expression vector and purified by ion exchange chromatography on a Mono Q® HR 5/5 anion exchange column. The eluted protein was concentrated by Centricon® YM-3 Centrifugal Filter Devices (Millipore, MA).

RraB was purified from BL21 (DE3) harboring plasmid pET-RraB-His-28a, which expresses RraB with a C-terminal his_6 tag, following the protocol suggested by the vendor of the Ni-NTA metal-affinity chromatography resin (Qiagen).

The C-terminal SPA tagged PNPase, RhlB or Enolase (Butland et al. 2005) were purified from the BL21 (DE3) strain transformed with pET21a-Pnp-SPA, pET21a-RhlB-SPA, or pET21a-Eno-SPA expression vector using anti-FLAG M2 beads and following the procedures outlined in the FLAG-tag immunoaffinity purification manual (Sigma).

RNA cleavage assay

The fluorogenic oligonucleotide P-BR14-FD was synthesized and HPLC-purified by TriLink (San Diego, CA). RNA cleavage was carried out at 25°C in RNase E cleavage buffer (pH 7.5, 20 mM Tris-HCl, 100 mM NaCl, 15mM $MgCl_2$, 5 % (v/v) glycerol, 0.1% TritonX-100, and 1 mM dithiothreitol). To establish the optimum level of $MgCl_2$, the concentration was varied from 0 to 150 mM. To measure the kinetics of hydrolysis of the fluorogenic substrate, various concentrations of P-BR14-FD were combined with a limiting amount of N-RNase E or RNase E845 (50nM) in a total volume of 50 μl. Measurements of initial rates were taken on a Synergy HT fluorescent plate reader (Bio-Tek, Burlington, VT) using a 485/20 excitation filter and a 516/20 emission filter. P-

BR14-FD substrate concentrations were varied from 0.05 to 5 μM (50 nM N-RNase E or RNase E 845); The PRISM 4 software (GraphPad, San Diego) was used for determination of V*max* and K_m values. The cleavage reactions were also monitored discontinuously by gel electrophoresis. Reaction mixtures were incubated at 25 °C, and aliquots were taken at appropriate time points. Samples were quenched by mixing aliquots with an equal volume of 20 mM EDTA and were analyzed by gel electrophoresis. This was followed by analysis with a Molecular Dynamics Fluor Imager.

To examine the effects of RraA/RraB on the *in vitro* hydrolysis of P-BR14-FD, 200 nM N-RNase E or RNase E845 and various amounts (0, 50, 100, 200, 400, and 1000-fold stoichiometric excess) of RraA or RraB were mixed in 1xRNA cleavage buffer and preincubated at 37°C for 10 minutes; the reaction was started by adding the RNA substrate P-BR14-FD at serial concentrations (0.1, 0.2, 0.5, 1, 2,5,10, 20 μM). This preincubation was necessary to obtain reproducible FRET kinetic data as well as maximal inhibition by these inhibitors. Longer preincubation was not performed because the enzymatic activity of RNase E started decreasing. The reaction was performed at 37°C. PRISM4 software (GraphPad, San Diego) was used for determination of kinetic parameter values.

RESULTS

Purification of C-terminal truncated RNase E

The full-length RNase E is highly unstable to degradation once the cells are lysed. Therefore, initial attempts at purification of the full-length RNase E under native conditions were unsuccessful largely. Even though a protease inhibitor cocktail was added prior to cell lysis and all steps were performed at 4˚C, the yield of full-length protein was negligible and the intact protein was barely detectable by Western bloting.

Since the preparative production of full length RNase E did not appear feasible in our hands, we elected to study four C-terminal truncated RNase E expression constructs. The plasmid pNRNE5 encodes a polypeptide (RNase E 499, i.e.N-RNase E) lacking the CTH, which has been employed previously for investigation of substrate specificity, mode of action, and inhibition by RraA/RraB. The other three longer truncated RNase E proteins contain binding sites for RraA, RraB and at least some of the degradosome components of interest (Figure3.1 A). The plasmid pET28a- *Rne*752-His encodes a polypeptide (RNase E 752) consisting of residues 1-752 of RNase E, which includes the RhlB and RraB binding sites. The plasmid pET28a-*Rne*845-His encodes a polypeptide (RNase E 845) which contains the residues 1-845 of RNase E and thus contains, the enolase binding epitope, in addition to those for RhlB and RraB. Finally, the plasmid pET28a-*Rne*1045-His expresses a polypeptide (RNase E1045) that covers nearly the full-length RNase E except the last 16 residues, which are potentially responsible for high-affinity binding of RraA. With the exception of the 1045 aa fragment of RNAse E the other three proteins could be expressed as fusions containing a C-terminal His_6 tag host. N-RNase E was purified to near homogeneity by Ni-NTA affinity chromatography under native condition using a step gradient of imidizole. About 600μg N-RNase E protein was obtained per liter per O.D. cell culture.

A

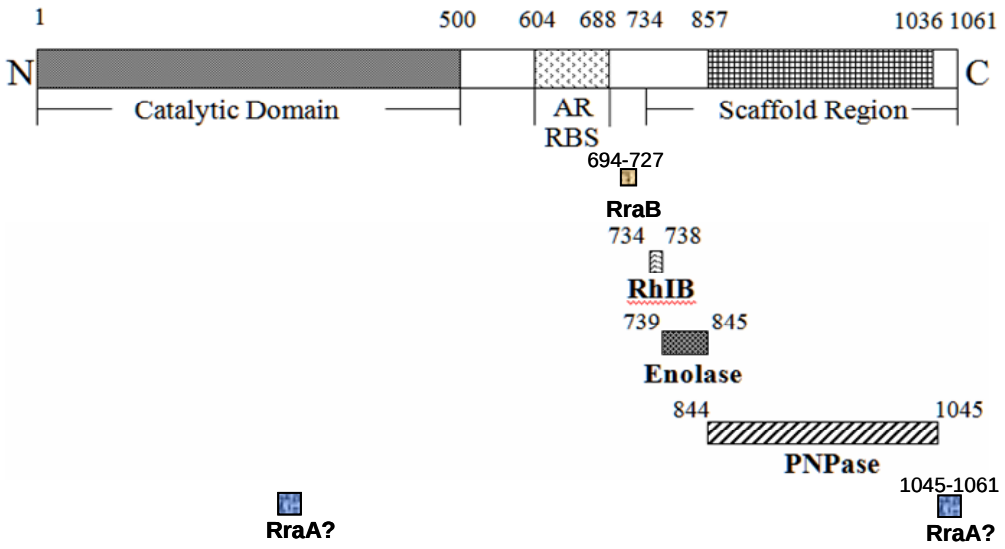

B

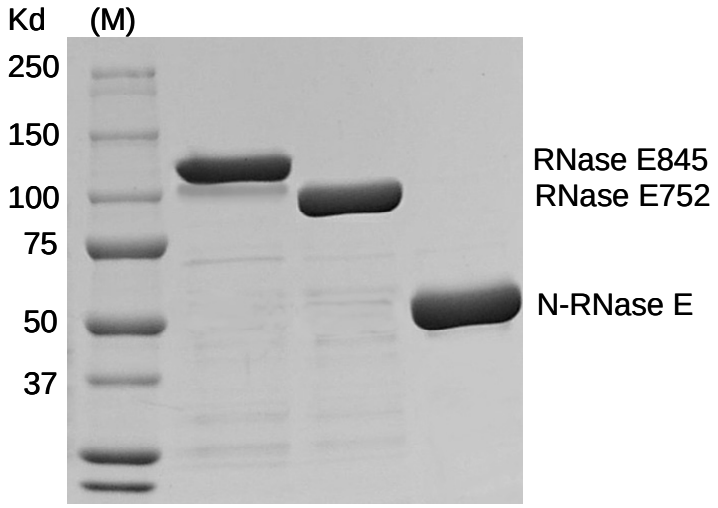

Figure 3.1 (A) Schematic illustration of the structure of full-length RNase E and the binding sites for RraA, RraB and the major degradosome components (see Chapter 3, also Vanzo et al 1998). (B) GelCode Blue Staining of the purified RNase E proteins. N-RNase E was purified under native conditions. RNase E 752 and RNase E 845 were purified under denaturing conditions.

For the other three truncated RNase E proteins, Ni-NTA affinity chromatography was carried out under denaturing conditions, i.e. in the presence of 8 M urea, to minimize proteolysis. Following purification, the denatured RNaseE proteins were refolded under optimized conditions. Unfortunately, the purification of RNase E1045 and full-length RNase E failed. This is presumably because the CTH is largely unstructured and therefore highly susceptible to proteolysis. The high susceptibility of the CTH domain to protease degradation cannot be completely overcome even under denaturing conditions.

RNase E752 and RNase E845 were successfully purified to near homogeneity (Figure 3.1 B). A yield of about 400 μg RNase E752 protein and 180 μg RNase E845 protein was obtained per liter per O.D. cell culture following the procedure described in the Materials and Methods section. The refolded proteins were active, as seen by their ability to cleave the FRET RNA substrate (P-BR14-FD). The specific cleavage was monitored continuously by fluorometry (excitation at 485 nm; emission at 516 nm) and discontinuously by gel electrophoresis of samples quenched at time intervals (Figure 3.2 B, C).

Determination of the kinetic parameters of RNase E

To determine the kinetic parameters for RNase E and the consequences of RraA and RraB binding on the kinetics of RNA degradation *in vitro,* we adopted the synthetic fluorogenic RNA substrate reported earlier by Jiang *et al.* (Jiang and Belasco 2004). This 14 nucleotide RNA substrate (P-BR14-FD; Figure 3.2 A) contains a sequence resembling the 5'-terminal segment of pBR322 RNA I, an untranslated regulatory RNA that bears a single major RNase E cleavage site. The key features of the synthetic substrate are a

fluorescein dye upstream of the expected RNase E cleavage site and a fluorescence-quenching dabcyl group downstream of the cleavage site, which quenches most of the fluorescein fluorescence in the uncleaved RNA. Five of the nucleotides upstream of the cleavage site were 2'-O-methylated to protect them from RNase E digestion. The extent of RNase E cleavage can be detected by the increase in fluorescence due to release of the dabcyl upon cleavage. The fluorogenic oligonucleotide was synthesized with a monophosphate group at the 5'-terminus (P-BR14-FD) which is cleaved much faster by RNase E than the corresponding primary transcripts with the terminal 5'-triphosphate group.

First, the reaction conditions for cleavage by N-RNaseE, which comprises of the catalytic N-terminal half of the protein (residues 1–499), were optimized using a stepwise approach. The optimum concentration of Mg^{2+} in a buffer containing 100 mM NaCl was found to be between 10 and 20 mM, with the highest cleavage rate obtained with 15 mM Mg^{2+}. The effect of salt on the rate of RNA hydrolysis by RNaseE was also investigated in a buffer containing 15 mM Mg^{2+}, and the optimum concentration was found to be 100 mM NaCl. The maximal rate of RNA hydrolysis was achieved under these conditions. Upon cleavage of P-BR14-FD by N-RNase E, there is an increase in fluorescence at 517 nm due to the release of the dabcyl group. To confirm that the increase in fluorescence accurately reflects the extent of RNA cleavage, digestion of P-BR14-FD by N-RNase E, RNase E752, and RNase E845 was monitored by both fluorometry and gel electrophoresis. The time course of cleavage reactions performed under the same reaction conditions was very similar when measured by either of these assays (Figure 3.2 B, C). As expected, the initial cleavage rates were dependent on the enzyme concentration and showed saturation at high substrate concentrations.

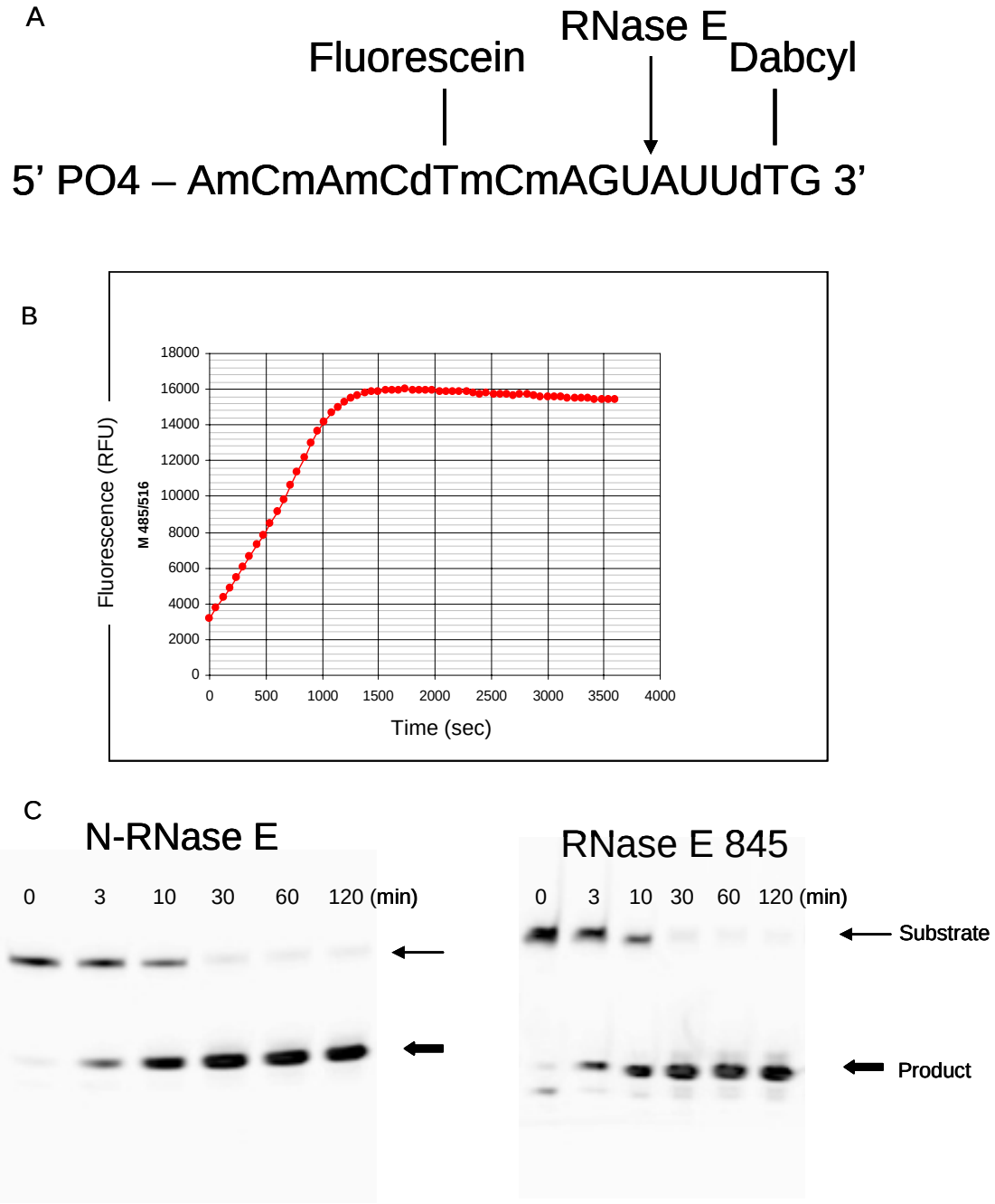

Figure 3.2 (A) Sequence of the fluorogenic oligonucleotide substrate, P-BR14-FD (modified from Jiang and Belasco, 2004). (B) Continuous fluorometric assay of P-BR14-FD (1 µM) cleavage by N-RNase E (50 nM). (C) Discontinuous electrophoretic assays comparing the cleavage of P-BR14-FD cleavage by N-RNase E and RNase E 845. The reactions were performed under the same conditions as in (A) and analyzed on a 16% polyacrylamide/7 M urea gel. thin arrow: substrate, thick arrow: product.

To measure the Michaelis-Menten parameters for the fluorogenic substrate, various concentrations of P-BR14-FD (0.05 to 5 μM) were mixed with a limiting amount of N-RNase E (50nM) or RNase E 845 (50nM) in the cleavage buffer (pH 7.5, 20mM Tris-HCl, 15 mM MgCl2 and 100mM NaCl), and the initial rate of RNA cleavage was measured by fluorometry. The data were then analyzed using the PRISM 4 software and V*max* and K*m* values were extracted. Each value is the average of three independent measurements using the same batch of purified enzyme. K_m values were within the same range: 0.57±0.1μM for N-RNase E versus 1.1±0.19μM for RNase E845 (Figure 3.3). Importantly, the Km value obtained with N-RNase E is statistically identical to the K_m value reported earlier by Jiang *et. al.* (0.60 ± 0.07μM). The V*max*/K*m* value of N-RNase E and RNase E 845 were 49.1 RFU/(μM*Sec) and 44.4 RFU/(μM*Sec), respectively. Since the same amount of enzymes (50nM) was used in each assay, the enzyme efficiency of N-RNase E and RNase 845 was essentially identical.

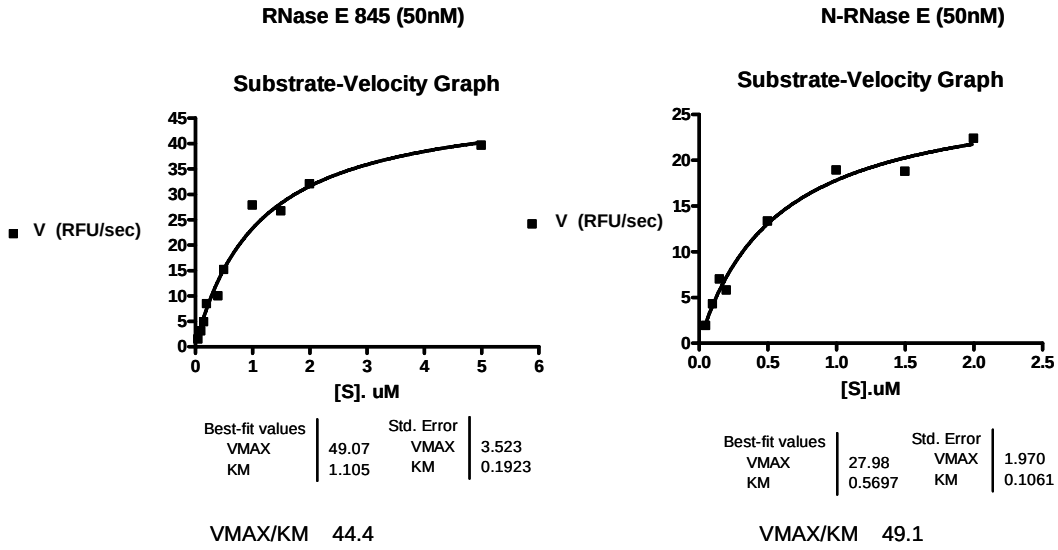

Figure 3.3 Michaelis-Menten parameters for the hydrolysis of P-BR14-FD oligonucleotide substrates. The reaction buffer used for these experiments had a pH of 7.5 and contained 15 mM MgCl2 and 100 mM NaCl. The concentration of RNase E protein in each reaction was 50 nM. Initial rates were determined as described in Materials and Methods. Each V value is the average of three independent measurements using the same batch of purified enzyme. The lines represent the best fit of data to the Michaelis-Menten equation.

Consequences of RraA and RraB binding to the kinetics of RNA degradation *in vitro*

As described earlier in chapter 2, the effect of RraA /RraB on RNA processing by RNase E was examined by monitoring the cleavage of a radiolabeled substrate by RNase E. That assay cannot be used to obtain quantitative information on the cleavage kinetics. By contrast, as shown above using the P-BR14-FD FRET substrate, kinetic parameters can be obtained with relative ease. On the basis of the *in vitro* binding affinities between RraA / RraB and the full-length RNase E measured by surface plasmon resonance analysis (K_D = 26μM for RraA and 28μM for RraB), assays were carried out

using 200 nM of N-RNase E or RNase E 845. To ensure the formation of the enzyme-inhibitor complex, the RNase Es and RraA/B were preincubated in 1x cleavage buffer at 37^{o}C for 10 minutes. Preincuation of truncated RNase E alone had no effect on the catalytic activity of the enzyme and did not result in a change in the initial rates of reaction. Consistent with *in vitro* observation (Kenneth J. McDowall, personal communication), no inhibitory effect on the processing of the FRET substrate by N-RNase E was detected with up to 200-fold molar excess of RraA monomer. For RNase E 845, weak inhibition (a 36% decrease in catalytic activity) was observed at a 200:1 molar excess of RraA to RNase E845 (Figure 3.4). Higher concentrations of RraA, e.g. 500-fold excess (100uM) or 1000-fold excess (200uM) RraA did not result in further inhibition. Additionally, up to 200-fold excess RraB had no effect on the FRET substrate cleavage by either RNase E 845 or N-RNase E.

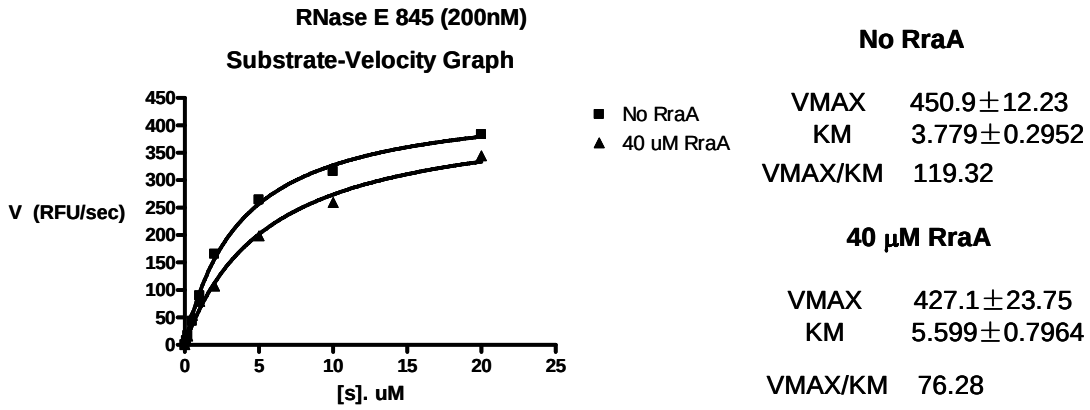

Figure 3.4 Substrate-Velocity graph for the hydrolysis of P-BR14-FD substrate by RNase E 845 with and without RraA. The concentration of RNase E845 in each reaction was 200 nM. Square: no RraA; Triangle: 200 fold excess (40μM) RraA. Each V value is the average of three independent measurements using the same batch of purified enzyme. The lines represent the best fit of data to the Michaelis-Menten equation.

Production and purification of PNPase, RhlB and Enolase

The recently reported sequential peptide affinity (SPA) purification makes use of two consecutive tags: a FLAG and a calmodulin binding peptide (CBP) separated by a tobacco etch virus (TEV) sequence. The presence of an SPA tag allows for the purification to near homogeneity, under native conditions, of proteins and protein complexes expressed in bacteria (Butland et al. 2005). To facilitate the purification of individual degradosome components, the individual gene, either *pnp*, *rhlB*, or *eno*, with a DNA cassette that encodes a carboxy-terminal SPA tag, was PCR amplified and moved into the pET21a expression vector. All SPA-tagged individual proteins were purified from the BL21 (DE3) strain using anti-FLAG M2 beads and following the procedures outlined in the manual (Sigma, St. Louis, MO). The proteins in each preparation were greater than 95% pure as judged by GelCode Blue Staining (Pierce, Rockford, IL) of samples run in SDS/polyacrylamide gel (Figure 3.5).

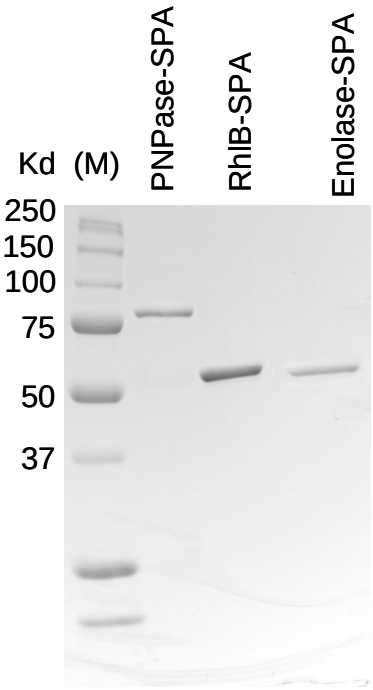

Figure 3.5 GelCode Blue staining of the purified degradosome components: PNPase-SPA, RhlB-SPA and Enolase-SPA.

DISCUSSION

The purification of full-length RNase E that forms the core of the degradosome posses a significant challenge. The full-length RNase E is a 1061 aa protein and is very susceptible to proteolytic degradation. For this reason, it has not yet been possible to purify full length RNase E in any significant amount. Nearly all biochemical analyses of RNase E have been carried out using the N-RNase E truncation, which contains the catalytically active N-terminal half, but lacks the C-terminal region which functions as the scaffold to assemble the degradosome and interact with RraA / RraB. Recent biophysical characterization of the RNase E CTH indicates that it is mainly unstructured

and hydrophobic (Callaghan et al. 2004). The CTH alone is extremely unstable and can be purified only under denaturing conditions. The susceptibility of the CTH to degradation accounts for the low yield of the intact RNase E protein. Here we have developed protocols to successfully overexpress and purify truncated forms of RNase E at the milligram scale under denaturing conditions. These RNase E truncation proteins can be used to assemble partial degradosomes *in vitro* and study the effects of the respective components (RhlB, enolase etc) or inhibitors (RraA and RraB) on RNA decay kinetics. Monitoring RNA cleavage by RNase E using electrophoretic techniques is not adequate for performing initial rate measurements needed for the in-depth kinetic analysis of the enzyme. Recently the Belacso lab developed a FRET (fluorescence resonance energy transfer) RNA substrate and showed that it can be used to monitor the catalytic properties of N-RNase E consisting of aa 1-499. We found that the FRET substrate allows for initial rate measurements to be taken very quickly (multiple rate measurements can be completed at once using 96 well plates, and hundreds of experiments can be done in an hour), something which is clearly not possible with techniques requiring the electrophoretic separation of RNA cleavage products. We examined the catalytic properties of the C-terminal truncated RNase E lacking residues 846-1061 (RNase E 845) and compared them to those of N-RNase E. The K_m values for the cleavage of the P-BR14-FD substrate were 0.57±0.1 μM and 1.1±0.19μM, for N-RNase E and RNase E845, respectively. For the same concentration of enzyme (50nM), the two enzymes exhibited identical catalytic efficiencies (V*max*/K*m* values) : 49.1 RFU/(μM*sec) for N-RNase E and 44.4 RFU/(μM*sec) for RNase E845. This result demonstrates that RNase E845 has the same catalytic properties as N-RNase E and can also to be used to study the effects of RhlB, Enolase, RraB and RraA.

The effect of RraA/RraB on the hydrolysis of P-BR14-FD substrate by N-RNase E or RNase E845 was examined as well. At 200-fold excess of inhibitor protein vs. RNase E, RraA cause a maximum of 36% inhibition on the processing of the 14-nucleotide substrate by RNase E 845, whereas 200-fold excess RraB hardly had an effect. In the case of N-RNase E, 200-fold excess RraA had no effect on the processing of the same substrate. Along these lines, 200-fold excess RraA failed to inhibit the cleavage of a similar, 3'-fluorescein-labeled short RNA substrate (p-BR13-Fl: 5'-pGGGACAGUAUUUG- fluorescein) by N-RNase E (Kenneth J. McDowall, personal communication). These results suggest that RraA and RraB exert at most minor effect on the cleavage of short RNAs.

Earlier studies by our lab showed that RraA and RraB at a much lower stoichiometric ratio to partially purified full-length RNase E result in significant inhibition of the cleavage of the p23 transcript (Gao et al. 2006). Thus, it is likely that RraA/RraB selectively affect the cleavage of longer transcripts. The 147 nucleotide p23 RNA is a truncated pM1 RNA transcript, which is processed by RNase E to a 111 nt product termed p23 RNA. The secondary structure of p23 RNA has the same structural features surrounding the processing site as those found in the intact pM1 RNA, a 415-nt RNA which is cleaved at sites near the 3' end by RNase E to give rise to M1, the 377-nt catalytic component of the tRNA processing ribozyme RNase P (Kim et al. 1996). Consistent with this hypothesis, it has been reported that the concentration of RraA that causes 50% inhibition of RNase E-mediated RNA cleavage (Ki) vary depending on RNA substrates (Lee et al. 2003). In addition, earlier microarray analysis has shown certain transcripts are stabilized by RraA, others by RraB and yet a third class stabilized by either inhibitor.

It will be of interest to examine the impact of the phosphorylation status of the RNA 5' terminus since RraA exhibits a stronger inhibitory effect on the cleavage of the RNA with a 5' triphosphate vs. a 5'monophosphate group (Lee, K., Cohen, S.N. and Georgiou, G, unpublished). Future studies need to focus on determining the kinetics of hydrolysis for RNAs of different length and complexity.

Alternatively, the lack of inhibition of RraA/B on the cleavage of the P-BR14-FD substrate by purified truncated RNase E proteins suggests their inhibitory effects may also be dependent on the assembled degradosome complex. To this end, other model short RNAs and well studied structured substrates will be used to evaluate how the degradosome components and RraA/RraB affect the hydrolysis of RNAs.

Chapter 4: Regulation of RraA, the Prototypical Protein Inhibitor of RNase E-mediated RNA Decay

INTRODUCTION

The *E. coli rraA* gene is located at 88.7 min in the chromosome, downstream of *menA* which encodes a 1, 4-dihydroxy-2-naphthoic acid (DHNA) octaprenyltransferase that catalyzes the prenylation of the redox mediator menaquinone (Shineberg and Young 1976). RraA was previously annotated as MenG in the database entirely on the basis of sequence analysis that had suggested it encodes an enzyme with S-adenosyl-L-methione-dependent methyltransferase activity capable of catalyzing the methylation of demethylmenaquinone, the last step in the biosynthesis of menaquinone (Meganathan 1996). However, the extensive biochemical, genetic and structural studies carried out in the Georgiou laboratory clearly demonstrated that RraA is not involved in the menaquinone synthesis pathway (Qiu 2001).

As described in Chapter 1, the function of RraA is to modulate RNA decay and processing by inhibiting the activity of RNase E. Interestingly, this function of RraA was uncovered in the course of genetic studies of a different pathway. *rraA* was isolated in a screen for multicopy genes that enhanced the yield of correctly folded v-tPA (a truncated variant of human tissue plasminogen activator (h-tPA) expressed in the *E. coli* periplasm. The higher tPA activity phenotype conferred by expression of RraA resulted from elevated levels of the disulfide isomerase DsbC protein, which in turn correlated with a dramatic increase in the steady-state abundance and half-life of the *dsbC* mRNA through the inhibition of RNase E. RraA binds to RNase E with an equilibrium

dissociation constant (K_D) in the low micromolar range. High affinity binding requires the C-terminal half (CTH) region of RNase E, which acts as a scaffold for the assembly of a large multiprotein complex called the degradosome (Vanzo et al. 1998). RraA serves as a *trans*-acting modulator of the endonuclease activity of the enzyme and it appears to interact only with the enzyme and not with RNA substrates (Lee et al. 2003). Gene chip analysis revealed that the action of RraA results in a dramatic change in the global abundance of mRNAs in *E.coli* affecting over 15% of all cellular transcripts. RraA homologs (>40% amino acid identity) are widely distributed in many organisms that contain endonuclease genes homologous to RNase E, including archae, proteobacteria, and Arabidopsis, suggesting a phylogenetically conserved function of RraA in modulating ribonuclease activity.

Earlier, Meganathan proposed that *rraA* is transcribed from the upstream *menA* promoter in a dicistronic mRNA (Meganathan 1996). Transcription of *menA* in turn was shown to occur from a σ^{70}-dependent promoter. In contrast to these earlier results, in the present study we demonstrate that *rraA* is transcribed predominantly from its own promoter (P*rraA*) located in the intergenic region between the *menA* and *rraA* genes. Transcription from P*rraA* is σ^{s}-dependent and is induced upon entry into stationary phase. Furthermore, we show that the synthesis of RraA is regulated at the post-transcriptional level by RNase E, suggesting the existence of a feedback regulatory circuit whereby induction of *rraA* transcription occurs in a σ^{s}-dependent manner and results in inhibition of RNase E activity, in turn decreasing the degradation rate of the *rraA* transcript and enhancing the cellular level of the RraA protein.

MATERIALS AND METHODS

Strains, plasmids and phage vectors

The strains, plasmid, and phage vectors used in this study are listed in Table 4.1. The *rpoS::kan* mutation from strain ZK1000 was introduced into various strains by P1 transduction as described by Miller (Miller 1992). The transduction of the *rpoS* disruption was confirmed by streaking single kanamycin-resistant transductants onto LB-kanamycin agar plates and testing the ability of catalase to hydrolyze hydrogen peroxide.

Growth conditions

Luria-Bertani broth (LB) and M9 minimal medium containing thiamin (50 μg/ml), 0.4% (w/v) glucose, and 0.2% (w/v) casein were supplemented with antibiotics, as required (50 μg/ml ampicilin, 25μg/ml kanamycin or 15μg/ml tetracycline). Unless otherwise stated, cells were grown in LB medium under aeration at 37^{o}C, and the growth was monitored by measuring the absorbance at 600 nm.

RNA methods

For reverse transcriptase-polymerase chain reaction (RT-PCR) analysis, total RNA was isolated with the RNeasy kit (Qiagen, Valencia, CA) and treated with RNase-free DNase (Ambion, Austin, TX). 50 ng of total RNA were subjected to RT-PCR analysis using the One Step RNA PCR kit (TaKaRa, New York, NY).

Northern blots were performed using total RNA isolated from *E. coli* JCB570 grown as above. Samples were collected in one hour intervals throughout the exponential and stationary phases. Five μg of total RNA per lane were loaded onto a denaturing gel containing formaldehyde, then transferred to a positively charged nylon

membrane (Hybond N+, Amersham, UK). The AlkPhos direct nucleic acid labeling and detection system (Amersham, UK) was used for probe (5'-tcgtttggcggacaaata-3') synthesis. Hybridization, washing of the membranes, and detection of signals were carried out according the manufacturer's protocol.

For primer extension, a 5' ^{32}P-labeled oligonucleotide (5'-gcggttccacgacgttaacatcttcttga-3', or 5'-ccgtccgccaaagttggagaacagc-3') was used as a primer for the RT reaction with 5 μg of total RNA (SuperScript III RNase H$^-$ Reverse Transcriptase (Invitrogen, Carlsbad, CA). The primer extension products were separated on 6% polyacrylamide/7M urea gels. The dideoxy-DNA sequence ladder from the same primer was prepared using the *fmol* DNA Cycle Sequencing System (Promega, Madison ,WI).

For Ribonuclease Protection Assays, *E. coli* CH1827 (MC1061, *zce-726::*Tn*10*) or CH1828 (CH1827, *rne-1*) were grown in LB at 30^{o}C to an OD_{600}=0.4 and then half of the culture was transferred to 43.5^{o}C and incubated for an additional 20 min. After the addition of rifampicin (500 ug/ml), aliquots were withdrawn every 45 sec., immediately chilled and stored in liquid nitrogen. Total RNA was prepared from the frozen samples using RNeasy kit (Qiagen, Valencia, CA) and Ribonuclease Protection Assays were performed using the RPA III kit (Ambion, Austin, TX) with the *in vitro* transcript from the complementary strand of *rraA* gene (nucleotides +13 to +318 of *rraA*) as the probe. The band intensity was quantified using the ImageQuant® software.

Construction of β-galactosidase fusions

We used polymerase chain reaction amplification to generate DNA fragments containing different regions upstream of *rraA*, i.e. -1075 to -1nt of the *rraA* upstream region that includes the P*menA*, the *menA* coding sequence, and the *menA-rraA* intergenic region, -1075 to -92 nt that includes the P*menA* and *menA* coding sequence, and -92 to -1 nt of the *menA-rraA* intergenic region. We then cloned each fragment upstream of the *lacZ* gene in a multicopy transcriptional fusion vector, pSP417 (Podkovyrov and Larson 1995). We generated plasmids pMZ002 {(-1075 to -1nt)-*lacZ* }, pMZ003{(-92 to -1nt)-*lacZ* }, and pMZ004 {(-1075 to -92nt)-*lacZ* }. pMZ001 was the negative control vector. The *lacZ* fusions in pMZ002, pMZ003 and pMZ004 were transferred onto the chromosome using the transducing lambda phage system (Simons et al. 1987). The fusions were transferred into λ*RS45,* whereas the negative control fusion in pMZ001 was transferred into λ*RS74* via a double recombination event. Plaques containing the recombinant lambda phages were isolated based on their blue plaque phenotype. The recombinant lambda phages were used to lysogenize EC-O (Δ(pro-*lacZ*)), and generated strains: MZ001(EC-O, λp0-*lacZ*) with a chromosomal promoterless *lacZ* gene, MZ002{EC-O, λ(-1075 to -1nt)-*lacZ*} encoding a *lacZ* fusion to nt -1075 to -1 of the *rraA* upstream region, *E. coli* MZ003{EC-O, λ(-92 to -1nt)-*lacZ*} encoding a *lacZ* fusion to -92 to -1nt of the *menA-rraA* intergenic region, and MZ004 {EC-O, λ(-1075 to -92nt)-*lacZ*} encoding a *lacZ* fusion to nt -1075 to -92 of the *rraA* upstream region. All lysogens were tested for mono-lysogenization by PCR (Powell et al. 1994).

β-galactosidase assays

Cultures grown with aeration at 37°C, in rich or M9 medium overnight, were subcultured into the fresh medium. Samples were collected at exponential and stationary phases. The samples were collected at 4°C and resuspended in an appropriate volume of ice-cold Z buffer (60 mM Na_2HPO_4, 40 mM NaH_2PO_4, 10 mM M KCl, 1 mM $MgSO_4$; pH 7.0) (Miller 1972) to give A_{600} in the range from 0.6 to 0.9. β-galactosidase activities were determined from at least three independent experiments, as previously described (Miller 1992).

Western Immunoblotting

Cells were grown as specified, harvested by centrifugation, re-suspended in PBS and lysed by passing through a French press (2,000 psi). The lysate was centrifuged for 15 minutes at 4^{o}C to remove cell debris and the protein concentration in the supernatant was determined by Bradford assay (Bio-Rad Laboratories, Hercules, CA). One μg of total protein was separated by SDS-12% polyacrylamide gels. Western blots were performed by standard methods using monoclonal ANTI-FLAG-M2-Peroxidase (HRP) antibody-conjugate (Sigma, St. Louis, MO). Signal intensities were measured (Bio-Rad Imaging Densitometer), quantified by using molecular analysis software (Quantity One, Bio-Rad), and displayed below the blot image.

Table 4.1 Strains, plasmid and phage vectors

Strains, Plasmids, Phage vectors	Description	Reference or Source
JCB570	(MC1000, *phoR*, *zih12::Tn10*)	(Bardwell et al., 1991)
ZK1000	(W3110, *ΔlacU16, tna-2*, *rpoS::kan*)	(Bohannon et al,. 1991)
EC-O	(*thi-1*, *relA1*, *Δ(pro-lac)X113[del = DE5] supE44 / F42-114(FTs) lac*)	Lab collection
DY330	W3110, *ΔlacU169 gal490 λc1857 Δ(cro-bioA)*	(Zeghouf et al.,2004)
MZ001	(EC-O, λp0-*lacZ*)	This study
MZ002	{EC-O, λ(-57 to 1019 nt)-*lacZ* }	This study
MZ003	{EC-O, λ(927 to 1019 nt)-*lacZ* }	This study
MZ004	{EC-O, λ(-57 to 927 nt)-*lacZ* }	This study
MZ013	(MZ003, *rpoS::kan*)	This study
MZ014	(MZ004, *rpoS::kan*)	This study
MZ100	(JCB570, *rpoS::kan*)	This study
CH1827	(MC1061, *zce-726::Tn10*)	(Ono et al., 1979)
CH1828	(CH1827, *rne-1*)	(Mudd et al., 1990)
pSP417	pBR ori, Amp^r,	(Podkovyrov, 1995)
pMZ002	{pSP417, (-57 to 1019 nt)-*lacZ* }	This study
pMZ003	{pSP417, (927 to 1019 nt)-*lacZ* }	This study
pMZ004	{pSP417, (-57 to 927 nt)-*lacZ* }	This study
λRS 45	*bla'-lacZ*$_{sc}$ *imm21 ind* +	(Simons et al., 1987)
λRS74	*placUV5-lacZ* + *imm21 ind* +	(Simons et al., 1987)
λMZ1	Same as λRS74, but with the p0-*lacZ* fusion	This study
λMZ2	Same as λRS45, but with the (-57 to 1019 nt)-*lacZ* fusion	This study
λMZ3	Same as λRS45, but with the (927 to 1019 nt)-*lacZ* fusion	This study
λMZ4	Same as λRS45, but with the (-57 to 927 nt)-*lacZ* fusion	This study

RESULTS

Identification of the P*rraA* promoter

Meganathan et al. had proposed that *rraA* is transcribed as a dicistronic mRNA from the P*menA* promoter (Meganathan 1996). The transcription initiation site for this putative dicistronic transcript was identified at 57bp upstream of the *menA* translation start site (Suvarna et al. 1998). Consistent with this hypothesis, a *menA-rraA* transcript of the expected size was detected by RT-PCR analysis (Figure 4.1A), suggesting that the *rraA* is transcribed together with the preceding *menA* gene as a dicistronic mRNA. However, Northern blot analysis with two different *rraA*-specific probes revealed that the predominant RNA in samples either in exponential or stationary phase corresponds to a shorter species, ca 550 bases in length, representing the *rraA* monocistronic transcript from an unidentified promoter that locates proximal to the *rraA* ORF. No bands around 1.5 kb (the expected size for *menA-rraA* dicistronic RNA) were detected even after a longer exposure of the membrane to the X-ray film (Figure 4.1B). The finding that the disictronic mRNA cannot be detected by Northern blotting suggests that most of the *rraA* mRNA is likely transcribed from the unidentified proximal promoter that is located proximal to the *rraA* ORF, throughout log to stationary phases. The contribution of P*menA* to *rraA* mRNA synthesis is negligible, when the cells were grown in LB media under aerobic condition.

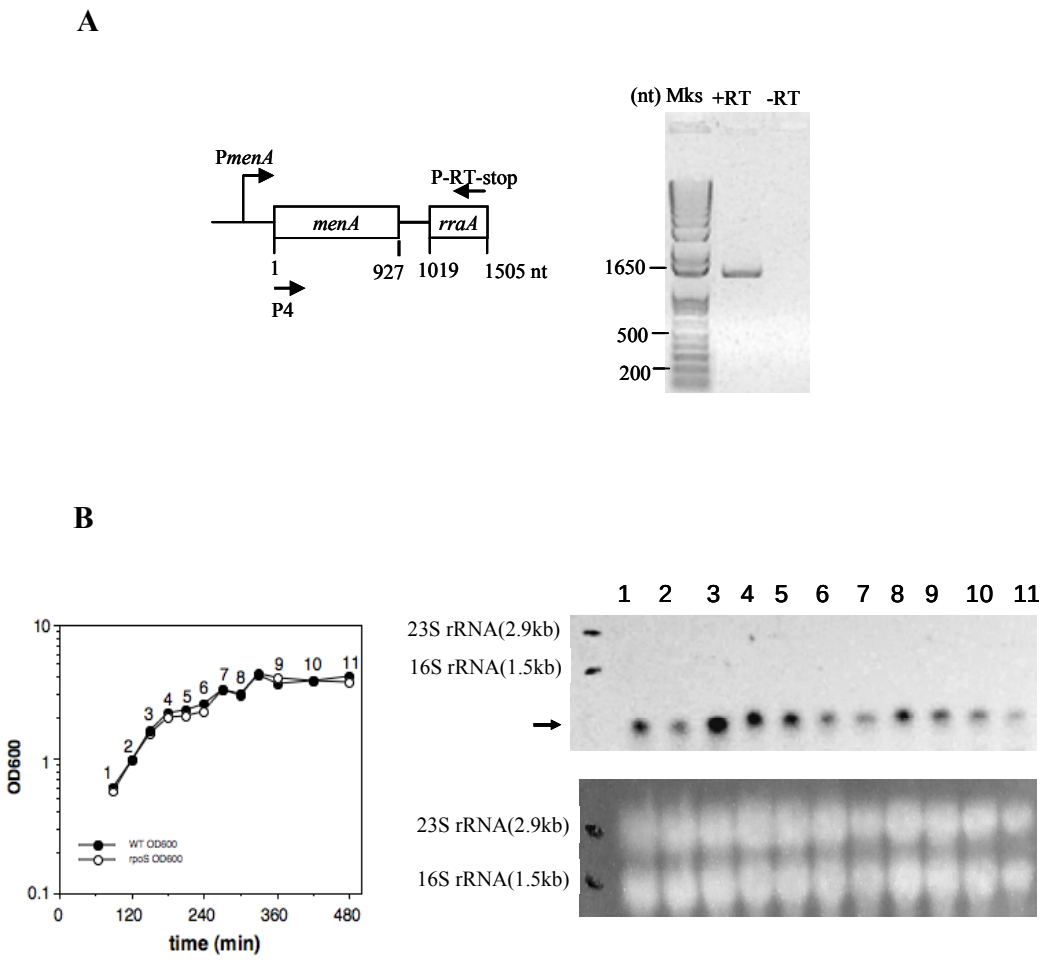

Figure 4.1: (A) RT-PCR analysis. (left) The annealing positions of the reverse primer (P-RT-stop) and forward primer (P4) used in the RT-PCR analysis of the *menA-rraA* region. (right) RT-PCR analysis of the *rraA* transcript using the primers P4 and P-RT-stop. - RT: the negative controls containing the same amounts of RNA, primers, and Taq polymerases, but no reverse transcriptase. (B) Northern Blotting. (left) The growth curve and sampling time. (right) The predominant *rraA* mRNA corresponds to the monocistronic transcript from a promoter that locates proximal to rraA ORF., ca 550 bases in length, throughout exponential and stationary phases. The result was confirmed using a different *rraA*-specific probe.

Primer extension of RNA isolated from *E. coli* JCB570 using the 5'-^{32}P labeled oligonucleotide probe ^{32}P-gcggttccacgacgttaacatcttcttga revealed an *rraA* transcript that is initiated at an A residue 28 nt upstream from the ATG codon (Figure 4.2A). In addition

to this major transcript, the data in Figure 4.2A also show a faint band at the position of the initiation codon of *rraA* (indicated by an open arrowhead). However, this band was not detected in a primer extension assay using an alternative primer (^{32}P-ccgtccgccaaagttggagaacagc) that anneals to a different location within the *rraA* RNA (located 23 bp upstream from the first primer) suggesting that the minor band likely corresponds to a premature stop product of the reverse transcriptase.

DNA sequence analysis of the *menA-rraA* intergenic region suggested the existence of a putative promoter (P*rraA*) (Figure 4.2B). *RraA* and *menA* are separated by a 92bp intergenic region that shows a significant degree of conservation among closely related bacteria such as *Shigella flexneri* (92/92 bp, 100% identity in the intergenic region), and *Salmonella typhimurium* (86/92bp, 93% identity in the intergenic region). A lower degree of sequence identity was observed for phylogenetically more distant bacteria such as *Yersinia pestis*, *Erwinia carotovora* and *Photorhabdus luminescens*. Analysis using GENETYX-MAC 11.2.5 identified regions that match the σ^{70} consensus -35 and -10 sequences, centered at 32 and 8 nucleotides, respectively, upstream of transcription initiation site (Figure 4.2B). Multiple sequence alignment, using CLUSTAL W 1.81, among the bacterial species which have close homologs (>80%) of the *E. coli* K-12 *rraA* revealed that the sequence of the P*rraA* promoter is conserved among γ-proteobacteria. As shown in Figure 4.2B, the -35 and -10 regions are identical, except from *Photorhabdus luminescens,* whose -35 region differs from that of *E. coli.* K-12 by one bp.

A

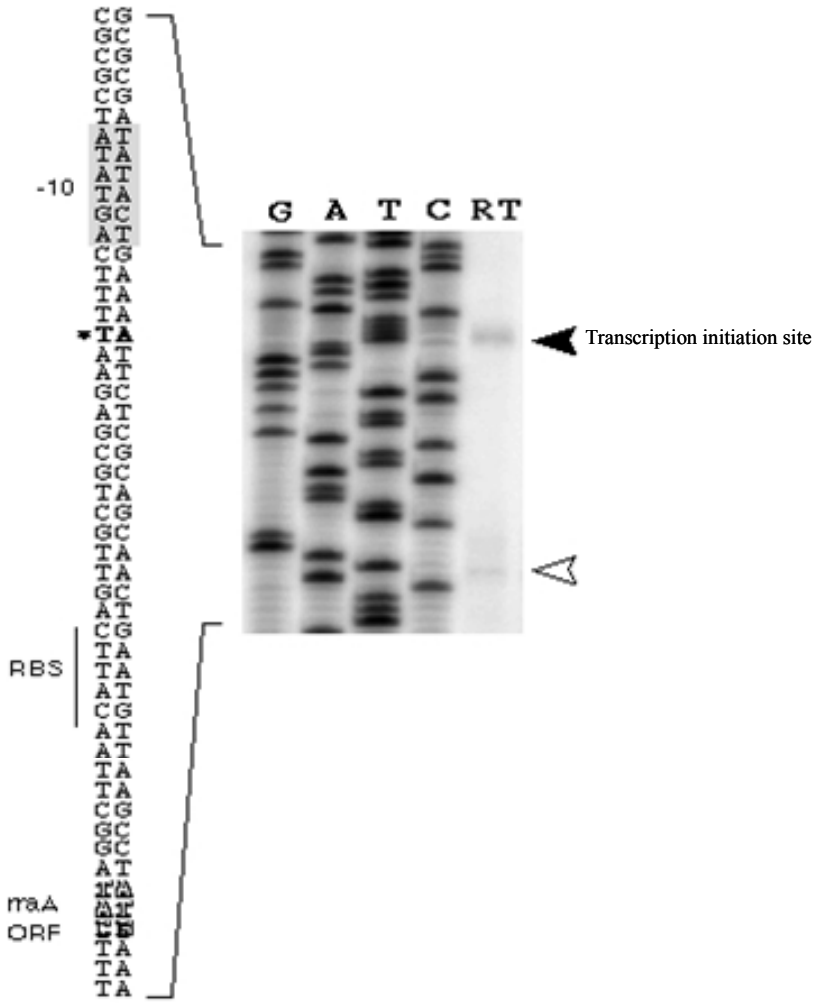

B

Figure 4.2 (A) Primer extension. Five µg total RNA isolated from *E. coli* JCB570 cells grown to log phase (A600 = 0.7) was reverse transcribed using the primer (5'-gcggttccacgacgttaacatcttcttga-3') complementary to nucleotides +36 to +64 of rraA. Filled arrowhead: the reverse transcription product; open arrowhead: the premature stop product of the reverse transcriptase. (B) Multiple sequence alignment of the *menA-rraA* intergenic sequence: Abbreviations: Eco, *Escherichia coli* K-12 ; Sfl, *Shigella flexner* I ; Sen, *Salmonella enterica* ; Ype, *Yersinia pestis* ; Eca, *Erwinia carotovora* ; Plu, *Photorhabdus luminescens*. Transcript start site is indicated by a solid arrow. -35, -10 sites are indicated by empty boxes.

Genetic analysis of expression PrraA using lacZ transcriptional fusions

We used PCR amplification to generate DNA fragments containing different regions upstream of *rraA* extending up to, and including, the *menA* promoter, as shown in Figure 4.3A: -57 to 1019 nt of the *rraA* upstream region that includes the P*menA*, the *menA* coding sequence, and the *menA-rraA* intergenic region; -57 to 927 nt that includes the P*menA* and *menA* coding sequence; 927 to 1019 nt of the *menA-rraA* intergenic region, and cloned each fragment upstream of the *lacZ* gene in a multicopy transcriptional fusion vector, pSP417 (Podkovyrov and Larson 1995). In this way, we

generated plasmids pMZ002 {(-57 to 1019 nt) -*lacZ* }, pMZ003{(927 to 1019 nt) -*lacZ* }, and pMZ004 {(-57 to 927 nt) -*lacZ* }; pMZ001 was the negative control vector.

To rule out the possibility that differences in the β-galactosidase activity expressed from the above transcriptional fusions might be partially due to plasmid copy number effects, we made single chromosomal copy isolates of each construct using the transducing lambda phage system (Simons et al. 1987). The *lacZ* fusions in pMZ001, pMZ002, pMZ003 and pMZ004 were transferred into either λ*RS74* or λ*RS45* via a double recombination event to generate λMZ1, λMZ2, λMZ3 and λMZ4. Subsequently, *E. coli* EC-O was lysogenized with the recombinant phages to generate strains carrying a single copy of each promoter-*lacZ* fusion. As show in Figure 4.3B, strain MZ003{EC-O, λ (927 to 1019 nt)-*lacZ* }, with only the *menA-rraA* intergenic region fused to *lacZ*, showed identical levels of β-galactosidase activity to those observed in MZ002 {EC-O, λ (-57 to 1019 nt)-*lacZ* } which contained a fusion to the *rraA* upstream region, including the P*menA* and the *menA* coding sequence. In contrast, MZ004 {EC-O, λ (-57 to 927 nt)-*lacZ*} containing a fusion to -57 to 927 nt of the *rraA* upstream region that lacked the *menA-rraA* intergenic region, showed 50% lower activity.

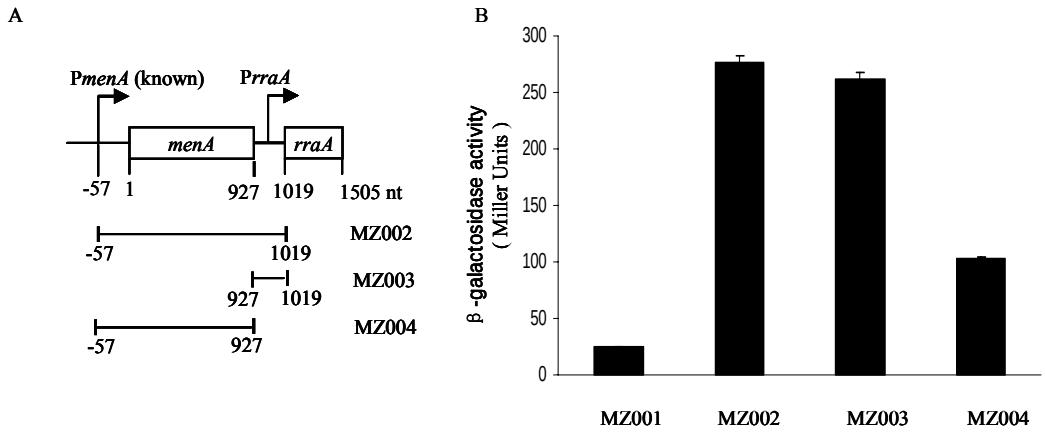

Figure 4.3 (A) Schematic of the transcriptional *rraA –lacZ* fusions used in this study. (B) β-galactosidease activities in MZ001, MZ002, MZ003 and MZ004 cells. MZ001 (EC-O, λp0-*lacZ*) has a chromosomal promoterless *lacZ* gene; strain MZ002{EC-O, λ(-57 to 1019 nt)-*lacZ* } encodes a *lacZ* fusion to nt -57 to 1019 of the *rraA* upstream region; MZ003 {EC-O, λ(927 to 1019 nt)-*lacZ* } encodes a *lacZ* fusion to nt 927 to 1019 of the *menA-rraA* intergenic region; MZ004{EC-O, λ(-57 to 927 nt)-*lacZ* } encodes a *lacZ* fusion to nt -57 to 927 of the *rraA* upstream region. Cells were grown in LB under aeration at 37°C, and harvested in log phase (A600= 0.5-0.8). Samples were normalized by O.D. and enzymatic activities were measured in Miller units. The data presented are the average of at least three independent determinations and error bars correspond to the standard deviation.

rraA expression in stationary phase

Earlier microarray studies had shown that the *rraA* mRNA level is increased upon entrance to stationary phase (https://asap.ahabs.wisc.edu/annotation/php/ASAP1.htm). The abundance of the RraA protein in exponential and stationary phase cells was examined by Western blotting using strain DY330-*rraASPA* (Butland et al. 2005) in which sequential peptide affinity (SPA) tags are fused to the C terminus of the *rraA* open reading frame within the chromosome. We found that the level of RraA protein reproducibly increased by about 2-fold in stationary phase (Figure 4.4).

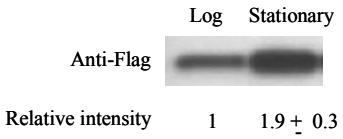

Figure 4.4 Western immunoblot analysis of RraA level in exponential and stationary phases. Strain DY330-*rraASPA*, bearing a sequential peptide affinity (SPA) tag at the C terminus of *rraA* open reading frame, was cultured in LB medium at 32°C and harvested during exponential growth (A600=0.4) and stationary phase (A600=3.5). RraA is expressed at endogenous levels from its chromosomal promoter and is detected by the highly specific anti-FLAG antibody. Blots were replicated from three independent protein preparations. Replicate measurements were made on the same membrane to determine the reproducibility of the analysis. The intensity of the signal was observed to be linear by using a dilution series of total protein. The data are the mean and error of three separate blots.

In order to determine if *rraA* gene transcription is dependent on the growth phase, we examined the *rraA* promoter activity in exponential or stationary phase cells grown in LB medium at 37^{o}C. Primer extension analysis of RNA from stationary phase cells revealed a marked increase in the *rraA* transcript in stationary phase cells (Figure 4.5). In addition to the *rraA* transcript, several minor bands were also evident in samples from stationary phase cells. These correspond to premature termination or mis-annealing products since they could neither be detected consistently nor were they detected in a primer extension assay using a different primer.

Transcriptional regulation of *rraA* by RpoS

Many genes that are upregulated in stationary phase are part of the *rpoS* regulon. The role of RpoS in the transcriptional regulation of *rraA* was examined using primer extension analysis. An *rpoS* mutant strain ,MZ100 (JCB570, *rpoS::kan*) was made by P1 transduction of a *kan* marked *rpoS* deletion allele (Bohannon et al. 1991). Primer extension analysis of RNA extracted from stationary phase cells of MZ100 did not show

any change in the intensity of the band corresponding to the *rraA* transcript (Figure 4.5). Together with the increased intensity of the *rraA* transcript in stationary phase observed in the wild type cell sample, these results indicate that transcription from the P*rraA* promoter increases in stationary phase and this effect is dependent on the transcription factor σ^s.

The effect of *rpoS* on the transcriptional activity of the P*rraA* promoter was also evaluated using *lacZ* fusions transcribed from the P*rraA* promoter. Specifically, β-galactosidase activity was determined in strains MZ003, MZ004, MZ013 (MZ003, *rpoS::kan*) and MZ014 (MZ004, *rpoS::kan*) grown to either exponential or stationary phase. As shown in Figure 4.6, in strain MZ003, the β-galactosidase activity increased more than 2-fold in stationary phase cultures ($A_{600}\approx$ 2.5) compared with log-phase cells ($A_{600}\approx$ 0.6). In the isogenic *rpoS* mutant MZ013 the β-galactosidase activity was comparable to the level observed in the parental *E. coli* MZ003 in exponential phase cells. However, unlike the wt control, MZ013 did not exhibit an increase in β-galactosidase activity in stationary phase. As a further control the β-galactosidase activity of MZ004 and MZ014 cells where *lacZ* is transcribed from the upstream *menA* promoter was neither growth phase dependent, nor was it affected by *rpoS*. These results clearly suggest that σ^s is responsible for the increased transcription from the P*rraA* upon entrance into stationary phase.

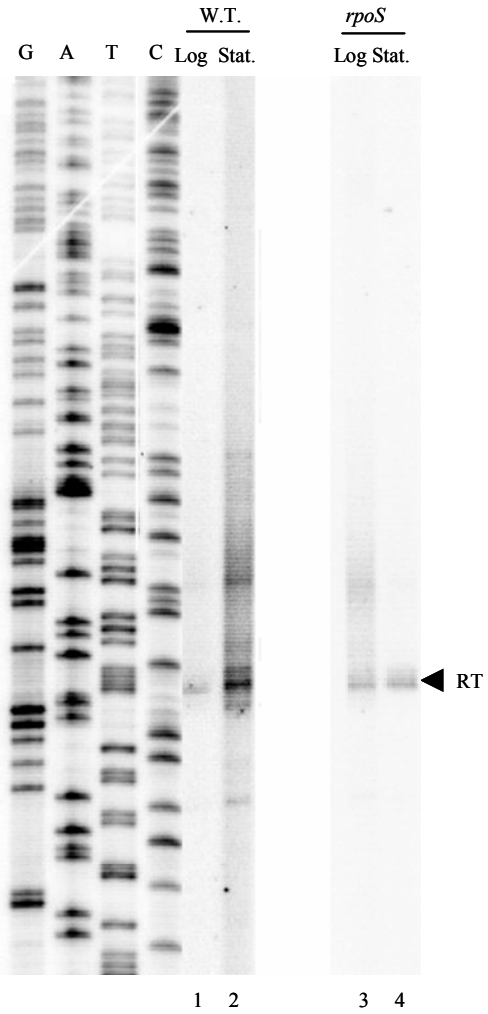

Figure 4.5 Primer extension analysis showing the transcription from P*rraA* in growth phases. Total RNA were prepared from isogenic strains JCB570 (w.t.) and MZ100 (JCB570, *rpoS::kan*) grown to log phase (A_{600}=0.6) and stationary phase (A_{600}=2.5). Equivalent amounts of RNA (5 μg) was reverse transcribed using the primer (5'-gcggttccacgacgttaacatcttcttga-3') complementary to nucleotides +36 to +64 of *rraA*. The position of the reverse transcription products are shown by the arrowhead.

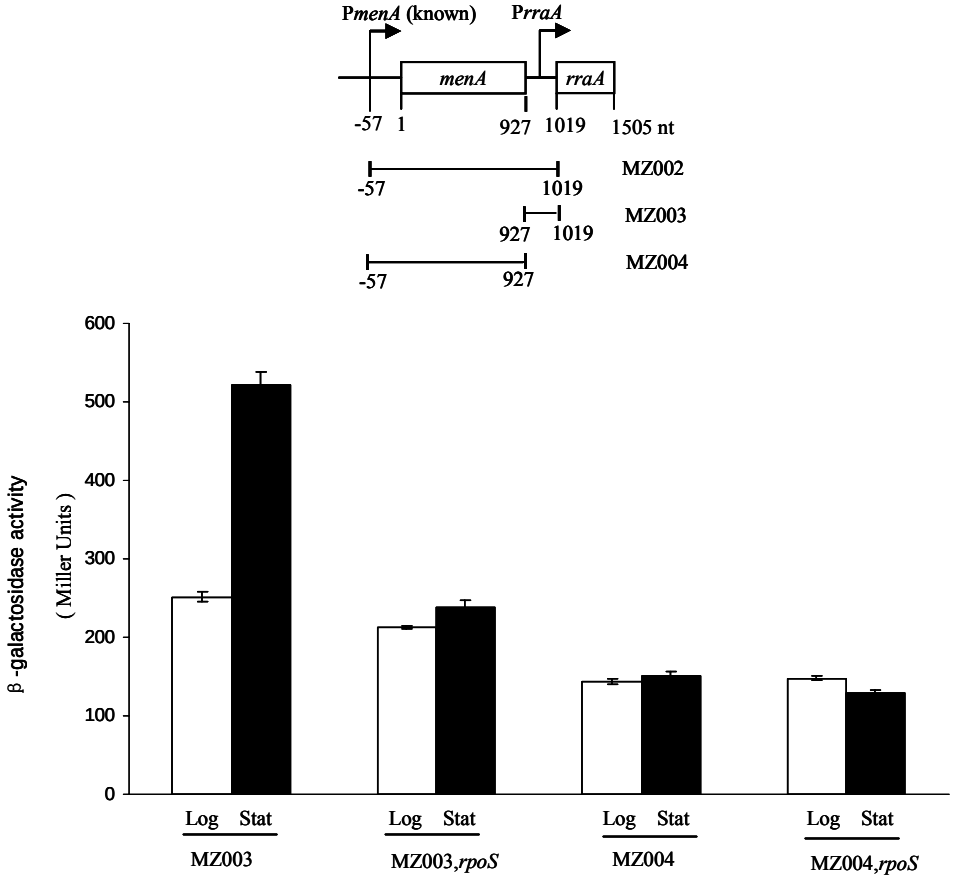

Figure 4.6 Effect of σ^s level on the transcriptional activity of the various *Prra - lacZ* fusions inexponential or stationary phase cells. Strains MZ003{EC-O, λ(927 to 1019 nt)-*lacZ* }, MZ004{ EC-O, λ(-57 to 927 nt)-*lacZ* }, MZ013 (MZ003, *rpoS::kan*) and MZ014 (MZ004, *rpoS::kan*) were in M9 medium supplemented with 0.2% casein with aeration, at 37°C and harvested either in exponential (A_{600}=0.6) or stationary phase (A_{600}=2.5). Samples were normalized by O.D. and enzymatic activities were measured in Miller units. The data presented are the average of at least three independent determinations and error bars correspond to the standard deviation.

The decay of the *rraA* transcript is dependent on RNase E

Since the function of RraA is to modulate the endonuclease activity of RNase E, it was of interest to examine whether RNase E plays a role in the decay of the *rraA* transcript. Because RNase E is an essential protein, the stability of the *rraA* mRNA was examined in *E. coli* CH1828 which contains the temperature sensitive *rne-1* allele. Cells were grown at 30^{o}C in LB medium under aerobic conditions to mid-logarithmic phase, followed by a temperature upshift to 43.5^{o}C for 20 min. Rifampicin was added to inhibit transcription, samples were withdrawn at different times, and the level of *rraA* was determined by Ribonuclease Protection Assays (Figure 4.5). In the parental strain CH1827, the half-life of *rraA*, determined by fitting a linear regression model, was virtually identical at 30^{o}C or at 43.5^{o}C, ($t_{1/2}$ = 2.4 ± 0.3 and 2.9 ± 0.2 min respectively). However, incubation of the *rne-1* mutant strain at the non-permissive temperature resulted in a significant (2-fold) stabilization of the *rraA* transcript, whose $t_{1/2}$ increased to 6.1 ± 1.1 min. Since RraA acts an inhibitor of RNase E activity, the finding that the processing of the *rraA* transcript is RNase E-dependent suggests the existence of a feedback mechanism: induction of *rraA* synthesis, possibly by environmental triggers that stimulate σ^{s}-dependent transcription, would be expected to result in higher accumulation of RraA protein, in turn inhibiting RNase E activity and thus leading to stabilization of the *rraA* transcript. The net result would be a further increase in the level of RraA protein and greater inhibition of RNase E activity.

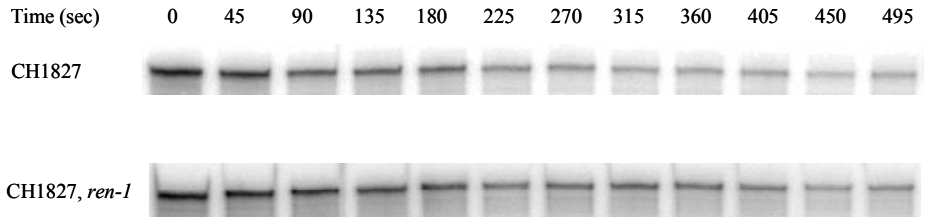

Figure 4.7 Ribonuclease protection assays and total RNA isolation were done as described in Materials and Methods on strains CH1827 (MC1061, zce-726::Tn*10)* and CH1828 (CH1827, *rne-1*). Time points in seconds were taken after rifampicin addition. Equivalent amounts of RNA (5 ug) were used in RNA protection assays and loaded into each lane of a 6% polyacrylamide/7M urea gel. The band intensity was quantified using the ImageQuant® software. Degradation rates were determined by fitting linear regression models and represent the average of two independent determinations.

DISCUSSION

The recently discovered RraA protein represents the prototypical cellular protein that modulates RNA decay and processing by binding to the essential endoribonuclease RNase E and inhibiting its activity. Interestingly, inhibition of RNase E activity by RraA does not require the RNase E carboxy-terminal scaffold region important in formation of the RNA degradosome; however, RraA binding is enhanced by the CTH of RNase E. RraA does not interact detectably with RNA substrates, suggesting that it affects the ability of RNase E to cleave phosphodiester bonds between nucleotides by a mechanism that is independent of substrate binding. Microarray profiling showed that adventitious expression of RraA affects the abundance of more than 2000 *E. coli* transcripts, giving rise to an mRNA profile that was very similar to the transcript signature observed during RNase E depletion. The absence of *rraA* altered the abundance of ~80 transcripts at least 2-fold. Most of these RNAs were destabilized in

an *rraA* null mutant, consistent with the inhibitory effect of RraA on the endoribonucleolytic activity of RNase E (Lee et al. 2003).

The relatively small number of transcripts affected in the *rraA* null strain, combined with the normal growth of this strain when cultured at 37˚C suggests that the physiological effects of RraA might occur under more specialized environmental conditions. Since RraA acts as an inhibitor of RNase E, its maximal effect on cell physiology is expected to occur under conditions where its cellular concentrations are elevated.

In this study we showed that *rraA* is expressed from its own promoter, P*rraA*, located in the *menA-rraA* intergenic region. Primer extension and *lacZ* fusion analysis revealed that transcription from P*rraA* is elevated upon entry into stationary phase in a σ^s–dependent manner. Finally, western blot confirmed that the RraA protein is accumulated in stationary phase.

E. coli cells experience morphological and physiological changes during the transition to stationary phase (Hengge-Aronis, 1999). In stationary phase, transcription is essentially controlled by the alternative sigma factor σ^s (or σ^{38}, RpoS), leading to the expression of more than 100 stationary phase-specific genes (Ishihama 1997).

The *E. coli rpoS* regulon also comprises genes that are upregulated under certain stress conditions such as hyperosmolarity, low PH, and oxidative and temperature stresses. They function largely in stress response, carbon metabolism and cell envelope biogenesis (Hengge-Aronis 2002). Recently, using microrarray analysis Hengge-Aronis's group identified over 400 genes which are positively controlled by σ^s in *E. coli*. While *rraA* was not recognized as an σ^s dependent gene in this study, we note that 33 out of the 87 genes which had been experimentally shown to be σ^s-controlled in earlier studies also failed to be detected in the microarray experiments (Weber et al. 2005).

Many σ^S promoters contain an extended -10 region KCTAYRCTTAA (nucleotide -14 to -4, K stands for T or G, Y stands for T or C, and R stands for A or G) (Weber et al. 2005). Particularly, C at -13 has been shown to interact directly with lysine 173 in the region 2.5 of σ^S (Becker and Hengge-Aronis 2001; Weber et al. 2005). Nevertheless, despite its importance, this C at -13 is not absolutely essential for more efficient promoter utilization by σ^S than by σ^{70}, as shown with mutant variants of the *aidB* promoter (Lacour et al. 202; Hengge-Aronis 2002). The extended -10 motif is found only on the genes which are σ^S-dependent under all three growth and stress conditions (i.e. transition into stationary phase growth, hyperosmotic shift and low pH). They account for less than 30% of the total genes which are positively controlled by *rpoS* and were named the "core set" of σ^S-dependent genes (Weber et al. 2005). Genes that display σ^S dependence only under certain conditions do not contain this extended -10. In P*rraA,* the -10 box (gaTATACT), contains an A rather than a C at -13 suggesting that additional factors may be involved in sigma factor selectivity. For example, the well-characterized σ^S-controlled gene, *csiD,* which is mainly induced by carbon starvation, contains an A at -13 (-10 sequence: gaTATTTT) (Weichart et al. 1993; Marschall et al. 1998) and requires cyclic AMP(cAMP) - cAMP receptor protein (CRP) for sigma factor selectivity. We could not identify sequences resembling either the distal or the proximal UP element which has been proposed to enhance σ^S selectivity. The absence of an apparent UP element is not surprising as such sequences are absent in more than 50% of the known σ^S-dependent promoters (Typas and Hengge-Aronis 2005). It should be noted that extensive earlier studies have revealed that σ^S promoter selectivity is affected by a number of factors including DNA supercoiling, topology and by the action of additional protein regulators (Kusano et al. 1996; Colland et al. 2000).

Along with changes in transcription, the mechanisms that control RNA stability are also altered during stationary phase, although very little is known about these latter effects. A possible biological role for the σ^S-dependent regulation of *rraA* expression is that it might provide a means for the stabilization of stationary phase-induced transcripts.

The translation of RpoS is positively regulated by the small non-coding RNA DsrA. DsrA interacts with one strand of the *rpoS* mRNA, interfering with the formation of the stem structure that otherwise inhibits translation. DsrA is degraded by RNase E (Repoila and Gottesman 2001). It is conceivable that the elevated expression of RraA reduces the cleavage of DsrA by RNase E ,and in turn stimulates the translation of *rpoS*, ultimately allowing further expression of *rraA*.

We found evidence that the expression of *rraA* may be regulated at the post-transcriptional level as well. The stability of the *rraA* transcript is dependent on RNase E activity suggesting the involvement of a feedback circuit in the regulation of the RraA level in *E. coli*: induction of *rraA* synthesis, possibly by environmental triggers that stimulate σ^S-dependent transcription, would be expected to result in higher accumulation of RraA protein, in turn inhibiting RNase E activity and thus leading to stabilization of the *rraA* transcript. The net result would be a further increase in the level of RraA protein and greater inhibition of RNase E activity.

Chapter 5: Studies on the Regulation of *rraB* Expression

INTRODUCTION

RraB is a 15.6 KDa protein which interacts with RNase E and inhibits RNase E endonucleolytic cleavages in *E. coli*, thus regulating gene expression at the posttranscriptional level. Similar to RraA, RraB does not alter RNase E cleavage site specificity or interact detectably with the substrate RNAs. RraB also possesses the same affinity for RNase E as RraA, with K_D values in the micromolar range. However, RraB exhibits key differences in its mode of action, its effects on transcript profile and its phylogenetic distribution. For example, RraB interacts with residue 694-727 at the CTH of RNase E. In contrast, no single contiguous epitope in RNase E has been found responsible for binding RraA. Adventitious expression of RraB induces dramatic and specific changes in degradosome composition that are distinct from RraA overexpression. DNA microarrays revealed that the action of RraB results in a dramatic change in the global abundance of mRNAs that is different from that obtained through the action of RraA (Gao et al. 2006). Finally, in contrast to the widely distributed RraA homologues, RraB homologues are only found in γ-proteobacteria, suggesting that these proteins may have a more specialized role in modulating RNA degradation.

The existence of two proteins that exert a differential effect on RNA decay via their interactions with RNase E and degradosome remodeling argues that modulation of RNA stability may be a mechanism for global control of transcript abundance in response to dynamic changes in the extracellular environment. The *E. coli rraB* gene is 417 bp in

length and is located at 96.4 minutes in the chromosome. Prior to the discovery of its function as an RNase E inhibitor, RraB protein was annotated as a hypothetical protein, YjgD, in the NCBI database.

As the first step to understanding the physiological significance of the modulation of mRNA decay by RraB, we studied the transcription and regulation of *rraB*. R*raB* was shown to be expressed throughout exponential and stationary phase growth. We demonstrated that *rraB* is transcribed from a promoter (P*rraB*) which is divergent from the *argI* promoter and overlaps with the arginine repressor binding site (ARG boxes) located in the *argI-rraB* intergenic region. This indicates that the expression of *rraB* could be regulated by the transcription factor ArgR and may be involved in arginine metabolism. Along these lines, previous microarray analysis suggested that the expression of *rraB* (*yjgD)* may be correlated with expression of *argI* in response to the changes in tryptophan metabolism (Ramelot et al. 2003; Khodursky et al. 2000).

In *E. coli* K-12 strains, arginine biosynthesis starts from glutamate and carbamoylphosphate. The enzymes responsible for these reactions are coded by the arginine regulon. This regulon is currently known to be composed of 12 genes, among which only a few are organized in an operon. However, all the genes in the arginine regulon are regulated by a master transcriptional regulator and repressor, ArgR, which functions as a direct sensor of arginine availability. The binding of six L-arginine molecules at the trimer-trimer interface of ArgR activates the regulator, allowing it to bind to the ARG boxes which spans nearly 40 bp and consist of two neighboring 18-bp palindromic sequences, separated by three nucleotides (Maas 1994).

E. coli has five principal operons, *trp, aroH, mtr, trpR,* and *aroL,* known to be involved in tryptophan biosynthesis, transport, and regulation. All of these operons are transcriptionally regulated by the tryptophan-activated Trp repressor (Pittard 1996). The five proteins, TrpA, TrpB, TrpC, TrpD and TrpE, required for tryptophan biosynthesis from the aromatic branch point intermediate, chorismate, are encoded by the *trp* operon. Transcription of the *trp* operon is regulated by transcription attenuation as well as by repression (Yanofsky et al. 1999).

We examined the possibility that the expression of *rraB* is regulated in response to changes in the availability of these two amino acids. However, we find that contrary to the gene chip data we could not find any evidence that *rraB* promoter activity, mRNA abundance and RraB protein level are affected by changes in either tryptophan or arginine metabolism.

MATERIALS AND METHODS

Strains, plasmids and phage vectors

The strains, plasmid, and phage vectors used in this study are listed in Table 5.1.

Growth conditions

Vogel and Bonner minimal medium (Heatwole and Somerville 1992) + 0.2% glucose, supplemented with L-tryptophan (50 μg/ml) or indole acrylic acid (15 μg/ml)

was used for tryptophan limited growth experiments. For arginine limitation, MD medium (Minimal medium with Davis salts) (Suiter et al. 2003) supplemented with amino acids (with excess arginine (20mM) or no arginine) and vitamins was used throughout. Arginine free medium (AF) is MD with the following added from a sterile 25-fold concentrated stock: 580 mg of DL-alanine, 60 mg of L-aspartatic acid, 70 mg of L-cysteine, 400 mg of L-glutamic acid, 160 mg of glycine, 50 mg of L-histidine, 320 mg of DL-isoleucine, 270 mg of L-leucine, 360 mg of L-lysine, 120 mg of L-methionine, 560 mg of DL-phenylalanine, 140 mg of L-proline, 330 mg of DL-serine, 55 mg of L-tryptophan, 60 mg of L-tyrosine, 200 mg of L-threonine, 330 mg of L-valine, 200 mg of L-asparagine, 20 mg of guanosine, 20 mg of adenosine, 20 mg of uracil, 1 mg of pantothenic acid, 1 mg of riboflavin, 1 mg of thiamine, 1 mg of nicotinic acid, 1 mg of biotin, and 1 mg of pyridoxine). Media were supplemented with antibiotics, as required (50 μg/ml ampicilin, 25μg/ml kanamycin or 10μg/ml chloramphenicol). Unless otherwise stated, cells were grown in Luria-Bertani broth (LB) under aeration at 37^{o}C, and the growth was monitored by measuring the absorbance at 600 nm of the culture.

Table 5.1 Strains, plasmid and phage vectors

Strains, plasmids, and phage vectors	Description	Reference or Source
JCB570	(MC1000, *phoR zih12::Tn10*)	(Bardwell et al., 1991)
W3110	(*lacL8, lacIq*)	(Khodursky et al., 2000)
AK11	(W3110, *argR::cam*)	(Kiupakis et al., 2002)
EC-O	(*thi-1, relA1, Δ(pro-lac)X113[del = DE5] supE44 / F42-114(FTs) lac*)	Lab collection
DY330	(W3110, *ΔlacU169 gal490 λc1857 Δ(cro-bioA)*)	(Zeghouf et al.,2004)
MZB001	(EC-O, λ p0-*lacZ*)	This study
MZB002	{EC-O, λ (-239 to -1 nt)-*lacZ* }	This study
MZB003	{EC-O, λ (-152 to -1 nt)-*lacZ* }	This study
MZB004	{EC-O, λ (-239 to -153 nt)-*lacZ* }	This study
CY15682	(W3110, *trpR2*)	(Khodursky et al., 2000)
pSP417	pBR ori, Amp^r,	(Podkovyrov et al., 1995)
pMZB002	{pSP417, (-239 to -1 nt)-*lacZ* }	This study
pMZB003	{pSP417, (-152 to -1 nt)-*lacZ* }	This study
pMZB004	{pSP417, (-239 to -153 nt)-*lacZ* }	This study
λRS 45	*bla'-lacZsc imm21 ind* +	(Simons et al., 1987)
λRS74	*placUV5-lacZ* + *imm21 ind* +	(Simons et al., 1987)
λMZB1	Same as λRS74, but containing the p0-*lacZ* fusion	This study
λMZB3	Same as λRS45, but containing the (-152 to -1 nt)-*lacZ* fusion	This study

Table 5.2 Growth condition examined and strains compared

A

Minimal medium vs. excess tryptophan
trpR$^+$ (Min) vs. *trpR*$^+$ (Min + Trp)*
Nonstarved vs. tryptophan-starved
trpR$^+$ (Min) vs. *trpR*$^+$ (Min + 15 μg/ml indole acrylate)*
trpR$^+$ vs. *trpR2* (repressor minus)
trpR$^+$ (Min) vs. *trpR2* (Min)

Strains used were: W3110 (wild type); CY15682, (*trpR2* , repressor minus)

(Min) = Vogel and Bonner Minimal medium; (Min + Trp) = minimal + 50 μg/ml L-tryptophan.

* Time-course experiments; samples taken at different intervals.

B

Minimal medium vs. excess arginine
argR$^+$ (Min) vs. *argR*$^+$ (Min + Arg)*
Nonstarved vs. arginine-starved
argR$^+$ (Min) vs. *argR*$^+$ (cells were shifted and incubated without arginine for 2 hrs to achieve transient arginine starvation)
argR$^+$ vs. *argR*$^-$ (repressor minus)
argR$^+$ (Min) vs. *argR*$^-$ (Min)

Strains used were: W3110 (wild type); AK11(*argR::cam*)

(Min) = MD minimal medium; (Min + Arg) = MD minimal + 20mM arginine.

* Time-course experiments; samples taken at different intervals.

RNA methods

For reverse transcriptase-polymerase chain reaction (RT-PCR) analysis, total RNA was isolated with the RNeasy kit (Qiagen, Valencia, CA) and treated with RNase-free DNase (Ambion, Austin, TX). 50 ng of total RNA were subjected to RT-PCR analysis using the One Step RNA PCR kit (TaKaRa, New York, NY). Northern blots were performed using total RNA isolated from *E. coli* JCB570 grown in LB medium under aeration at 37^{o}C. Samples were collected in one hour intervals throughout the exponential and stationary phase. Five μg of total RNA per lane were loaded onto a denaturing gel containing formaldehyde, then transferred to a positively charged nylon membrane (Hybond N+, Amersham, UK). The AlkPhos direct nucleic acid labeling and detection system (Amersham, UK) was used to synthesize the oligonucleotide probe specific to *rraB* gene (5'-aacaactgatgacgctggca-3'). Hybridization, washing of the membranes, and detection of signals were carried out according the manufacturer's protocol.

For primer extension, 5' ^{32}P-labeled oligonucleotide (5'-acaccactgacattgcctccaccttt -3') was used as a primer for the RT reaction with 5 μg of total RNA (SuperScript III RNase H^{-} Reverse Transcriptase (Invitrogen, Carlsbad, CA). The primer extension products were separated on 6% polyacrylamide/7M urea gels. The dideoxy-DNA sequence ladder from the same primer was prepared using the *fmol* DNA Cycle Sequencing System (Promega, Madison ,WI).

Construction of β-galactosidase fusions

PCR amplification was used to generate DNA fragments containing three different regions: -239 to -1 nt, -152 to -1 nt, and -239 to -153 nt, upstream of *rraB*, and each fragment was cloned upstream of the *lacZ* gene in the multicopy transcriptional fusion vector, pSP417. Plasmids pMZB002 {(-239 to -1 nt)-*lacZ* }, pMZB003{(-152 to -1 nt)-*lacZ* }, pMZB004 {(-239 to -153 nt)-*lacZ* } were thus constructed. pMZB001 was used as a negative control. The *lacZ* fusion in pMZB003 was transferred onto the chromosome using the transducing lambda phage system. The fusions were transferred into λ*RS45,* whereas the negative control fusion in pMZB001 was transferred into λ*RS74* via a double recombination event (Simons et al. 1987). Plaques containing the recombinant lambda phages were isolated based on their blue plaque phenotype. The recombinant lambda phages were used to lysogenize EC-O (*Δ(pro-lacZ)*), and generated strains: MZB001 (EC-O, λp0-*lacZ*) with a chromosomal promoterless *lacZ* gene; MZB002 {EC-O, λ(-239 to -1 nt)-*lacZ*}, MZB003{EC-O, λ(-152 to -1 nt)-*lacZ*} encodes a *lacZ* gene fused to nt -239 to -1 and nt -152 to -1 of the *rraB* upstream region, respectively. All lysogens were tested for mono-lysogenization by PCR.

β-galactosidase assays

Cultures were grown with aeration at 37°C, in the medium specified in Table 5.2. Samples were collected during exponential and stationary phases. The samples were collected at 4°C and resuspended in an appropriate volume of ice-cold Z buffer (60 mM Na_2HPO_4, 40 mM NaH_2PO_4, 10 mM M KCl, 1 mM $MgSO_4$; pH 7.0) to give A_{600} in the

range from 0.6 to 0.9. β-galactosidase activities were determined from at least three independent experiments, as described in Chapter 4.

Western Immunoblotting

Western Blots were performed as described in Chapter 4.

Real-Time PCR

E. coli strains were grown in the conditions described in Table 5.2. Total RNA was isolated with the RNeasy kit (Qiagen, Valencia, CA) and treated with RNase-free DNase (Ambion, Austin, TX). To exclude the possibility of DNA contamination during RNA preparation, RNA samples were subjected to PCR amplification without prior reverse transcription. No amplification was obtained during this step. Reverse transcription of 2 μg of total RNA was performed with random hexanucleotides and SuperScript III RNase H^- Reverse Transcriptase (Invitrogen, Carlsbad, CA) according to the instructions of the manufacturer. For expression analysis, the primers specific for the genes, *rraB, trpE, argI,* and *dnaX*, were used. Real-time PCR was performed with an ABI Prism 7700 machine (Applied Biosystems) using the relative standard curve method under the universal cycling conditions (2 min at 50°C, 10 min at 95°C, 40 cycles of 15 s at 95°C, and 1 min at 60°C) as described by the manufacture. The reaction mixture (20 μl) for SYBR Green assay contained 2× SYBR Green PCR Master Mix (PE Applied Biosystems), 10 pmol of forward and reverse primers, and 5 μl of cDNA (0.1-100 ng). Reat time PCR was carried

out in a MicroAmp optical 96-well reaction plate with optical caps (PE Applied Biosystems). At each cycle, accumulation of PCR products was detected by monitoring the increase in fluorescence of the dsDNA-binding SYBR Green. After the PCR, a dissociation curve (melting curve) was constructed in the range of 60°C to 95°C. Sequence-specific standard curves were generated by using 10-fold serial dilutions of cDNA. The quantity of cDNA for the investigated genes was normalized to the quantity of *dnaX* cDNA in each sample. The *dnaX* gene encoding the DNA polymerase III holoenzyme was chosen as an internal standard because it is a ubiquitously expressed housekeeping gene that is frequently used for the normalization of gene expression in quantitative reverse transcription-PCR experiments in *E. coli*. Cycle threshold (CT) values were determined by automated threshold analysis with ABI Prism version 1.0 software. Calculations were performed with Microsoft Excel. Analysis of dissociation profiles was performed with ABI Prism version 1.6 software. Each experiment was performed at least three times with two independent RNA preparations.

RESULTS

Identification of the *rraB* promoter by DNA sequence analysis

First, the DNA sequence around the *rraB* gene was analyzed using bioinformatics tools. A promoter search using GENETYX-MAC 11.2.5 suggested the existence of two putative promoters that match the σ^{70} consensus -35 and -10 sequences. The proximal

pair is centered at 128 and 104 nucleotides upstream of the *rraB* translation start site. The distal pair is located at a further 64 nucleotides upstream of the start codon of *rraB* (Figure 5.1A). Sequence similarity search using BLAST revealed that the *E. coli* K-12 *rraB* gene and its upstream region containing the putative promoter sequence are well conserved (>=80% sequence identity) among γ-proteobacteria including *E. coli, Shigella flexneri, Salmonella typhimurium, Yersinia pestis, Erwinia carotovora* and *Photorhabdus luminescens*. Multiple sequence alignment using CLUSTAL X 1.8, among the bacterial species which have close homologues of the *E. coli* K-12 *rraB,* revealed that the sequence of the -35 and -10 regions of the putative *rraB* promoter is conserved among γ-proteobacteria (Figure 5.1B). Moreover, a protein BLAST search identified eight bacterial homologues of approximately the same length as RraB (134–153 residues) with significant sequence identity (>50%).

RraB is located at 96.4 minutes in the *E. coli* chromosome and is adjacent to *argI* which is transcribed from the opposite strand and codes for ornithine carbamoyltransferase I and is involved in arginine biosynthesis. Thus, *rraB* and *argI* are adjacent genes arranged in a head-to-head alignment on opposite DNA strands in *E. coli*. Interestingly, genome context analysis showed that the *rraB* homologues in *S. typhimurium* and *Y. pestis* are in the same head-to-head alignment with *argI*. Although a homologue of *argI* is not found near the *rraB* homologue, VC0424, in the *V. cholerae* genome, VC0424 is in a similar head-to-head alignment with VC0423, which codes for an arginine deiminase (ADI) that is involved in arginine catabolism (Figure 5.1C). Inspection of the nucleotide sequence in the *argI-rraB* intergenic region revealed an arginine repressor (ArgR) binding site ARG boxes, which consists of two neighboring 18-bp palindromic sequence separated by three nucleotides (Figure 5.1A). Based on these observations we decide to examine whether the expression of *rraB* is regulated by the

transcription factor ArgR . Earlier,the transcription of *RraB* was found to be correlated with *argI* expression in previous microarray analysis (Ramelot et al. 2003; Khodursky et al. 2000).

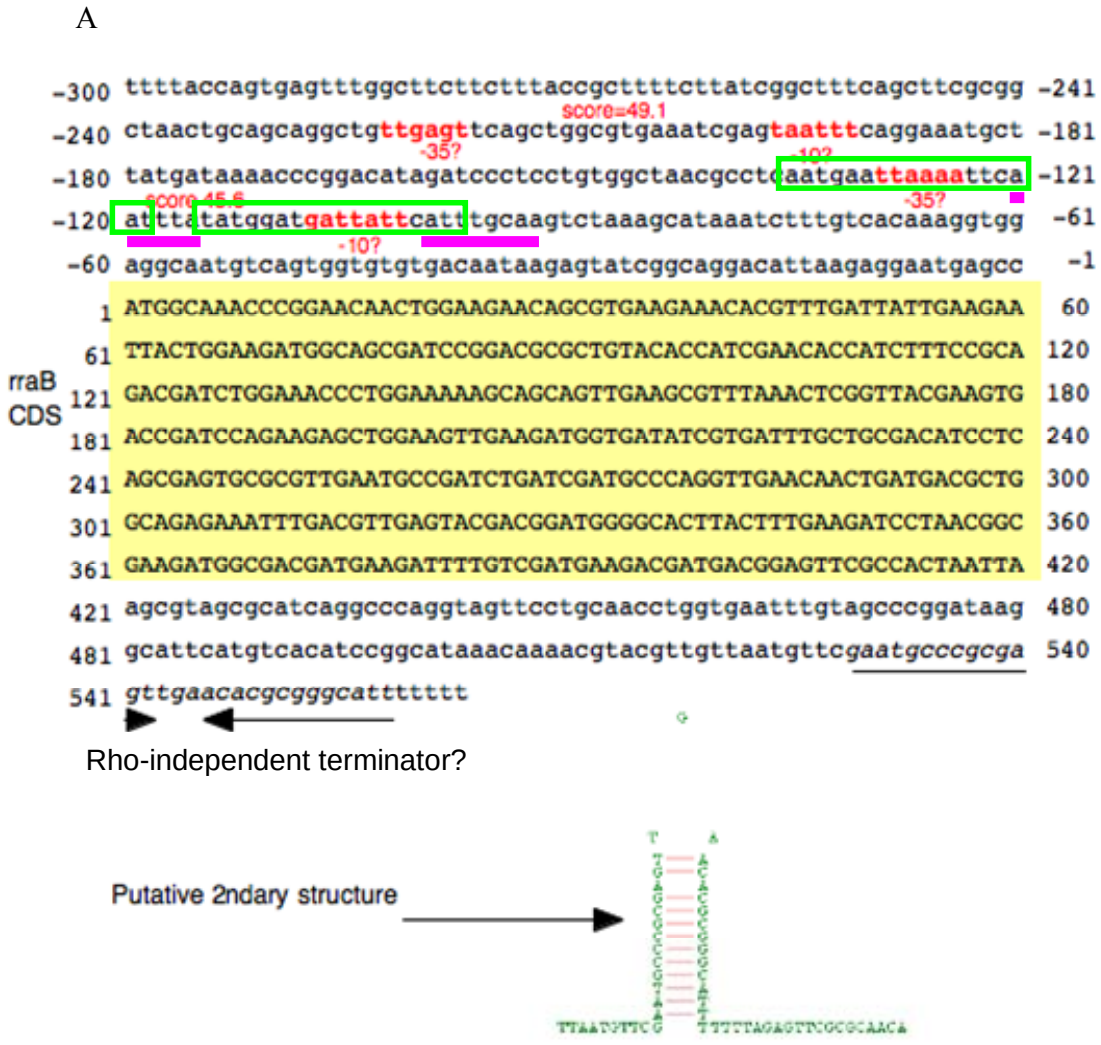

Figure 5.1 (A) Two pairs of putative promoters (red letter) that match the σ^{70} consensus -35 and -10 sequences were identified using GENETYX-MAC 11.2.5. Green box: arginine repressor binding sites (ARG boxes); underlined letter: previously identified *argI* promoter sequence.

B

Figure 5.1 (B) Multiple sequence alignment of the *argI-rraB* intergenic sequence: Abbreviations: Eca, *Erwinia carotovora* ; EcoB, *Escherichia coli* B, EcoK12, *Escherichia coli K-12* ; EcoO157, *Escherichia coli* O-157, EcoCFT073 *Escherichia coli* CFT073, Sfl, *Shigella flexner I* ; Salmonella, *Salmonella enterica ;* Ype, *Yersinia pestis* ; Plu, *Photorhabdus luminescens.* Transcript start codon, -35, -10 sites are indicated by empty boxes.

C

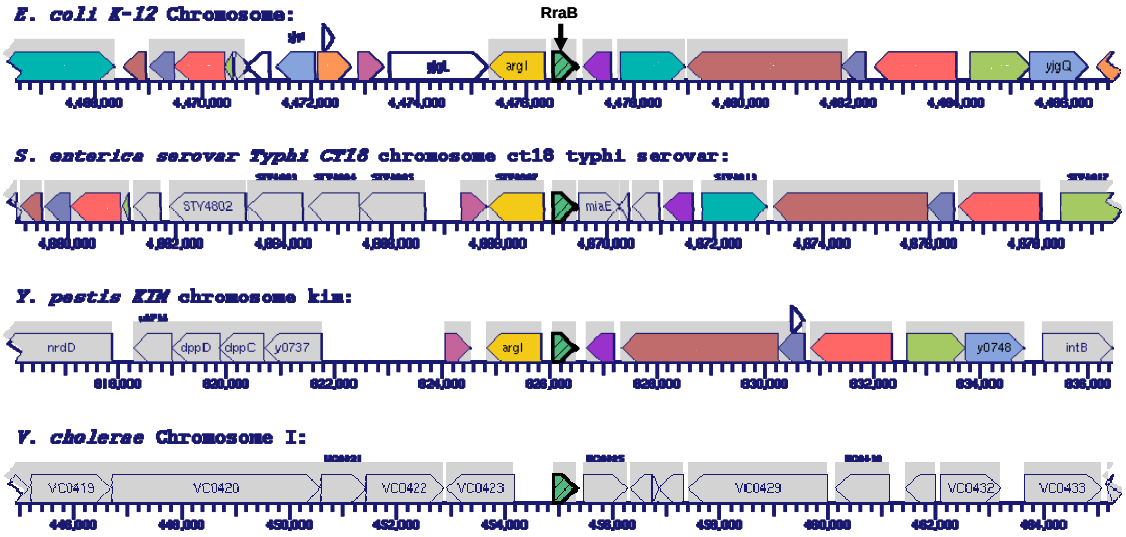

Figure 5.1 (C) Genome context analysis showed the head-to-head alignment of *rraB* and *argI* is conserved in *E. coli* and related bacteria.

Experimental identification of the *rraB* promoter

Northern blot analysis with *rraB*-specific probes revealed that *rraB* mRNA is expressed from its chromosomal copy throughout exponential and stationary phase. The transcript is around 500 bases in length, thus corresponding to a monocistronic mRNA transcribed from the putative promoter predicted by the sequence analysis (Figure 5.2A). Primer extension of RNA isolated from wild-type *E. coli* JCB570 using the 5'-32P labeled oligonucleotide probe 32P-gcggttccacgacgttaacatcttcttga revealed a single *rraB* transcript that is initiated at a T residue 88bp upstream from the ATG codon (Figure 5.2B), which corresponds to the predicted proximal promoter (-35:ttaaaa, -10:attatt). This promoter was designated P*rraB*. No other bands were detected.

A

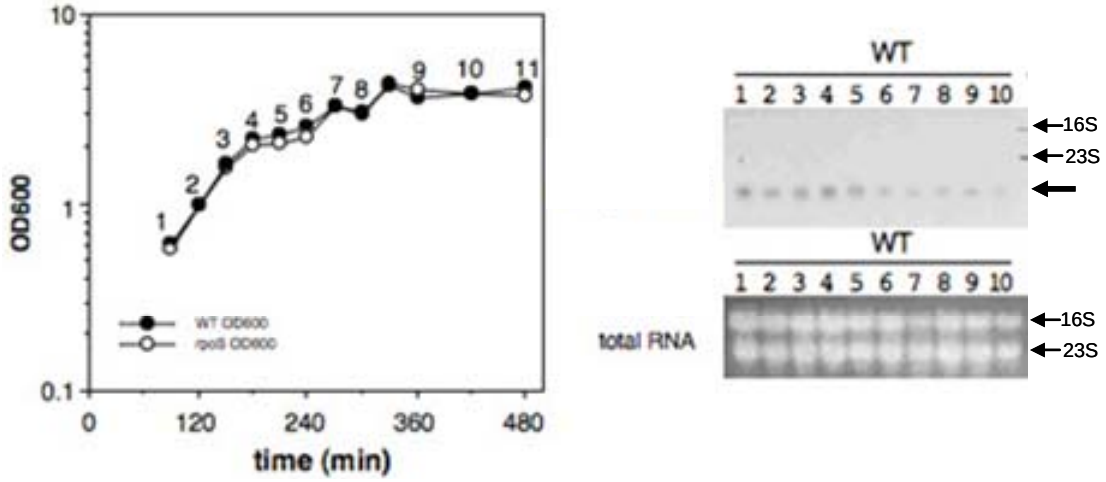

Figure 5.2 (A) Northern Blotting (left) The growth curve and sampling time. (right) *rraB* transcript is around 500 bases in length and is expressed constitutively throughout exponential and stationary phase growths.

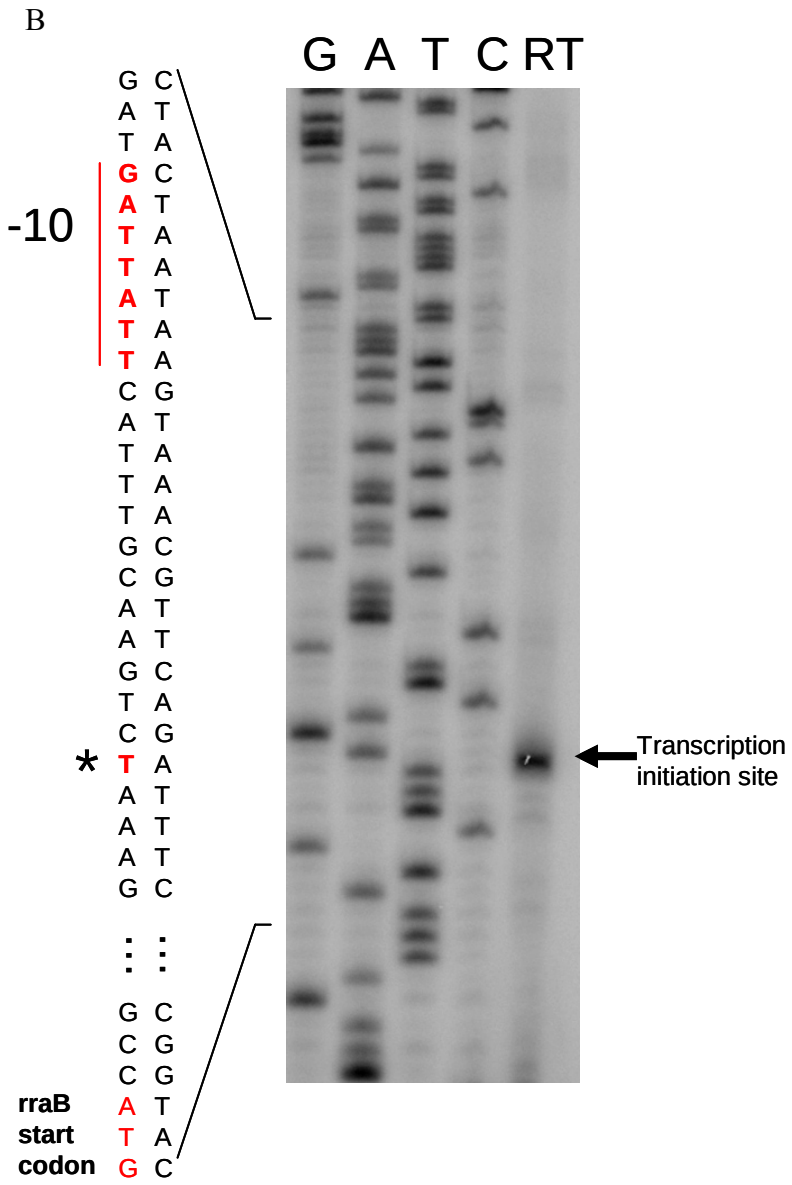

Figure 5.2 (B) Primer extension. Five µg total RNA isolated from *E. coli* JCB570 cells grown to log phase (A600 = 0.7) was reverse transcribed using the primer (5'-acaccactgacattgcctccaccttt -3') complementary to *rraB*. Arrow: the reverse transcription product.

The promoter activity of P*rraB* was further analyzed using l*acZ* transcriptional fusions. The different regions upstream of *rraB* extending up to the putative distal promoter as shown in Figure 5.3A, were amplified by PCR and cloned upstream of the *lacZ* gene in the low copy transcriptional fusion vector, pSP417. In this way, we generated plasmids pMZB002 {(-239 to -1 nt)-lacZ}, pMZB003{(-152 to -1 nt) -lacZ }, and pMZB004 {(-239 to -153 nt)-lacZ }; pMZ001 was the negative control vector.

To rule out the possibility that differences in the β-galactosidase activity expressed from the above transcriptional fusions might be partially due to plasmid copy number effects, we made single chromosomal copy isolates of each construct using the transducing lambda phage system (Simons et al. 1987). The *lacZ* fusions in pMZ001, pMZB002, pMZB003 were transferred into either λRS74 or λRS45 via a double recombination event. Subsequently, *E. coli* strain EC-O was lysogenized with the recombinant phages to generate strains carrying a single copy of each promoter-*lacZ* fusion.

As shown in Figure 5.3B, strain MZB003{EC-O, λ(-152 to -1 nt)-*lacZ* }, with the *rraB* upstream region including the proximal promoter fused to *lacZ*, showed identical levels of β-galactosidase activity to those observed in MZB002 {EC-O, λ(-239 to -1 nt)-*lacZ* } which contains a fusion to the *rraB* upstream region including both the proximal and the distal putative promoter sequences. In contrast, MZB004 {EC-O, λ(-239 to -153 nt)-*lacZ*} containing a fusion to -239 to -153 nt of the *rraB* upstream region that lacks the proximal promoter region did not give any activity higher than the background. Thus, the transcriptional fusion experiments also confirmed that the *rraB* is transcribed from the proximal promoter (P*rraB*).

In Chapter 4 we showed that expression of the *rraA* gene is induced in stationary phase. We now examined the transcription of *rraB* in both the exponential and

stationary phase. In contrast to *rraA*, the transcription level of *rraB* remained unchanged during various growth phases. Specifically, there is no change in the β-galactosidase activities from the P*rraB-lacZ* fusion in cells grown in exponential or stationary phases (Figure 5.3C). Northern blot analysis also showed that the *rraB* mRNA level stays same during both growth phases (Figure5.2).

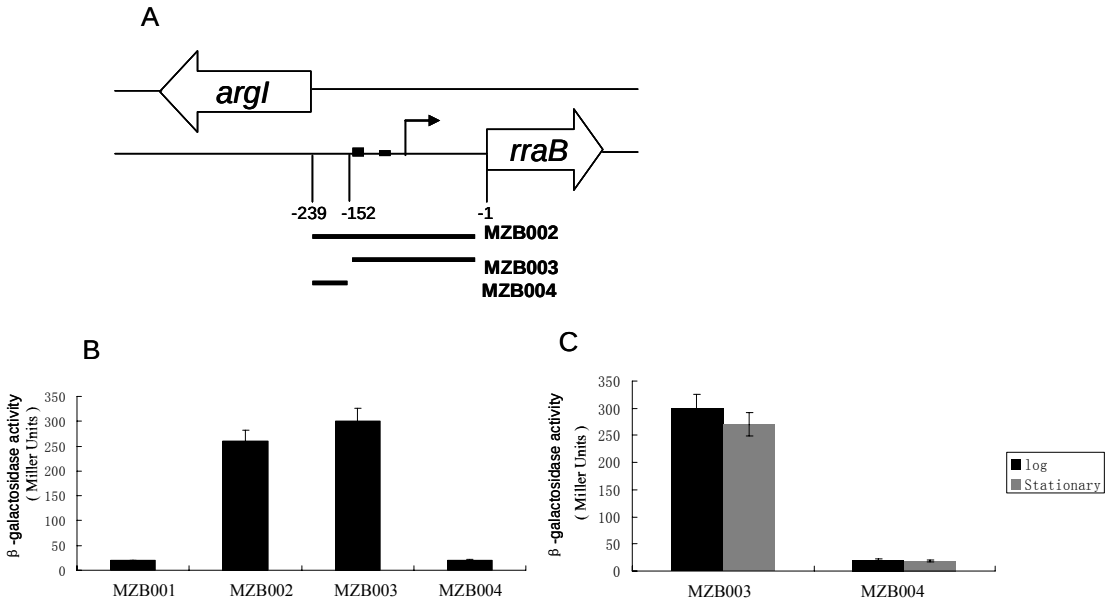

Figure 5.3 (A) Schematic of the transcriptional *rraB –lacZ* fusions used in this study. (B) and (C): β-galactosidease activities in MZB001, MZB002, MZB003 and MZB004 cells. MZB001 (EC-O, λ p0-*lacZ*) has a chromosomal promoterless *lacZ* gene; strain MZ002{EC-O, λ (-239 to -1 nt)-*lacZ* } encodes a *lacZ* fusion to nt -239 to -1 of the *rraB* upstream region; MZ003 {EC-O, λ (-152 to -1 nt)-*lacZ* } encodes a *lacZ* fusion to nt -152 to -1 of the *argI-rraB* intergenic region; MZ004{EC-O, λ (-239 to -153 nt)-lacZ } encodes a *lacZ* fusion to nt -239 to -153 of the *rraB* upstream region. Cells were grown in LB under aeration at 37°C, and harvested in log phase (A600= 0.5) and stationary phase (A600= 1.6). Samples were normalized by O.D. and enzymatic activities were measured in Miller units. The data presented are the average of at lease three independent determinations and the error bars correspond to the standard deviation.

RraB expression is not affected by tryptophan availability

Previous DNA microarray analysis of gene expression in response to physiological and genetic changes affecting tryptophan metabolism showed that expression of the *rraB* gene is repressed in response to tryptophan starvation (Khodursky et al. 2000). To evaluate the expression pattern of *rraB* in the context of tryptophan availability, we examined the transcriptional activity level and steady state mRNA level from *rraB* under three conditions, which have distinct effects on tryptophan metabolism (Table 5.2). First, excess tryptophan was added to cultures growing in minimal medium (+Trp). Second, cultures were partially starved of tryptophan (-Trp) by addition of the tryptophan analog, indole acrylate. The presence of indole acrylate in the growth medium relieves both repression and attenuation of the *trp* operon because it prevents the *trp* repressor from acting and inhibits the charging of tRNATrp by tryptophanyl-tRNA synthetase. Third, the effect of inactivating the tryptophan repressor was examined using a strain which does not produce a functional trp repressor because of a frameshift mutation in *trpR* (*trpR2*).

As shown in Figure 5.4, similar β-galactosidase activities of the *PrraB::lacZ* fusion were obtained from cell grown in normal minimal medium, with excess tryptophan or with tryptophan starvation. This indicates that *rraB* promoter activity is not altered by changes in tryptophan availability.

The steady state level of the *rraB* gene was examined by real-time PCR. Cells were subjected to tryptophan starvation induced by addition of indole acrylate, to excess tryptophan, or neither, and the changes in mRNA levels with time were measured and compared.

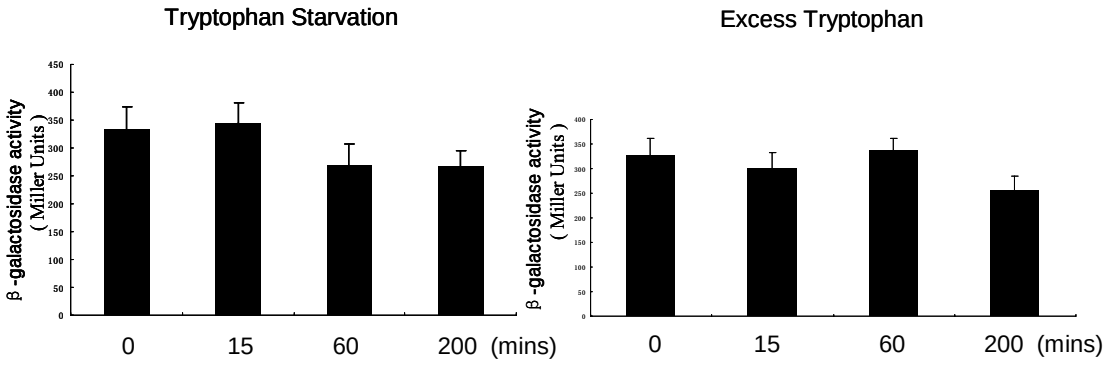

Figure 5.4 β-galactosidase activities from the P*rraB::lacZ* fusion were measured with excess tryptophan (+50 μg/ml L-tryptophan) or with tryptophan starvation (+15 μg/ml indole acrylate), as described in the Material and Methods. Samples taken at different intervals as indicated.

The change in *rraB* mRNA level was also analyzed in *trpR* mutant and its parental strain W3110. *trpE*, encoding the anthranilate synthase component I, was used as a positive control because it belongs to the *trp* operon and is known to be negatively regulated by TrpR. Equal amounts of total RNA from cells grown under the various experimental conditions described above were reverse transcribed and used to quantitate the transcript levels of *rraB* and *trpE* genes by real-time PCR. The data were normalized to the expression of the *dnaX* gene in the two strains and different growth conditions. Instead of using a specific fluorescence-labeled probe (TaqMan) for the detection of amplicons, we used SYBR green dye. Since SYBR green binds only to double-stranded and not to single stranded DNA molecules, PCR product concentrations can be recorded at each cycle, yielding a real-time amplification curve suitable for automated threshold analysis and quantification. The specificity of SYBR green-based real-time RT-PCR was ascertained by comparing the melting temperatures (Tms) of the amplification products from different samples to that of the positive control sample. Dissociation curves of all PCR products showed a sharp peak at the expected Tm of the products (Zhao and

Georgiou, unpublished data). These results indicate that each real-time PCR specifically amplified the target DNA. A twofold difference in transcription was interpreted as a significant difference in expression under different conditions. As shown in Table 5.4, *trpE* mRNA abundance is decreased in response to excess tryptophan {(6.67±0.55)-fold decrease after 15 mins, (3.75±0.46)-fold decrease after 60 mins}. It is dramatically increased in response to tryptophan starvation {(259.27±30.89)-fold increase after 15 mins, (392.92±38.67) -fold increase after 60 mins}. Expression of *trpE* increased (18.12±1.36) fold in the *trpR* mutant compared to the wild type. The results obtained with *trpE* confirmed the reliability of the real-time PCR system. However, contrary to the earlier microarray data, the *rraB* mRNA level was not affected by any of the physiological or genetic changes in tryptophan metabolism tested.

We further examined the abundance of the RraB protein under these conditions by Western blotting using strain DY330-rraBSPA in which sequential peptide affinity (SPA) tags are fused to the C terminus of the *rraB* open reading frame within the chromosome. Consistent to what was observed in steady mRNA level, the abundancy of RraB protein was not influenced by changes in tryptophan availability (Zhao and Georgiou, unpublished data).

The regulation of *rraB* expression is not affected by arginine metabolism

The expression of *rraB* expression as a function of arginine availability was also investigated. The influence of changes in arginine availability was examined following arginine up shift and down shift. First, excess arginine (20mM) was added to cultures growing in minimal medium (+Arg). Second, arginine-grown cells were shifted and incubated without arginine for two hours to achieve transient arginine starvation. Third,

the arginine repressor was inactivated to examine its effect on *rraB* transcription. The transcription activity of P*rraB*, deduced from the β-galactosidase activity levels from cells grown in medium with excess amount of arginine or without arginine, were in the same range as those from cells grown in medium with a normal amount of arginine (Figure5.5). In addition, the steady level of *rraB* mRNA was measured by real-time PCR using *argI* as a positive control. As shown in Table 5.4, *argI* mRNA level decreased in response to excess arginine {(1.92±0.23)-fold decrease after 15 mins, (2.86±0.32)-fold decrease after 200 mins}. It increased under condition of arginine starvation {(144.98±20.45)-fold increase after 2hours}. Expression of *argI* increased (93.51±12.32) fold in the *argR* mutant compared to the wild type. The expected pattern of *argI* expression validated the real-time PCR system. In contrast, no statistically significant change in the level of *rraB* mRNA was detected under the conditions tested.

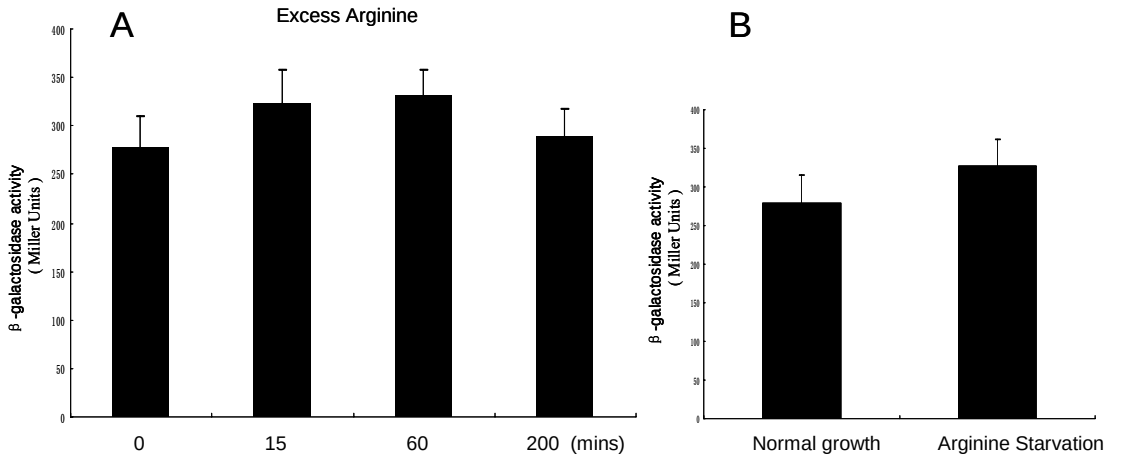

Figure 5.5 β-galactosidase activities of the P*rraB::lacZ* fusion were measured with excess arginine (+20mM arginine) or with arginine starvation, as described in the Material and Methods. Samples taken at different intervals as indicated.

Table 5.4 mRNA abundance measured by Real-Time PCR		
Growth condition examined and strains compared	Relative Abundance	
Tryptophan Metabolish	*rraB*	*trpE*
trpR$^+$ (Min)	1	1
trpR$^+$ (Min + Trp) (15min)	1.06	0.15
trpR$^+$ (Min + Trp) (60min)	1.35	0.27
trpR$^+$ (Min, tryptophan-starved) (15min)	1.21	259.27
trpR$^+$ (Min, tryptophan-starved) (60min)	0.83	392.92
trpR2 (repressor minus)	1.02	18.12
Arginine Metabolism	*rraB*	*argI*
argR$^+$ (Min)	1	1
argR$^+$ (Min + Arg) (15min)	0.99	0.52
argR$^+$ (Min + Arg) (200min)	0.87	0.35
argR$^+$ (Min, arginine-starved)	1.11	144.98
ArgR- (repressor minus)	1.36	93.51

Strains used were W3110 (wild type); CY15682, (*trpR2*), AK11(*argR::cam*). The results were the average of three independent measurements (variance was ≦20% of the mean). mRNA abundance were measured as described in Material and Methods.

Toward understanding the physiological significance of RraA and RraB

Three null mutant strains JQ004 (*rraA*-), JG002 (*rraB*-) and JG004 (*rraA*- *rraB*-) were used to examine the effect of RraA and RraB on growth under different condistions. Earlier, DNA microarray analysis by K Lee at Stanford had revealed that the absence of *rraA* or *rraB* altered the abundance of a small set of transcripts. Most of these RNAs were destabilized in the *rraA* or *rraB* deleted strains, consistent with the inhibitory effect of RraA/RraB on the endoribonucleolytic activity of RNase E. However, the three null mutant strains exhibited normal growth under typical growth conditions (37^{o}C, in LB

media). To further discern any phenotypes resulting from deletion of the RNAse E inhibitors the *rraA- rraB-* double mutant (JG004) was subjected to Phenotype MicroArray (Biolog, Hayward, CA) analysis, which is a comprehensive method that determines the phenotype of bacterial mutant. These studies showed that the *rraA- rraB-* double mutant is unable to grow when L-Tryptophan was used as the sole nitrogen source and it was more susceptible to toxic compounds, e.g. patulin, hexachlorophene, 8-hydroxyquinoline.

DISCUSSION

The identification of RraB as the second protein inhibitor of RNase E led to the discovery of a new mechanism for the global regulation of mRNA stability. In comparison RraB modulates the composition of the degradosome and differentially affects the ability of the RNA degrading machinery to recognize and cleave different RNAs. Understanding the regulation of *rraB* gene expression is essential to pinpointing the physiological significance of these effects. RT-PCR and Northern blot analysis confirmed that *rraB* is expressed from its chromosomal copy throughout exponential and stationary growth phases. Primer extension and *lacZ* transcriptional fusion experiments demonstrated that *rraA* is transcribed from its own promoter (P*rraB*) located 88 bp upstream from the translation start codon. In the genomes of *E. coli* and other bacteria, such as *S. typhimurium, Y. pestis* and *V. cholerae, rraB* homologues are arranged in a head-to-head alignment with the adjacent gene, *argI. argI,* a member of the arginine regulon, encoding the ornithine carbamoyltransferase I, is known to be regulated by the

specific repressor, ArgR. The binding site for ArgR i.e. ARG boxes, is located in the *rraB-argI* intergenic region and overlaps the *argI* promoter in *E. coli.* Interestingly, the -10 and -35 boxes of the experimentally confirmed *rraB* promoter completely reside in these two ARG boxes. It was presumed that by binding to the -10 and -35 boxes of the promoter, ArgR would block the access of DNA polymerase to both the *rraB* and *argI* promoter elements, thus preventing transcription initiation. In fact, this simultaneous regulation of two divergent promoters by ArgR has been described for a number of adjacent genes, for example, *argE* and *argC*, both are involved in arginine biosynthesis; *argG* and *metY*, *argG* is involved in arginine biosynthesis and *metY* encodes one of the two methionine tRNAs required for the initiation of protein synthesis (Krin et al. 2003).

This assumption that *rraB* expression may be related to arginine availability was further supported by several independent, global analyses. Previous microarray analysis indicated that the expression of *rraB* (*yjgD)* is correlated with expression of *argI* in response to the changes in tryptophan metabolism. The microarray data suggested that the expression of *argI* and *rraB* genes is repressed in response to tryptophan starvation (Khodursky AB et al. 2000; Ramelot et al. 2003). Consistent with these observations the *rraA- rraB-* double mutant was unable to grow when tryptophan was used as the sole nitrogen source in a phenotype microarray analysis. The expression of *rraB* gene in response to that the availability of tryptophan or arginine metabolism was examined. Contrary to the microarray data, we found that expression of *rraB* does not respond to the changes in neither tryptophan nor arginine availability. This unexpected result emphasizes that information from public databases should be used with caution.

As with other posttranslational mechanisms of regulation, RraB may facilitate rapid alterations in RNA decay and/or processing in response to specific environmental stimuli, although at this time, cellular conditions that may affect RraB production and/or

activity have not been identified. While homologues of RraA are widely distributed among archea, proteobacteria and plants, RraB homologues are found only in γ-proteobacteria, suggesting that these proteins may have a more specialized role in modulating RNA degradation. The different effect on RNA decay via its distinctive interactions with RNase E and degradosome remodeling also argues that modulation of RNA stability by RraB may be a response to different stimuli (e.g. stress response) in the extracellular or intracellular environment. There are several explanations for the lack of a strong phenotype in the *rraA, rraB* deletion strains JQ004 (*rraA*-), JG002 (*rraB*-) and JG004 (*rraA- rraB*-). First, since RraA and RraB act as inhibitors of RNase E, their maximal effect on cell physiology is expected under conditions where their cellular concentrations are elevated. Therefore, it is not surprising that so far we have only detected rather subtle defects of these null mutants. The lack of a strong phenotype for the *rraA rraB* null mutation may also be due to the presence of additional cellular proteins capable of modulating the catalytic function of RNase E and whose functions may partially overlap that of RraA/RraB.

Chapter 6: Conclusions and Recommendations

The significance of the RNase E based degradosome in RNA metabolism has been studied extensively over the past decade. However, the mechanistic details of how the ribonucleolytic activity and degradosome composition are modulated and how this in turn affects the decay of transcripts, remains to be resolved. In this work, different approaches were used to understand and characterize the newly discovered regulatory proteins which modulate RNA abundance by interacting with the RNase E. Comparison of the actions of RraB and RraA revealed a novel mechanism whereby the selective remodeling of the degradosome by adaptor proteins serves to dramatically modulate RNA degradation and processing in *E. coli*. A system was developed for investigating the function of the degradosome and the role of RraA/RraB in RNA processing *in vitro*. The expression of RraA and RraB is regulated differently, suggesting their physiological role is to modulate transcript abundance in response to distinct changes in the cellular environment.

The discovery of RraA as the prototypical protein inhibitor of RNase E-mediated RNA decay prompted us to look for additional cellular proteins which might participate in the regulation of RNase E activity. In a manner analogous to RraA, RraB was isolated as a consequence of its ability to inhibit the cleavage of the *dsbC* mRNA by RNase E. Similar to RraA, RraB inhibited endoribonucleolytic cleavage of the 5' UTR of *rne* transcripts strongly enough to circumvent the autoregulation of *rne* that normally maintains the level of the enzyme within a narrow range. RraB physically interacts with full length RNase E *in vivo* and *in vitro* with an affinity that is nearly indistinguishable

from RraA. Importantly, however, RraA and RraB interact differently with the enzyme: Co-precipitation analysis with a set of RNase E mutants bearing deletions within the degradosome organizing domain demonstrates that RraB recognizes a well defined epitope located between aa residues 694-727 whereas RraA requires both the N-terminus and the distal C-terminus (aa residues 1045-1061) of RNase E for binding. Proteomic analysis further shows that RraA and RraB exert dramatic, distinct, and inhibitor-specific effects on the composition of the degradosome, most notably on the amount of degradosome-bound PNPase and RhlB. Microarray analysis reveals that RraA and RraB exert differential effects on the ability of the RNA degrading machinery to cleave various mRNAs, in turn giving rise to distinct transcript profiles. Certain transcripts are stabilized by RraA, others by RraB and yet a third class is stabilized by either inhibitor. Notably, the global transcript abundance profiles associated with RraA or RraB expression are dissimilar to the profile observed during RNase E deficiency. Our results revealed a novel mechanism whereby binding of inhibitors to distinct sites within RNase E serves to differentially regulate RNA cleavages in *E. coli*.

As a continuing study to explore the molecular details of this novel mechanism, we developed a system for the partial reconstitution of degradosomes and determination of the consequences of RraA and RraB binding to the kinetics of RNA degradation *in vitro*. To overcome the susceptibility to proteolytic degradation of RNase E CTH, we made a series of C-terminal truncated forms of RNase E containing the binding sites for RraA, RraB and some of the degradosome components. We have developed protocols to successfully overexpress and purify the C-terminal truncated RNase E proteins at the milligram scale under denaturing condition. RraA, RraB, PNPase, RhlB and enolase expression constructs have been made and the proteins have been purified via ion

exchange chromatography or affinity chromatography. This work laid the foundation for reconstituting partial degradosomes *in vitro* and for examining the effect of RrA/RraB on the composition of the complex. A system for the detailed kinetic analysis of degradation of a model short RNA substrate (P-BR14-FD) has been established. RNase E845 (1-845aa) was found to have the same catalytic properties as N-RNase E (1-499aa) for P-BR14-FD and can also be used to study the effects of RhlB, enolase, RraB and RraA. Interestingly, the inhibition parameters of RraA/B on RNase E-mediated RNA cleavage seem to vary depending on RNA substrates of different length and structure.

To understand the physiological significance of the differential modulation of *E. coli* RNA decay and processing by inhibitory proteins, we studied the regulation of RraA/ RraB expression. Transcription of *rraA* had been proposed to occur from the upstream *menA* promoter which was shown to be σ^{70}-dependent (Meganathan 1996). In contrast to these earlier results, we demonstrate that *rraA* is transcribed predominantly from its own promoter (P*rraA*) located in the *menA* - *rraA* intergenic region. Transcription from P*rraA* is σ^{s}-dependent and is induced upon entry into stationary phase. Moreover, the synthesis of RraA is regulated at the post-transcriptional level by RNase E, suggesting the existence of a feedback regulatory circuit whereby induction of *rraA* transcription occurs in a σ^{s}-dependent manner and results in inhibition of RNase E activity, in turn decreasing the degradation rate of the *rraA* transcript and enhancing the cellular level of the RraA protein.

We showed that *rraB* is transcribed from a promoter (P*rraB*) which is divergent from the *argI* promoter and overlaps with the arginine repressor binding site (ARG boxes) located in the *argI-rraB* intergenic region. Based on previous gene chip analysis

data, we examined the possibility that the expression of *rraB* is regulated in response to changes in the availability of tryptophan or arginine. However, we find that, contrary to earlier published data, there is no evidence that *rraB* promoter activity, mRNA abundance and RraB protein level are affected by changes in metabolism of either amino acid. In contrast to *rraA, rraB* is expressed constitutively during exponential and stationary phases.

RECOMMENDATION FOR FURTHER STUDIES

As described in Chapter 4, we found RraA and RraB exert a small effect on the cleavage of the short RNAs (P-BR14-FD and p-BR13-Fl) by N-RNase and RNase E845 *in vitro*. In contrast, RraA and RraB significantly inhibit the cleavage of a longer transcript (149 nt p23) by the partially purified full-length RNase E. Thus, it is likely that the effect of RraA/RraB is dependent on the assembled degradosome complex and on the intrinsic character of the substrate RNAs. To understand both the function of degradosome and of the role of RraA/RraB, purified degradosome component proteins (C-terminal truncated RNase E proteins, PNPase, RhlB and enolase) could be used to reconstitute the degradosome *in vitro* and determine the consequences of RraA and RraB binding to the kinetics of RNA degradation. The subunit stoichiometry of the reconstituted degradosomes complexes could be evaluated by SDS-PAGE. The effect of RraA/RraB on the composition of the complex could be determined by adding different molar ratios of these proteins. Subsequently, the reconstituted degradosomes with or without the inhibitory proteins could be used to determine the kinetics of cleavage of RNAs of different length and structure. For examples, the 14 nt FRET RNA (P-BR14-

FD) could be used as a model short RNA whereas the 147 nt transcript p23 could be used to evaluate how the degradosome components and RraA/RraB affect the hydrolysis of structured RNAs. Michaelis-Menten parameters and enzyme inhibition constants for RrA/RraB could be obtained. It would also be of interest to examine the impact of the phosphorylation status of the RNA 5' terminus since RraA has been shown to exhibit a stronger inhibitory effect on the cleavage of the RNA with a 5' triphosphate vs. a 5'monophosphate group (Lee, K., Cohen, S.N., and Georgiou, G., unpublished).

Alternative strategies should be considered to understand the regulation of *rraB* expression. Screening a plasmid-encoded genomic library in the strain with the chromosomal P*rraB::lacZ* fusion is a promising way to identify genes encoding regulatory factors for *rraB* expression. Gene products that up-regulate the transcription from *rraB* promoter will enhance the β-galactosidase activity encoded from the P*rraB::lacZ* fusion; hence a positive regulator will be identified as blue colonies on X-gal plates. The genes down-regulating *rraB* expression will be identified as white colonies as a result of decreased β-galactosidase activity. Complementarily, a transposon mutagenesis library could be used to screen the *rraB* transcription regulators based on loss-of-function. Moreover, analysis of the structural characteristics of RraB by solving its crystal structure will also provide key insight about its physiological function and regulation.

Gene chip studies showed that overexpression of RraA and RraB differentially altered the steady state level of hundreds of transcripts in *E. coli.* Microarray analysis carried out by other groups revealed that all of the four degradosome components, including. RNase E, PNPase, RhlB, and enolase, are required for the normal turn over of

mRNA. It is of great interest to determine to what extent these degradosome components and inhibitory proteins that modulate RNA degradation affect the abundance of protein in cell. Shotgun proteomics, in which proteins are digested into peptide fragments, and analyzed by 2D-HPLC coupled with tandem mass spectrometry LC/LC/MS/MS (Mirgorodskaya et al. 2000; Washburn et al. 2001; Yao et al. 2001; Conrads et al. 2002; Yi et al. 2005), provides a high throughput measurement of the complete set of proteins expressed by a genome. Various approaches have been developed to quantify the relative abundance of proteins by introducing internal reference standards. Recently, Marcotte et al. developed a method for large-scale absolute protein expression measurements (APEX) by mass spectrometry (Marcotte, E., personal communication). Proteomic profiles of cells under the following conditions: 1) RraA or RraB overexpression, 2) deletion mutation in RraA or RraB, and 3) deletion mutation in the major degradasome components, could be determined using these quantitative proteomic studies. Furthermore, comparison between the protein expression profiles with the transcript profiles will allow us to determine whether protein abundance levels are correlated to mRNA steady levels, thus leading to an estimation of the relative contributions of transcriptional and translational regulation in the steady state levels of proteins.

The lack of a strong phenotype for the *rraA rraB* null mutant strain may be due to the presence of additional cellular proteins capable of modulating the catalytic function of RNase E and whose functions may partially overlap that of RraA/RraB. As both RraA and RraB were isolated as a result of their abilities to stabilize *dsbC* mRNA, other proteins that bind to RNase E and selectively affect the stability of sets of transcripts with different features could be discovered by the application of alternative genetic screens.

For example, a transcriptional fusion, in which the autoregulatory region of *rne* gene fused to an antibiotic resistance gene (e.g. *rne-kan*) or an enzyme gene (e.g. *rne-lacZ*), could be used for the screening. Genes encoding other *E. coli* proteins that inhibit the activity of RNase E based degradosome could be identified by screening a plasmid-encoded genomic library in the *rraA rraB* mutant background. Any cellular proteins that suppress the catalytic activity of RNAse E activity would result in less cleavage of the *rne-kan* or *rne-lacZ* mRNA, thus producing more antibiotic resistant protein or higher β-galactosidase activity. Hence, RNase E inhibitor genes will be identified as colonies able to grow on higher concentration of antibiotic plates or as bluer colonies on X-gal plates. The effect of the respective proteins on the inhibition of RNase E activity, on degradosome composition, and on the transcript profile could also be determined.

Author's Publication List

Zhao M, Zhou L, Kawarasaki Y, Georgiou G. Regulation of RraA, the Protein Inhibitor of RNase E-mediated RNA Decay. *Journal of Bacteriology*, 2006 May;188(9):3257-63.

Gao J, Lee K, Zhao M, Qiu J, Zhan X, Saxena A, Moore CJ, Cohen SN, Georgiou G. Differential Modulation of E. coli mRNA Abundance by Inhibitory Proteins that Alter the Composition of the Degradosome. *Molecular Microbiology*, 2006 Jul; 61(2):394-406.

Xu L, Zhao WL, Xiong SM, Su XY, Zhao M, Wang C, Gao YR, Niu C, Cao Q, Gu BW, Zhu YM, Gu J, Hu J, Yan H, Shen ZX, Chen Z, Chen SJ. Molecular Cytogenetic Characterization and Clinical Relevance of Additional, Complex and/or Variant Chromosome Abnormalities in Acute Promyelocytic Leukemia. *Leukemia*. 2001 Sep;15(9):1359-68.

Zhang QH, Ye M, Wu XY, Ren SX, Zhao M, Zhao CJ, Fu G, Shen Y, Fan HY, Lu G, Zhong M, Xu XR, Han ZG, Zhang JW, Tao J, Huang QH, Zhou J, Hu GX, Gu J, Chen SJ, Chen Z. Cloning and Functional Analysis of cDNAs with Open Reading Frames for 300 Previously Undefined Genes Expressed in CD34+ Hematopoietic Stem/Progenitor Cells. *Genome Research*. 2000 Oct; 10(10):1546-60.

Zhao M, Chen S. Centric and Pericentric Chromosome Rearrangements in Hematopoietic Malignant Diseases. *Hereditas*. 2001; 23(4): 384-388.

Zhao M, Chen SJ, Chen Z. 2002. Gene Amplification in Human Tumor: the Biological and Clinical Significance, P60-75. in Chen SJ, Huang W, Fan QS (ed.), *Technologies in Human Genome Research*. People's Military Medical Publisher, Beijing, China.

Zhao M, Chen B, Wang L, Xu L, Cao Q, Su X, Chen S. Establishment and Application of Multiplex FISH in Detection of the Complex Chromosome Abnormalities in Leukemia. *Chinese Journal of Medical Genetics*. 2002 Oct; 19(5):375-8.

Chen S, Zhao M, Chen Z. Progress of All-Trans Retinoic Acid Plus Arsenic Trioxide in Treating Active Promyelocytic Leukemia. *Tumor*. 2001 Nov; 21(6):415-418.

Wu Y, Xue Y, Zhao M, Chen S, Pan J, Lu D. Clinical and Experimental Study of Two Cases of Myelodysplastic Syndrome with t(3; 5) (q25; q34) Translocation. *Chinese Journal of Hematology*. 2002 Jun; 23(6):304-6.

Bibliography

Abee, T. and J. A. Wouters (1999). "Microbial stress response in minimal processing." Int J Food Microbiol **50**(1-2): 65-91.

Adams, P., R. Fowler, N. Kinsella, G. Howell, M. Farris, P. Coote and C. D. O'Connor (2001). "Proteomic detection of PhoPQ- and acid-mediated repression of Salmonella motility." Proteomics **1**(4): 597-607.

Anderson, J. S. J. and R. Parker (1998). "The 3' to 5' degradation of yeast mRNA is a general mechanism for mRNA turnover that requires the SKI2 DEVH box protein and 3' to 5' exonucleases of the exosome complex." EMBO J **17**: 1497-1506.

August, J. T., P. J. Ortiz and J. Hurwitz (1962). "Ribonucleic acid-dependent ribonucleotide incorporation. I. Purification and properties of the enzyme." J Biol Chem **237**: 3786-93.

Babitzke, P. and S. R. Kushner (1991). "The Ams (altered mRNA stability) protein and ribonuclease E are encoded by the same structural gene of Escherichia coli." Proc Natl Acad Sci U S A **88**(1): 1-5.

BAKER, K. E. and C. CONDON (2004). Under the Tucson sun: A meeting in the desert on mRNA decay. RNA. **10:** 1680-1691.

Becker, G. and R. Hengge-Aronis (2001). "What makes an *Escherichia coli* promoter sigma(S) dependent? Role of the -13/-14 nucleotide promoter positions and region 2.5 of sigma(S)." Mol Microbiol. **39**: 1153-65.

Belasco, J. G. (1993). Control of mRNA Stability. San Diego, Academic Press.

Bernstein, J. A., A. B. Khodursky, P. H. Lin, S. Lin-Chao and S. N. Cohen (2002). "Global analysis of mRNA decay and abundance in Escherichia coli at single-gene resolution using two-color fluorescent DNA microarrays." Proc Natl Acad Sci U S A **99**(15): 9697-702.

Bernstein, J. A., P. H. Lin, S. N. Cohen and S. Lin-Chao (2004). "Global analysis of Escherichia coli RNA degradosome function using DNA microarrays." Proc Natl Acad Sci U S A **101**(9): 2758-63.

Blattner, F. R., G. Plunkett, 3rd, C. A. Bloch, N. T. Perna, V. Burland, M. Riley, J. Collado-Vides, J. D. Glasner, C. K. Rode, G. F. Mayhew, J. Gregor, N. W. Davis, H. A. Kirkpatrick, M. A. Goeden, D. J. Rose, B. Mau and Y. Shao (1997). "The complete genome sequence of Escherichia coli K-12." Science **277**(5331): 1453-74.

Blum, E., B. Py, A. J. Carpousis and C. F. Higgins (1997). "Polyphosphate kinase is a component of the Escherichia coli RNA degradosome." Mol Microbiol **26**(2): 387-98.

Bohannon, D. E., N. Connell, J. Keener, A. Tormo, M. Espinosa-Urgel, M. M. Zambrano and K. Roberto (1991). "Stationary-phase-inducible "gearbox" promoters: differential effects of *katF* mutations and role of sigma 70." J Bacteriol. **173**: 4482-492.

Butland, G., J. M. Peregrin-Alvarez, J. Li, W. Yang, X. Yang, V. Canadien, A. Starostine, D. Richards, B. Beattie, N. Krogan, M. Davey, J. Parkinson, J. Greenblatt and A. Emili (2005). "Interaction network containing conserved and essential protein complexes in Escherichia coli." Nature **433**(7025): 531-7.

Bycroft, M., T. J. Hubbard, M. Proctor, S. M. Freund and A. G. Murzin (1997). "The solution structure of the S1 RNA binding domain: a member of an ancient nucleic acid-binding fold." Cell **88**(2): 235-42.

Callaghan, A. J., J. P. Aurikko, L. L. Ilag, J. Gunter Grossmann, V. Chandran, K. Kuhnel, L. Poljak, A. J. Carpousis, C. V. Robinson, M. F. Symmons and B. F. Luisi (2004). "Studies of the RNA degradosome-organizing domain of the Escherichia coli ribonuclease RNase E." J Mol Biol **340**(5): 965-79.

Callaghan, A. J., J. G. Grossmann, Y. U. Redko, L. L. Ilag, M. C. Moncrieffe, M. F. Symmons, C. V. Robinson, K. J. McDowall and B. F. Luisi (2003). "Quaternary structure and catalytic activity of the Escherichia coli ribonuclease E amino-terminal catalytic domain." Biochemistry **42**(47): 13848-55.

Callaghan, A. J., M. J. Marcaida, J. A. Stead, K. J. McDowall, W. G. Scott and B. F. Luisi (2005). "Structure of Escherichia coli RNase E catalytic domain and implications for RNA turnover." Nature **437**: 1187-1191.

Cao, G. J., J. Pogliano and N. Sarkar (1996). "Identification of the coding region for a second poly(A) polymerase in Escherichia coli." Proc Natl Acad Sci U S A **93**(21): 11580-5.

Carpousis, A. J., G. Van Houwe, C. Ehretsmann and H. M. Krisch (1994). "Copurification of E. coli RNAase E and PNPase: evidence for a specific association between two enzymes important in RNA processing and degradation." Cell **76**(5): 889-900.

Caruthers J. M. , Feng Y, McKay DB and C. SN (2006). "Retention of core catalytic functions by a conserved minimal ribonuclease E peptide that lacks the domain required for tetramer formation." J Biol Chem **15**(28): 27046-51.

Caruthers, J. M. and D. B. McKay (2002). "Helicase structure and mechanism." Curr. Opin. Struct. Biol **12**: 123-133.

Cheng, Z.-F., Y. Zuo, Z. Li, K. E. Rudd and M. P. Deutscher (1998). "The vacB gene required for virulence in Shigella flexneri and Escherichia coli encodes the exoribonuclease RNase R." J. Biol. Chem **273**: 14077-14080.

Coburn, G. A., X. Miao, D. J. Briant and G. A. Mackie (1999). "Reconstitution of a minimal RNA degradosome demonstrates functional coordination between a 3' exonuclease and a DEAD-box RNA helicase." Genes Dev **13**(19): 2594-603.

Colland, F., M. Barth, R. Hengge-Aronis and A. Kolb (2000). "Sigma factor selectivity of *Escherichia coli* RNA polymerase: role for CRP, IHF and lrp transcription factors." EMBO J **19**: 3028-37.

Coller, J. and R. Parker (2004). "Eukaryotic mRNA decapping." Annu.Rev. Biochem. **73**: 861-890.

Conrads, T. P., H. J. Issaq and T. D. Veenstra (2002). "New tools for quantitative phosphoproteome analysis." Biochem Biophys Res Commun **290**(3): 885-90.

Datsenko, K. A. and B. L. Wanner (2000). "One-step inactivation of chromosomal genes in Escherichia coli K-12 using PCR products." Proc Natl Acad Sci U S A **97**(12): 6640-5.

de la Cruz, J., D. Kressler, D. Tollervey and P. Linder (1998). "Dob1p (Mtr4p) is a putative ATP-dependent RNA helicase required for the 3' end formation of 5.8s rRNA in Saccharomyces cerevisiae." EMBO J **17**: 1128-1140.

Deutscher, M. P. (2006). "Degradation of RNA in bacteria: comparison of mRNA and stable RNA." Nucleic Acids Research **34**(2): 659-666.

Diwa, A. A. and J. G. Belasco (2002). "Critical features of a conserved RNA stem-loop important for feedback regulation of RNase E synthesis." J Biol Chem **277**(23): 20415-22.

Diwa, A. A., X. Jiang, M. Schapira and J. G. Belasco (2002). "Two distinct regions on the surface of an RNA-binding domain are crucial for RNase E function." Mol Microbiol **46**(4): 959-69.

Ehretsmann, C. P., A. J. Carpousis and H. M. Krisch (1992). "Specificity of Escherichia coli endoribonuclease RNase E: in vivo and in vitro analysis of mutants in a bacteriophage T4 mRNA processing site." Genes Dev **6**(1): 149-59.

Emory, S. A., P. Bouvet and J. G. Belasco (1992). "A 5'-terminal stem-loop structure can stabilize mRNA in Escherichia coli." Genes Dev **6**(1): 135-48.

Feng, Y., T. A. Vickers and S. N. Cohen (2002). "The catalytic domain of RNase E shows inherent 3' to 5' directionality in cleavage site selection." Proc Natl Acad Sci U S A **99**(23): 14746-51.

Folichon, M., F. Allemand, P. Regnier and E. Hajnsdorf (2005). "Stimulation of poly(A) synthesis by Escherichia coli poly(A)polymerase I is correlated with Hfq binding to poly(A) tails." Febs J **272**(2): 454-63.

Gao, J., K. Lee, M. Zhao, J. Qiu, X. Zhan, A. Saxena, C. Moore, S. Cohen and G. Georgiou (2006). "Differential modulation of E. coli mRNA abundance by inhibitory proteins that alter the composition of the degradosome." Mol Microbiol. **61**(2): 394-406.

Georgellis, D., Barlow, T., Arvidson, S. and von Gabain, A., 1993. Retarded RNA turnover in Escherichia coli: a means of maintaining gene expression during anaerobiosis. Mol. Microbiol. 9, pp. 375–381.

Ghora, B. K. and D. Apirion (1978). "Structural analysis and in vitro processing to p5 rRNA of a 9S RNA molecule isolated from an rne mutant of E. coli." Cell **15**(3): 1055-66.

Ghosh, S. and M. P. Deutscher (1999). "Oligoribonuclease is an essential component of the mRNA decay pathway." Proc Natl Acad Sci U S A **96**(8): 4372-7.

Gorbalenya, A. E. and E. V. Koonin (1993). "Helicases: amino acid sequence comparisons and structure-function relationships." Curr. Opin. Struct. Biol **3**: 419-429.

Gottesman, S. (2005). "Micros for microbes: non-coding regulatory RNAs in bacteria." Trends Genet **21**(7): 399-404.

Gupta, R. S., T. Kasai and D. Schlessinger (1977). "Purification and some novel properties of Escherichia coli RNase II." J Biol Chem **252**(24): 8945-9.

Hajnsdorf, E., F. Braun, J. Haugel-Nielsen and P. Regnier (1995). "Polyadenylylation destabilizes the rpsO mRNA of Escherichia coli." Proc Natl Acad Sci U S A **92**(9): 3973-7.

Hajnsdorf, E., O. Steier, L. Coscoy, L. Teysset and P. Regnier (1994). "Roles of RNase E, RNase II and PNPase in the degradation of the rpsO transcripts of Escherichia coli: stabilizing function of RNase II and evidence for efficient degradation in an ams pnp rnb mutant." Embo J **13**(14): 3368-77.

Hayes, R., J. Kudla, G. Schuster, L. Gabay, P. Maliga and W. Gruissem (1996). "Chloroplast mRNA 3'-end processing by a high molecular encoded RNA binding proteins." EMBO J **15**: 1132-1141.

Heatwole, V. and R. Somerville (1992). "Synergism between the Trp repressor and Tyr repressor in repression of the aroL promoter of Escherichia coli K-12." J Bacteriol. **174**(1): 331-5.

Hengge-Aronis, R. (2002). "Signal transduction and regulatory mechanisms involved in control of the sigma(S) (RpoS) subunit of RNA polymerase." Microbiol Mol Biol Rev **66**(3): 373-95, table of contents.

Hengge-Aronis, R. (2002). "Stationary phase gene regulation: what makes an *Escherichia coli* promoter σ^s -selective?" Curr Opin Microbiol **5**: 591-5.

Iost, I. and M. Dreyfus (1995). "The stability of Escherichia coli lacZ mRNA depends upon the simultaneity of its synthesis and translation." EMBO J **14**: 3252-3261.

Iost, I. and M. Dreyfus (2006). "DEAD-box RNA helicases in Escherichia coli." Nucleic Acids Research.

Ishihama, A. (1997). "Adaptation of gene expression in stationary phase bacteria." Curr Opin Genet Dev **7**: 582-588.

Jain, C. and J. G. Belasco (1995). "RNase E autoregulates its synthesis by controlling the degradation rate of its own mRNA in Escherichia coli: unusual sensitivity of the rne transcript to RNase E activity." Genes Dev **9**(1): 84-96.

Jiang, X. and J. G. Belasco (2004). "Catalytic activation of multimeric RNase E and RNase G by 5'-monophosphorylated RNA." Proc Natl Acad Sci U S A **101**(25): 9211-6.

Kaberdin, V. R. (2003). "Probing the substrate specificity of Escherichia coli RNase E using a novel oligonucleotide-based assay." Nucleic Acids Res **31**(16): 4710-6.

Kaberdin, V. R., A. Miczak, J. S. Jakobsen, S. Lin-Chao, K. J. McDowall and A. von Gabain (1998). "The endoribonucleolytic N-terminal half of Escherichia coli RNase E is evolutionarily conserved in Synechocystis sp. and other bacteria but not the C-terminal half, which is sufficient for degradosome assembly." Proc Natl Acad Sci U S A **95**(20): 11637-42.

Kawamoto, H., T. Morita, A. Shimizu, I. T. and H. Aiba (2005). " Implication of membrane localization of target mRNA in the action of a small RNA: mechanism of post-transcriptional regulation of glucose transporter in Escherichia coli." Genes Dev. **19**: 328-338.

Khemici, V. and A. J. Carpousis (2004). "The RNA degradosome and poly(A) polymerase of Escherichia coli are required in vivo for the degradation of small mRNA decay intermediates containing REP-stabilizers." Mol Microbiol **51**(3): 777-90.

Khemici, V., L. Poljak, I. Toesca and A. J. Carpousis (2005). "Evidence in vivo that the DEAD-box RNA helicase RhlB facilitates the degradation of ribosome-free mRNA by RNase E." Proc Natl Acad Sci U S A **102**(19): 6913-8.

Khemici, V., I. Toesca, L. Poljak, Vanzo, NF and A. Carpousis (2004). "The RNase E of Escherichia coli has at least two binding sites for DEAD-box RNA helicases: functional replacement of RhlB by RhlE." Mol Microbiol. **54**(5): 1422-30.

Khodursky, A., B, B. J. Peter, N. R. Cozzarelli, D. Botstein, P. O. Brown and C. Yanofsky (2000). "DNA microarray analysis of gene expression in response to physiological and genetic changes that affect tryptophan metabolism in Escherichia coli." PNAS **97**(22): 12170-12175.

Khodursky AB, Peter BJ, Cozzarelli NR, Botstein D, Brown PO and Y. C (2000). "DNA microarray analysis of gene expression in response to physiological and genetic changes that affect tryptophan metabolism in Escherichia coli." Proc Natl Acad Sci U S A. **97**(22): 12170-12175.

Khodursky, A. B., B. J. Peter, N. R. Cozzarelli, D. Botstein, P. O. Brown and C. Yanofsky (2000). "DNA microarray analysis of gene expression in response to physiological and genetic changes that affect tryptophan metabolism in Escherichia coli." Proc Natl Acad Sci U S A **97**(22): 12170-5.

Kido, M., K. Yamanaka, T. Mitani, H. Niki, T. Ogura and S. Hiraga (1996). "RNase E polypeptides lacking a carboxyl-terminal half suppress a mukB mutation in Escherichia coli." J Bacteriol **178**(13): 3917-25.

Kim, S., H. Kim, I. Park and Y. Lee (1996). "Mutational analysis of RNA structures and sequences postulated to affect 3' processing of M1 RNA, the RNA component of Escherichia coli RNase P." J Biol Chem **271**(32): 19330-7.

Krin, E., C. Laurent-Winter, P. Bertin, A. Danchin and A. Kolb (2003). "Transcription regulation coupling of the divergent argG and metY promoters in Escherichia coli K-12." J Bacteriol. **185**(10): 3139-3146.

Kusano, S., Q. Ding, N. Fujita and A. Ishihama (1996). " Promoter selectivity of *Escherichia coli* RNA polymerase E sigma 70 and E sigma 38 holoenzymes. Effect of DNA supercoiling." J Biol Chem **271**: 1998-2004.

Kushner, S. (2004). "mRNA decay in prokaryotes and eukaryotes: different approaches to a similar problem." IUBMB Life. **56**(10): 585-94.

Kushner, S. R. (2002). "mRNA decay in Escherichia coli comes of age." J Bacteriol **184**(17): 4658-65; discussion 4657.

Lacour, S., A. Kolb, A. Boris Zehnder and P. Landini (202). "Mechanism of specific recognition of the aidB promoter by sigma(S)-RNA polymerase." Biochem Biophys Res Commun **292**: 922-30.

Lee, K., J. A. Bernstein and S. N. Cohen (2002). "RNase G complementation of rne null mutation identifies functional interrelationships with RNase E in Escherichia coli." Mol Microbiol **43**(6): 1445-56.

Lee, K., X. Zhan, J. Gao, J. Qiu, Y. Feng, R. Meganathan, S. N. Cohen and G. Georgiou (2003). "RraA. a protein inhibitor of RNase E activity that globally modulates RNA abundance in E. coli." Cell **114**(5): 623-34.

Leroy, A., N. F. Vanzo, S. Sousa, M. Dreyfus and A. J. Carpousis (2002). "Function in Escherichia coli of the non-catalytic part of RNase E: role in the degradation of ribosome-free mRNA." Mol Microbiol **45**(5): 1231-43.

Li, Z. and M. P. Deutscher (2002). "RNase E plays an essential role in the maturation of Escherichia coli tRNA precursors." Rna **8**(1): 97-109.

Li, Z. and M. P. Deutscher (2004). "Exoribonucleases and endoribonucleases." In Curtiss, R., III (Ed.). EcoSal-Escherichia coli and Salmonella: Cellular and Molecular Biology, Chapter 4.6.3.

Li, Z., S. Pandit and M. P. Deutscher (1999). "RNase G (CafA protein) and RNase E are both required for the 5' maturation of 16S ribosomal RNA." Embo J **18**(10): 2878-85.

Lin-Chao, S., C. L. Wei and Y. T. Lin (1999). "RNase E is required for the maturation of ssrA RNA and normal ssrA RNA peptide-tagging activity." Proc Natl Acad Sci U S A **96**(22): 12406-11.

Lin, P.-H. and S. Lin-Chao (2005). "RhlB helicase rather than enolase is the -subunit of the Escherichia coli polynucleotide phosphorylase (PNPase)–exoribonucleolytic complex." PNAS **102** (46): 16590-16595.

Lin, P. H. and S. Lin-Chao (2005). "RhlB helicase rather than enolase is the beta-subunit of the Escherichia coli polynucleotide phosphorylase (PNPase)-exoribonucleolytic complex." Proc Natl Acad Sci U S A **102**(46): 16590-5.

Liou, G., W. Jane, S. Cohen, N. Lin and S. Lin-Chao (2001). "RNA degradosomes exist in vivo in Escherichia coli as multicomponent complexes associated with the

cytoplasmic membrane via the N-terminal region of ribonuclease E." Proc Natl Acad Sci U S A. **98**(1): 63-8.

Liou, G. G., H. Y. Chang, C. S. Lin and S. Lin-Chao (2002). "DEAD box RhlB RNA helicase physically associates with exoribonuclease PNPase to degrade double-stranded RNA independent of the degradosome-assembling region of RNase E." J Biol Chem **277**(43): 41157-62.

Lundberg, U., A. von Gabain and O. Melefors (1990). "Cleavages in the 5' region of the ompA and bla mRNA control stability: studies with an E. coli mutant altering mRNA stability and a novel endoribonuclease." Embo J **9**(9): 2731-41.

Maas, W. K. (1994). "The arginine repressor of Escherichia coli." Microbiol Rev. **58**(4): 631-40.

Mackie, G. A. (1991). "Specific endonucleolytic cleavage of the mRNA for ribosomal protein S20 of Escherichia coli requires the product of the ams gene in vivo and in vitro." J Bacteriol **173**(8): 2488-97.

Mackie, G. A. (1992). "Secondary structure of the mRNA for ribosomal protein S20. Implications for cleavage by ribonuclease E." J Biol Chem **267**(2): 1054-61.

Mackie, G. A. (1998). "Ribonuclease E is a 5'-end-dependent endonuclease." Nature **395**(6703): 720-3.

Margossian, S. P., H. Li, H. P. Zassenhaus and R. A. Butow (1996). "The DExH box protein Suv3p is a component of a yeast mitochondrial 3' to 5' exoribonuclease that suppresses group I intron toxicity." Cell **84**: 199-209.

Marschall, C., V. Labrousse, M. Kreimer, D. Weichart, A. Kolb and R. Hengge-Aronis (1998). "Molecular analysis of the regulation of *csiD*, a carbon starvation-

inducible gene in *Escherichia coli* that is exclusively dependent on sigma s and requires activation by cAMP-CRP." J Mol Biol **276**: 339-53.

Masse, E., F. E. Escorcia and S. Gottesman (2003). "Coupled degradation of a small regulatory RNA and its mRNA targets in Escherichia coli." Genes Dev **17**(19): 2374-83.

Masse, E. and S. Gottesman (2002). "A small RNA regulates the expression of genes involved in iron metabolism in Escherichia coli." Proc Natl Acad Sci U S A **99**(7): 4620-5.

Masse, E., N. Majdalani and S. Gottesman (2003). "Regulatory roles for small RNAs in bacteria." Curr Opin Microbiol **6**(2): 120-4.

Mata, J., S. Marguerat and J. Bahler (2005). "Post-transcriptional control of gene expression: a genome-wide perspective." TRENDS in Biochemical Sciences **30**(9): 506-514.

McDowall, K. J. and S. N. Cohen (1996). "The N-terminal domain of the rne gene product has RNase E activity and is non-overlapping with the arginine-rich RNA-binding site." J Mol Biol **255**(3): 349-55.

McDowall, K. J., R. G. Hernandez, S. Lin-Chao and S. N. Cohen (1993). "The ams-1 and rne-3071 temperature-sensitive mutations in the ams gene are in close proximity to each other and cause substitutions within a domain that resembles a product of the Escherichia coli mre locus." J Bacteriol **175**(13): 4245-9.

McDowall, K. J., S. Lin-Chao and S. N. Cohen (1994). "A+U content rather than a particular nucleotide order determines the specificity of RNase E cleavage." J Biol Chem **269**(14): 10790-6.

Meganathan, R. (1996). Biosynthesis of the isoprenoid quinones menaquinone (vitamin K2) and ubiquinone (coenzyme Q). Washington, D.C., American Society for Microbiology.

Melefors, O. and A. von Gabain (1991). "Genetic studies of cleavage-initiated mRNA decay and processing of ribosomal 9S RNA show that the Escherichia coli ams and rne loci are the same." Mol Microbiol **5**(4): 857-64.

Miczak, A., V. R. Kaberdin, C. L. Wei and S. Lin-Chao (1996). "Proteins associated with RNase E in a multicomponent ribonucleolytic complex." Proc Natl Acad Sci U S A **93**(9): 3865-9.

Miller, J. H. (1972). "Experiments in Molecular Genetics."

Miller, J. H. (1992). A short course in bacterial genetics: a laboratory manual and handbook for Escherichia coli and related bacteria, Cold spring harbor laboratory press.

Mirgorodskaya, O. A., Y. P. Kozmin, M. I. Titov, R. Korner, C. P. Sonksen and P. Roepstorff (2000). "Quantitation of peptides and proteins by matrix-assisted laser desorption/ionization mass spectrometry using (18)O-labeled internal standards." Rapid Commun Mass Spectrom **14**(14): 1226-32.

Misra, T. K. and D. Apirion (1979). "RNase E, an RNA processing enzyme from Escherichia coli." J Biol Chem **254**(21): 11154-9.

Mitchell, P., E. Petfalski, A. Shevchenko, M. Mann and D. Tollervey (1997). "The exosome: A conserved eukaryotic RNA processing complex containing multiple 3'-5' exoribonucleases." Cell **91**: 457-466.

Mohanty, B. K., V. F. Maples and S. R. Kushner (2004). "The Sm-like protein Hfq regulates polyadenylation dependent mRNA decay in Escherichia coli." Mol Microbiol **54**(4): 905-20.

Moll I, Afonyushkin T, Vytvytska O, Kaberdin VR and B. U. (2003). "Coincident Hfq binding and RNase E cleavage sites on mRNA and small regulatory RNAs." RNA **9**(11): 1308-14.

Monzingo, A. F., J. Gao, J. Qiu, G. Georgiou and J. D. Robertus (2003). "The X-ray structure of Escherichia coli RraA (MenG), A protein inhibitor of RNA processing." J Mol Biol **332**(5): 1015-24.

Morita, T., H. Kawamoto, T. Mizota, T. Inada and H. Aiba (2004). "Enolase in the RNA degradosome plays a crucial role in the rapid decay of glucose transporter mRNA in the response to phosphosugar stress in Escherichia coli." Mol Microbiol **54**(4): 1063-75.

Morita, T., K. Maki and H. Aiba (2005). "RNase E-based ribonucleoprotein complexes: mechanical basis of mRNA destabilization mediated by bacterial noncoding RNAs." Genes Dev. **19**: 2176-2186.

Mudd, E. A. and C. F. Higgins (1993). "Escherichia coli endoribonuclease RNase E: autoregulation of expression and site-specific cleavage of mRNA." Mol Microbiol **9**(3): 557-68.

Mudd, E. A., H. M. Krisch and C. F. Higgins (1990). "RNase E, an endoribonuclease, has a general role in the chemical decay of Escherichia coli mRNA: evidence that rne and ams are the same genetic locus." Mol Microbiol **4**(12): 2127-35.

Nilsson, P. and B. Uhlin (1991). "Differential decay of a polycistronic Escherichia coli transcript is initiated by RNaseE-dependent endonucleolytic processing." Mol. Microbiol. **5**: 1791- 99.

O'Hara, E. B., J. A. Chekanova, C. A. Ingle, Z. R. Kushner, E. Peters and S. R. Kushner (1995). "Polyadenylylation helps regulate mRNA decay in Escherichia coli." Proc Natl Acad Sci U S A **92**(6): 1807-11.

Ono, M. and M. Kuwano (1979). "A conditional lethal mutation in an Escherichia coli strain with a longer chemical lifetime of messenger RNA." J Mol Biol **129**(3): 343-57.

Ow, M. C. and S. R. Kushner (2002). "Initiation of tRNA maturation by RNase E is essential for cell viability in E. coli." Genes Dev **16**(9): 1102-15.

Ow, M. C., Q. Liu and S. R. Kushner (2000). "Analysis of mRNA decay and rRNA processing in Escherichia coli in the absence of RNase E-based degradosome assembly." Mol Microbiol **38**(4): 854-66.

Ow, M. C., T. Perwez and S. R. Kushner (2003). "RNase G of Escherichia coli exhibits only limited functional overlap with its essential homologue, RNase E." Mol Microbiol **49**(3): 607-22.

Pittard, A. J. (1996). "in Escherichia coli and Salmonella: Cellular and Molecular Biology, eds. Neidhardt, F. C., Curtis, R., III, Ingraham, J. L., Lin, E. C. C., Low, K. B., Magasanik, B., Reznikoff, W. S., Riley, M., M., Schaecter, A. & Umbarger, H. E." **1**: 458-484.

Podkovyrov, S. M. and T. J. Larson (1995). "A new vector-host system for construction of lacZ transcriptional fusions where only low-level gene expression is desirable." Gene **156**(1): 151-2.

Powell, B. S., M. P. Rivas, D. L. Court, Y. Nakamura and C. L. Turnbough (1994). "Rapid confirmation of single copy lambda prophage integration by PCR." Nucleic Acids Res **22**: 5765-766.

Prud'homme-Genereux, A., R. K. Beran, I. Iost, C. S. Ramey, G. A. Mackie and R. W. Simons (2004). "Physical and functional interactions among RNase E, polynucleotide phosphorylase and the cold-shock protein, CsdA: evidence for a 'cold shock degradosome'." Mol Microbiol **54**(5): 1409-21.

Py, B., H. Causton, E. A. Mudd and C. F. Higgins (1994). "A protein complex mediating mRNA degradation in Escherichia coli." Mol Microbiol **14**(4): 717-29.

Py, B., C. F. Higgins, H. M. Krisch and A. J. Carpousis (1996). "A DEAD-box RNA helicase in the Escherichia coli RNA degradosome." Nature **381**(6578): 169-72.

Qiu, J. (2001). Ph. D. Thesis. Austin, The University of Texas at Austin.

Qiu, J., J. R. Swartz and G. Georgiou (1998). "Expression of active human tissue-type plasminogen activator in Escherichia coli." Appl Environ Microbiol **64**(12): 4891-6.

Ramelot, T. A., S. Ni, S. Goldsmith-Fischman, J. R. Cort, B. Honig and M. A. Kennedy (2003). "Solution structure of Vibrio cholerae protein VC0424: a variation of the ferredoxin-like fold." Protein Sci **12**(7): 1556-61.

Raynal, L. C. and A. J. Carpousis (1999). "Poly(A) polymerase I of Escherichia coli: characterization of the catalytic domain, an RNA binding site and regions for the

interaction with proteins involved in mRNA degradation." Mol Microbiol **32**(4): 765-75.

Regnier, P. and E. Hajnsdorf (1991). "Decay of mRNA encoding ribosomal protein S15 of Escherichia coli is initiated by an RNase E-dependent endonucleolytic cleavage that removes the 3' stabilizing stem and loop structure." J Mol Biol **217**(2): 283-92.

Regonesi, M. E., M. Del Favero, F. Basilico, F. Briani, L. Benazzi, P. Tortora, P. Mauri and G. Deho (2005). "Analysis of the Escherichia coli RNA degradosome composition by a proteomic approach." Biochimie.

Repoila, F. and S. Gottesman (2001). "Signal transduction cascade for regulation of RpoS: temperature regulation of DsrA." J Bacteriol. **183**(13): 4012-23.

Sauter, C., J. Basquin and D. Suck (2003). "Sm-like proteins in eubacteria: the crystal structure of the Hfq protein from Escherichia coli." Nucleic Acids Res **31**: 4091-4098.

Schatz, P. J. (1993). "Use of peptide libraries to map the substrate specificity of a peptide-modifying enzyme: a 13 residue consensus peptide specifies biotinylation in Escherichia coli." Biotechnology (N Y) **11**(10): 1138-43.

Schena, M., D. Shalon, R. W. Davis and P. O. Brown (1995). "Quantitative monitoring of gene expression patterns with a complementary DNA microarray." Science **270**(5235): 467-70.

Schlee, S., P. Beinker, A. Akhrymuk and J. Reinstein (2004). "A chaperone network for the resolubilization of protein aggregates: direct interaction of ClpB and DnaK." J Mol Biol **336**(1): 275-85.

Schubert, M., R. E. Edge, P. Lario, M. A. Cook, N. C. Strynadka, G. A. Mackie and L. P. McIntosh (2004). "Structural characterization of the RNase E S1 domain and identification of its oligonucleotide-binding and dimerization interfaces." J Mol Biol **341**(1): 37-54.

Shineberg, B. and I. Young (1976). "Biosynthesis of bacterial menaquinones: the membrane-associated 1,4-dihydroxy-2-naphthoate octaprenyltransferase of Escherichia coli." Biochemistry **15**: 2754-8.

Silverman, E., G. Edwalds-Gilbert and R. J. Lin (2003). "DExD/H-box proteins and their partners: helping RNA helicases unwind." Gene **312**: 1-16.

Simons, R. W., F. Houman and N. Kleckner (1987). "Improved single and multicopy lac-based cloning vectors for protein and operon fusions." Gene **53**(1): 85-96.

Singer, R. H. and S. Penman (1973). "Messenger RNA in HeLa cells: kinetics of formation and decay." J Mol Biol **78**(2): 321-34.

Soreq, H. and U. Z. Littauer (1977). "Purification and characterization of polynucleotide phosphorylase from Escherichia coli. Probe for the analysis of 3' sequences of RNA." J Biol Chem **252**(19): 6885-8.

Steege, D. A. (2000). "Emerging features of mRNA decay in bacteria." Rna **6**(8): 1079-90.

Storz, G., J. A. Opdyke and A. Zhang (2004). "Controlling mRNA stability and translation with small, noncoding RNAs." Curr Opin Microbiol **7**(2): 140-4.

Suiter, A., O. Banziger and A. Dean (2003). "Fitness consequences of a regulatory polymorphism in a seasonal environment." Proc Natl Acad Sci U S A. **100**(22): 12782-6.

Suvarna, K., D. Stevenson, R. Meganathan and M. E. Hudspeth (1998). "Menaquinone (vitamin K2) biosynthesis: localization and characterization of the menA gene from Escherichia coli." J Bacteriol **180**(10): 2782-7.

Tanner, N. K. and P. Linder (2001). "DExD/H box RNA helicases: from generic motors to specific dissociation functions." Mol. Cell **8**: 251-262.

Taraseviciene, L., A. Miczak and D. Apirion (1991). "The gene specifying RNase E (rne) and a gene affecting mRNA stability (ams) are the same gene." Mol Microbiol **5**(4): 851-5.

Tsao, K. L., B. DeBarbieri, H. Michel and D. S. Waugh (1996). "A versatile plasmid expression vector for the production of biotinylated proteins by site-specific, enzymatic modification in Escherichia coli." Gene **169**(1): 59-64.

Typas, A. and R. Hengge-Aronis (2005). "Differential ability of sigma and sigma of *Escherichia coli* to utilize promoters containing half or full UP-element sites." Mol Microbiol **55**: 250-260.

Vanzo, N. F., Y. S. Li, B. Py, E. Blum, C. F. Higgins, L. C. Raynal, H. M. Krisch and A. J. Carpousis (1998). "Ribonuclease E organizes the protein interactions in the Escherichia coli RNA degradosome." Genes Dev **12**(17): 2770-81.

Wachi, M., G. Umitsuki, M. Shimizu, A. Takada and K. Nagai (1999). "Escherichia coli cafA gene encodes a novel RNase, designated as RNase G, involved in processing of the 5' end of 16S rRNA." Biochem Biophys Res Commun **259**(2): 483-8.

Wah, D. A., I. Levchenko, T. A. Baker and R. T. Sauer (2002). "Characterization of a specificity factor for an AAA+ ATPase: assembly of SspB dimers with ssrA-tagged proteins and the ClpX hexamer." Chem Biol **9**(11): 1237-45.

Warner, J. R. and C. Gorenstein (1978). "Yeast has a true stringent response." Nature **275**(5678): 338-9.

Washburn, M. P., D. Wolters and J. R. Yates, 3rd (2001). "Large-scale analysis of the yeast proteome by multidimensional protein identification technology." Nat Biotechnol **19**(3): 242-7.

Weber, H., T. Polen, J. Heuveling, V. F. Wendisch and R. Hengge-Aronis (2005). "Genome-wide analysis of the general stress response network in *Escherichia coli*: sigmaS-dependent genes, promoters, and sigma factor selectivity." J Bacteriol. **187**: 1591-603.

Weichart, D., R. Lange, N. Henneberg and R. Hengge-Aronis (1993). "Identification and characterization of stationary phase-inducible genes in *Escherichia coli*." Mol. Microbiol. **10**: 407-420.

Xu, F. and S. N. Cohen (1995). "RNA degradation in Escherichia coli regulated by 3' adenylation and 5' phosphorylation." Nature **374**(6518): 180-3.

Yanofsky, C., E. W. Miles, K. Kirschner and R. Bauerle (1999). "in The Encyclopedia of Molecular Biology, ed. Creighton, T. E." **4**: 2676-2689.

Yao, X., A. Freas, J. Ramirez, P. A. Demirev and C. Fenselau (2001). "Proteolytic 18O labeling for comparative proteomics: model studies with two serotypes of adenovirus." Anal Chem **73**(13): 2836-42.

Yi, E. C., X. J. Li, K. Cooke, H. Lee, B. Raught, A. Page, V. Aneliunas, P. Hieter, D. R. Goodlett and R. Aebersold (2005). "Increased quantitative proteome coverage with (13)C/(12)C-based, acid-cleavable isotope-coded affinity tag reagent and modified data acquisition scheme." Proteomics **5**(2): 380-7.

Zhan, X., J. Gao, C. Jain, M. J. Cieslewicz, J. R. Swartz and G. Georgiou (2004). "Genetic analysis of disulfide isomerization in Escherichia coli: expression of DsbC is modulated by RNase E-dependent mRNA processing." J Bacteriol **186**(3): 654-60.

Zhang, A., K. M. Wassarman, C. Rosenow, B. C. Tjaden, G. Storz and S. Gottesman (2003). "Global analysis of small RNA and mRNA targets of Hfq." Mol Microbiol **50**(4): 1111-24.

Zhang, X., L. Zhu and M. P. Deutscher (1998). "Oligoribonuclease is encoded by a highly conserved gene in the 3'-5' exonuclease superfamily." J Bacteriol **180**(10): 2779-81.

Zuo, Y. and M. P. Deutscher (2001). "Exoribonuclease superfamilies: structural analysis and phylogenetic distribution." Nucleic Acids Res **29**(5): 1017-26.

Vita

Meng Zhao was born in Henan, China on January 29, 1975, the daughter of Fengqin Yao and Tieshan Zhao. She graduated with High Honors from Shanghai's Higher Education and received the degree of Bachelor of Medicine (equivalent of M.D. in U.S.) in Clinic Medicine from Medical College of TongJi University, Shanghai, China, in July 1998. She then entered Shanghai Second Medical University, Shanghai, China, where she received the degree of Master of Medicine with a specialization in Biomedical Science in July 2001. In August 2001 she entered the Graduate School of The University of Texas at Austin to work towards her Doctorate in Cell and Molecular Biology.

Permanent address: 302, 22, 177 Nong, TianShan Road, Shanghai, China, 200336

This dissertation was typed by the author.